Fabrication & Characterization of Ti-Ce MOFs based silk electro spun membrane for bone Regeneration
A combined DFT and Experimental Approach

MS Thesis

by

Tayyaba Fatima

CIIT/SP24-R06-027/LHR

COMSATS University Islamabad
Pakistan

Fall 2025

Fabrication & Characterization of Ti-Ce MOFs based silk electro spun membrane for bone Regeneration
A combined DFT and Experimental Approach

A thesis submitted to

COMSATS University Islamabad

In partial fulfilment

Of the requirement for the degree of

Master of Science

In

Chemistry

By

Tayyaba Fatima

CIIT/SP24-R06-027/LHR

Department of Chemistry

Faculty of Science

COMSATS University Islamabad
Pakistan Fall 2025

Fabrication & Characterization of Ti-Ce MOFs based silk electro spun membrane for bone Regeneration A combined DFT and Experimental Approach

This Thesis is submitted to the Department of Chemistry as partial fulfillment of the requirements for the award of the Degree of MS in Chemistry.

Name	Registration Number
Tayyaba Fatima	CIIT/SP24-R06-027/LHR

Supervisory Committee

Supervisory Committee	
Name and Designation	Role
Prof. Dr. Mazhar Amjad Gilani/ Professor	Supervisor
Prof. Dr. Ather Farooq Khan /Tenured Professor , IRCBM	Co-supervisor/Member
Dr. Hamad Khalid, Associate Professor	Member
Dr. Hafsa Akhtar, Research Associate	Member

Certificate of Approval

This thesis is titled

Fabrication & Characterization of Ti-Ce MOFs based silk electro spun membrane for bone Regeneration A combined DFT and Experimental Approach

By

Tayyaba Fatima

CIIT/SP24-R06-027/LHR

Has been approved

For COMSATS University Islamabad, Lahore Campus.

External Examiner:_____

Dr. External Examiner

University Name

Supervisor:_____

Prof. Dr. Mazhar Amjad Gilani
Director, (CUI) Sahiwal Campus

Head of Department:_____

Dr Muhammad Shahid Nazir

Department of Chemistry, (CUI) Lahore Campus

Author's Declaration

I, Tayyaba Fatima CIIT/SP24-R06-027/LHR, hereby declare that I have produced the work presented in this thesis, during the scheduled period of study. I also declare that I have not taken any material from any source except referred to wherever due to that amount of plagiarism within an acceptable range. If a violation of HEC rules on research has occurred in this thesis, I shall be liable to punishable action under the plagiarism rules of HEC.

Date:_____ _____

Tayyaba Fatima

CIIT/SP24-R06-027/LHR

Certificate

It is certified that Tayyaba Fatima CIIT/SP24-R06-027/LHR has carried out all the work related to this thesis under my supervision at the Department of Mathematics, COMSATS University Islamabad, Lahore Campus and the work fulfill the requirement for award of MS degree.

Date:_____

Supervisor

Prof. Dr. Mazhar Amjad Gilani

Director, CUI Sahiwal Campus

_____

Dedication

I Wholeheartedly Dedicate This Work to My

Parents and my Siblings

Acknowledgments

After the Gracious, the Most Merciful, Beneficent, Loving, and Kind **Almighty Allah**, I want to pay gratitude to my family including my **parents** and my **siblings** who helped me achieve this feat through their constant support, endless love, and prayers. My most profound appreciation goes to my supervisor, **Prof. Dr. Mazhar Amjad Gilani**, who deserves my gratitude for all his time, effort, and patience in helping me get my MS degree. In addition, I want to thank my Co. supervisor, **Prof. Dr. Ather Farooq khan,** for his support throughout and for backing me up in times of need and also thanks to my research group **Dr. Hamad Khalid** and **Dr Hafsah Akhter** for their assistance in times of need. I want to thank everyone from the Department of Chemistry for their help, especially HOD **Dr Muhammad Shahid Nazir** and PG Coordinator. I would also like to extend thanks to IRCBM for providing me with the opportunity to perform advance research in Pakistan. It gives me immense pleasure and honor to be able to convey my sincere gratitude and commitment to the head of IRCBM, **Prof. Anila Asif**, and **Mr. Muhammad Usman (Manager IRCBM)** for giving me a suitable environment and the necessary resources for carrying out this research. I am indebted to my lab fellows, friends, and family.

Tayyaba Fatima

SP24-R06-027

Abstract

Fabrication & Characterization of Ti-Ce MOFs based silk electro spun membrane for bone Regeneration A combined DFT and Experimental Approach

By

Tayyaba Fatima

Neurosurgical procedures, traumatic brain injury, tumor resection, and cerebrovascular disorders may lead to leaking cerebrospinal fluid and development of severe complications such as infection, inflammation, and dysfunction of the nervous system. The traditional methods of dural repairs like sutures, sealants, and hydrogels are usually constrained by factors such as partial repair, immunogenic response, lack of accessibility and mechanical efficacy. In solving these issues, a mechanically stable, biocompatible and biodegradable scaffold should be developed. In this work we have fabricated a bilayer electrospun scaffold that was created using silk fibroin, calcium magnesium silicates (SILK+CMS), poly(epsilon-caprolactone) (PCL), with metal-organic frameworks (PCL+MOF) to regenerate the dura mater. The scaffolds were prepared and characterized in a systematic way by application of different techniques of analysis. The FTIR analysis showed that all components had characteristic functional groups, which correspond to the successful fabrication of the scaffolds. The bilayer scaffolds also had optimized hydrophilicity, swelling characteristics, porosity, and density that were beneficial in cell attachment, growth, diffusion of nutrients, and tissue integration. SEM examination demonstrated a consistent fibrous pattern and well organization of the fibers which were very similar to the normal dura mater structure. In vitro degradation tests proved that the scaffolds had a programmed rate of degradation that could be adjusted to the rate of healing in the dura mater. Moreover, in vitro biocompatibility tests revealed that there is a good cellular response, which indicates that the scaffold can facilitate cell attachment and viability. Altogether, the findings indicate that the developed bilayer scaffold can be regarded as the promising biomaterial candidate to repair dura mater, and it may help avoid the cerebrospinal fluid leakage and promote successful tissue regeneration.

Table of Contents

Chapter 01 1
Introduction 1
1.1 Background 1
1.2 Anatomy of Dura Mater 3
1.3 Function of Dura Mater: 4
1.4 Origins of Dural defects: 7
1.5 Classical Approaches to Dural Closure 7
1.5.1 Sealants: 7
1.5.2 Hydrogels: 8
1.5.3 Sutures: 8
1.6 Categories of Dural Repair Materials: 9
1.6.1 Homologous materials: 9
1.6.2 Acellular materials: 10
1.6. 3 Natural materials: 10
1.6.3.1 Collagen 10
1.6.3.2 Other natural materials: 12
1.6.4 Synthetic materials: 12
1.6.4.1 non-biodegradable materials: 12
1.6.4.2 Biodegradable materials: 13
1.6.5 Composite materials: 13
1.7 Tissue Engineering: 14
1.7.1 Scaffolds for Tissue Engineering: 15
1.7.2 Physiochemical and biochemical properties of Tissue Engineering Scaffolds: 16
1.7.3 Biomaterials for Scaffold Fabrication: 17
1.7.3.1 Bioinert Materials: 18
1.7.3.2 Biodegradable Materials: 18
1.7.3.3 Bioactive Materials: 18
1.8 Scaffold Manufacturing Techniques: 19
i)1.8.1 Electrospinning: 19

1.8.1.1 Fundamental principle of Electro spinning: 21
ii) 1.8.2 Freeze drying: 22
1.8.2.1 Fundamental Principle of freeze drying: 23
1.9 Fabrication materials for bi-layered scaffolds: 24
1.9.1 Silk -A natural Polymer 24
1.9.2 Silk: Structural and Chemical Composition 25
1.9.3 Fibroin Protein: 26
1.9.4 Sericin Protein: 28
1.9.5 Essential properties of silk fibroin as biomaterial: 29
1.9.6 Poly-ε-caprolactone (PCL) 30
1.9.7 Metal-Organic Framework (MOFs): 33
1.9.7.1 Titanium-based MOFs 35
1.9.7.2 Cerium-based MOFs 36
1.9.8 Calcium Magnesium Silicates (CMS) 36
1.10 Theoretically (Software and Computational studies) 38
Chapter 02 40
Literature review 40
Chapter 03 44
Materials and Methodology 44
3.1 Materials: 44
3.2 Computational Methodology 45
3.3 Experimental Methodology 45
3.3.1 Fabrication of Silk Fibroin Scaffold 45
3.3.2 Dissolution of Silk Fibroin 46
3.3.3 Freeze drying of Silk Fibroin 46
3.3.4 Fabrication of SF+CMS Scaffolds: 47
3.3.4.1 Preparation of Silk+CMS Solution 47
3.3.4.2 Freeze drying of SILK+CMS scaffolds: 48
3.3.4.3 Electrospinning of PCL 48

3.3.4.4 Electrospinning of PCL+MOF 48
3.3.5 Fabrication of Bi-layered Scaffold: 49
3.4 Characterization techniques 50
3.4.1 Fourier transform-infrared spectroscopy (FT-IR) 50
3.4.2 Scanning Electron Microscope (SEM) 51
3.4.3 Contact Angle (Biolin Scientific Attention Theta Measurement) 52
3.4.4 X-rays Diffraction (XRD) 53
3.4.5 Migration Assay 54
3.4.6 Swelling ratio measurement 56
3.4.7 Porosity measurement: 56
3.4.8 Density measurement: 57
3.4.9 *In Vitro* Degradation studies 57
Chapter 04 58
Results and discussion 58
4.1 Theory Results and Discussion 58
4.1.2 Geometry optimization 58
4.1.3 Interaction Energies 58
4.2 Experimental Results and Discussion 60
4.2.1 Functional Group Detection-FTIR Spectroscopy 60
4.2.2 X-ray Diffraction (XRD) 63
4.2.3 Scanning Electron Microscopy (SEM) 65
4.2.5 Contact Angle 68
4.2.6 Swelling ratio measurement 69
4.2.7 Porosity Measurement 70
4.2.8 Density Measurement 71
4.2.9 *In vitro*-Degradation studies 73
4.2.10 Cell Migration Study 74
Chapter 5 75
Conclusion 76

List of Figures

Figure 1. 1Anatomy of Dura Mater……4
Figure 1. 2 Magnified view of structure of meninges-dura mater, arachnoid mater, pia mater..... 6
Figure 1. 3 Classical Approaches to Dural Closure [45] 9
Figure 1. 4 Classification of materials used for dural repair [57] 11
Figure 1. 5 Bilayered Scaffold with tissue engineering [86] 16
Figure 1. 6 Biomaterials with tissue engineering [104] 19
Figure 1. 7 Electrospinning setup 20
Figure 1. 8 Electrospinning set up with parameters [112] 21
Figure 1. 9 Freeze drying Setup 22
Figure 1. 10 Freeze drying Theory [118] 24
Figure 1. 11 Silk Cocoons from Bombyx mori 25
Figure 1. 12 Structure of Silkworm thread [121] 26
Figure 1. 13 Structure of Silk Fibroin [122] 27
Figure 1. 14 Molecular Crystalline structure of Silk Fibroin [124] 28
Figure 1. 15 Formation of polycaprolactone [131] 30
Figure 1. 16 Polycaprolactone Composites/Blends and Their Applications [134] 31
Figure 1. 17 Key Properties of PCL [134] 32
Figure 1. 18 Representation of Metal-Organic Frameworks [136] 33
Figure 1. 19 Applications of MOFs in the biomedical field [137] 34
Figure 1. 20 Input structure of Ti-Ce Pyridine-2,4,6-tricarboxylic acid MOFs 38
Figure 1. 21 Input structure of PCL (polycaprolactone) 39

Figure 3. 1 Fabrication of Silk scaffold 47
Figure 3. 2 Fabrication of Bilayer Scaffold 49
Figure 3. 3 Thermo Nicolet Scientific 6700 FTIR, USA 51
Figure 3. 4 Thermo Fisher SCIENTIFIC Electron Microscope 1142267 52
Figure 3. 5 Biolin Scientific Attention Theta Measurement 53
Figure 3. 6 Rigaku MiniFlex XRD Measurement ……55

Figure 4. 1 FTIR Analysis of CMS, SF, SF+CMS, PCL, MOF, PCL+MOF 61
Figure 4. 2 XRD Analysis of (a) Ce-Ti MOF (b) CMS 64
Figure 4. 3 FESEM Analysis of SF, SF+CMS, PCL, PCL+MOF and BL SCAFFOLD……...66
Figure 4. 4 FESEM Cross section area of BL SCAFFOLD……..67
Figure 4. 5 Contact angle of SF, SF+CMS, PCL, PCL+MOF and BL SCAFFOLDS 69
Figure 4. 6 %Swelling measurement of SF, SF+CMS, PCL, PCL+MOF and BL SCAFFOLDS 70
Figure 4. 7 %Porosity measurements of SF, SF+CMS, PCL, PCL+MOF, BL in absolute ethanol 71

Figure 4. 8 Density measurement of SF, SF+CMS, PCL, PCL+MOF and BL SCAFFOLDS.... 73
Figure 4. 9 %Degradation profile of scaffolds after 1, 7, 14 and 28 days 74
Figure 4. 10 Migration Assay of SF, SF+CMS, PCL, PCL+MOF, BL and Control SCAFFOLD 75

List of Tables

Table 1.1 List of Chemicals 44
Table 4.1 Interaction energies……...59
Table 4.2 Characteristics peaks for the functional groups of scaffolds……..63
Table 4.3 Contact Angle of the scaffolds ……..69

List of Abbreviation

CNS	Central Nervous System
CSF	Cerebrospinal Fluid
SF	Silk Fibroin
CMS	Calcium Magnesium Silicates
PCL	Polycaprolactone
MOF	Metal organic framework
BL	Bilayer scaffold
ES	Electrospinning
FD	Freeze drying
FTIR	Fourier Transform infrared spectroscopy
SEM	Scanning Electron Microscopy
XRD	X-rays Diffraction

Chapter 01

Introduction

1.1 Background

The dura mater is the most external covering of preservation of the central nervous system (CNS) enveloping the brain (cranial dura mater) and the spinal cord[1].The dura mater in addition to acting as a barrier has a role in blood transportation of brain to the heart, causing the intracranial pressure to be stabilized and containing the cerebrospinal fluid (CSF)[2]. Dura mater integrity is fundamental in the preservation of the protection of the central nervous system. Traumatic injury, neoplastic invasion, cerebrovascular pathology or surgery may disrupt this membrane and cause cerebrospinal fluid (CSF) leakage, which is a condition that poses a great risk to developing neurological complications[3].One of the difficulties in neurosurgery is the attainment of a watertight closure of the dura mater when it is violated. The dura does not possess self-healing ability like other tissues. It is thus important in neurosurgical practice to regenerate or reconstruct the dura mater effectively [4]. After rupture, the CSF spills into extradural space resulting in severe neurological complications, including meningitis, abscess, and ventriculitis[5]. The anatomy of dural defects makes the direct repair complex, resulting in poor outcomes of the traditional methods like epidural blood patches[6]. Clinical reports have indicated that CSF leaks have occurred in the rates of 30-40 percent stipulating the enormity of the problem[7]. Minor defects (less than 1 cm) of the dura (e.g. iatrogenic injury, fistula of the CSF) are commonly remedied using multilayered grafting methods, which have shown over 90% success rates. Conversely, the bigger defects (>3 cm) are more challenging to contain[8]. In these instances, several various free grafting materials have been used, such as acellular dermis, cadaveric pericardium, fascia lata, titanium meshes, and nasal turbinate mucosa. Nevertheless, large reconstructions have poor clinical outcomes with a leak rate that is higher than 30%[9]. The limitations present the necessity of more efficient tactics. There

are several types of dural substitutes developed and tested over the years in the clinical and experimental settings such as autologous grafts (e.g., temporal facia, periosteal flaps, facia lata feminina), allografts (e.g., freeze dried human cadaveric dura) and xenografts (e.g., bovine, porcine heart capsule, small intestinal submucosa, dermis, equine Achilles tendon)[10]. As much as these substitutes offer short-term closure, they are more of a limited usage. The main disadvantages are a morbidity of the donor site, limited availability of tissues, chances of infections or transmission of diseases, and chances of immune rejection[11]. Notably, such grafts usually do not recapitulate the natal architecture of the dura mater, limiting their capacity to have intracranial homeostasis and cushion the brain in a long-term period[12]. Tissue engineering has in recent years become a worthy subject in efforts to come up with more advanced dural substitutes. The strategy is the production of biomimetic scaffolds, which can provide the required conditions of cellular adhesion, proliferation, and differentiation.

A good scaffold must combine the following major characteristics:

- 10 mmHg tensile strength to counter intracranial pressure.
- Biocompatibility to prevent immune or inflammatory responses.
- Regulated biodegradability to allow the material to be slowly substituted by native tissue.
- Large porosity and surface area, which facilitates the transport of nutrients and migration of cells[13].

Synthetic polymers, natural polymers, metals and ceramics are some of the wide array of biomaterials under investigation in fabrication of scaffolds[14]. Nevertheless, none of the materials is linked to strengths. An example is that synthetic polymers are generally strong and non-biodegradable whereas natural ones are biodegradable and not very strong[15]. Composite scaffolds have been suggested as a remedy to these problems. Composite systems can enhance natural polymers complex functioning because by adding the structural benefits of synthetic materials, the biochemical characteristic of natural polymers can be employed further[16]. These materials, which have hybrid characteristics, have been proven to possess a great potential in preclinical applications and, a very important milestone in reliable dural regeneration in the clinical environment[17].

1.2 Anatomy of Dura Mater

The dura mater is the hard outermost layer of the meninges that has a protective layer around the brain and spinal cord in the central nervous system (CNS)[18]. The cranial dura is structurally organized into two layers, one of which is an outer periosteal sheet that is against and absorbed into the inner surface of the skull and another inner meningeal sheet that is against and absorbed into the brain[19]. The innermost layer is relatively smaller and the periosteal layer is twice as the periosteum of the skull and it forms a good attachment to the bone[20]. These two layers are fused in most of the areas but they differentiate at certain locations to constitute the dural venous sinuses which are special vascular channels of conducting the venous drainage of the brain[21]. Histologically, the cranial dura is composed mostly of collagenous bundles belonging to collagen interspersed with elastic fibers and fibroblasts[22]. The fiber arrangement varies between the layers and in the upper layers, there is a greater amount of elastin that appears and in the lower strata, there is greater concentration of collagen. The dura has high tensile strength due to the longitudinal orientation of the collagen fibrils, and the resilience and stretching and mechanical stress resistance of the dura is attained by the presence of elastin fibers. Combined, this composite design gives it rigidity and flexibility, which are important in its protection purposes[23]. The spinal dura mater, however, has one layer and meets at the cranial sheet of mesenchymal. It descends to the second sacral vertebra, and gains sharpness as it passes to the lumbar region, and proceeds to wrap up the final filament until it is attached to the coccyx[24].The epidural space separates the spinal dura and the vertebral canal, and is found to contain connective tissue, adipose tissue, venous networks, lymphatic vessels, and roots of spinal nerves. This is a particularly significant space clinically because it is the point of epidural anesthesia[25]. In addition to a barrier action, the dura plays an important role in the physiology of cerebrospinal fluid (CSF). It envelops the CSF, sustaining circulation, absorption and pressure dynamics, which are required to ensure neural homeostasis and allow physiological fluctuation[26].

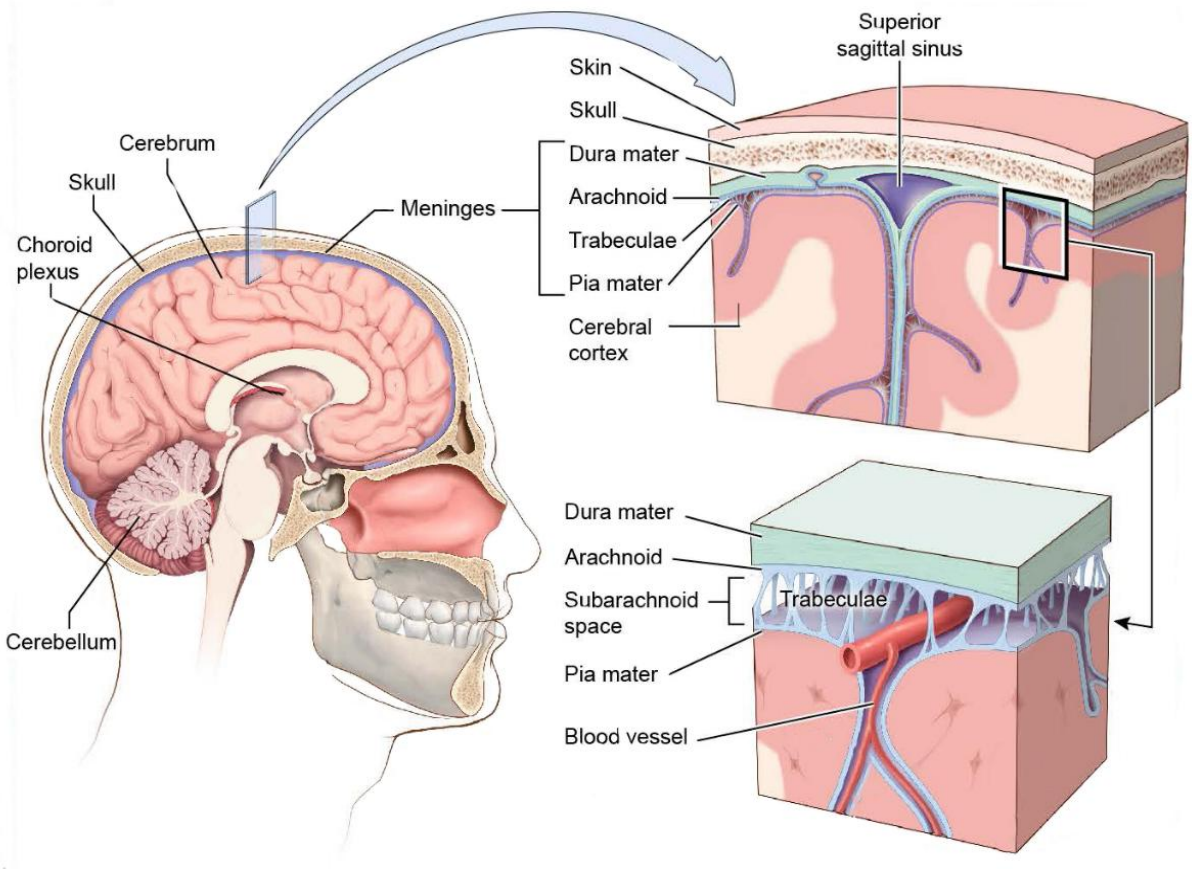

Figure 1. 1Anatomy of Dura Mater [27]

Moreover, the dura has a vascular supply, especially in the periosteal part, which is sufficient in blood delivery. The average thickness of the human dura is about 1.06 ± 0.22 mm but there are some regional differences based on physiological conditions and the site of the anatomy[27].

1.3 Function of Dura Mater:

The dura mater of central nervous system is known to be a viscoelastic connective tissue, which can withstand physiological loads like bending, stretching and compression[28]. This feature allows it to serve as a mechanical buffer to shield the neural structures against strain-related damage during normal movement and mechanical loading. In addition to the mechanical support, the dura acts as a primary biological barrier that allows it to protect against infections and reduce the likelihood of secondary complications[29]. An essential

role played by the dura is that it is used in the maintenance of cerebrospinal fluid (CSF) homeostasis[30]. The dura ensures a regulated environment, which cushions the brain and spinal cord, absorbing the external shocks and alleviating the effect of the mechanical force impact by enclosing the CSF in a closed compartment. The critical role of this role is maintaining the fine structure and functioning of the CNS[31].Also, the dura is essential in blood circulation to the brain. It directs the blood flow out of the brain to the heart through the dural venous sinuses, which is part of an efficient venous flow. By this bilateral action of the preservation of CSF dynamics and the sustenance of the venous blood circulation. The dura mater helps stabilize intracranial pressure, which is imperative to normal neurologic functioning.

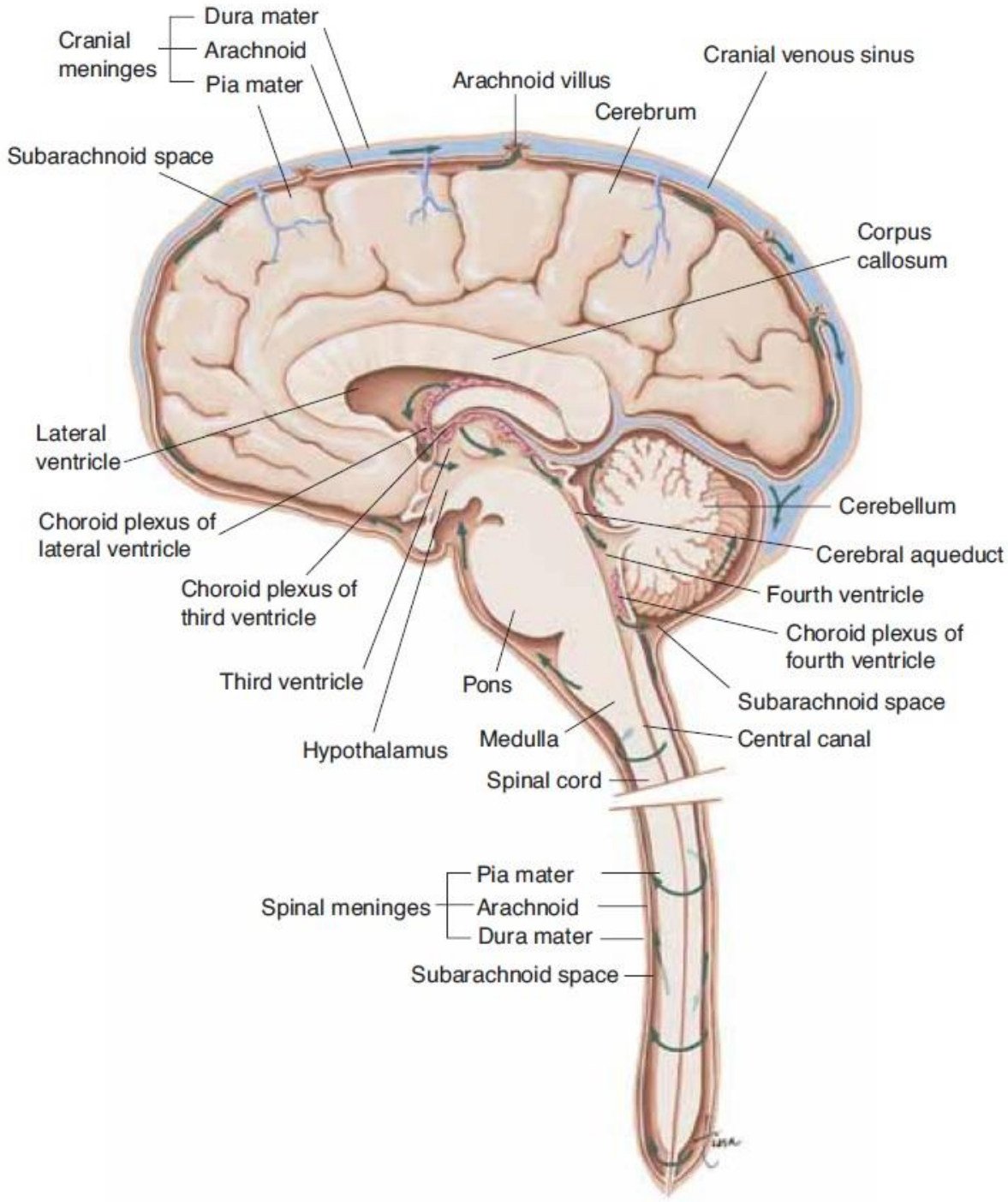

Figure 1. 2 Magnified views of structure of meninges-dura mater, arachnoid mater, pia mater [33]

1.4 Origins of Dural defects:

The dura mater defects can be caused by various conditions, such as traumatic brain injury, tumor infiltration, congenital anomalies, iatrogenic damages, inflammation and cerebrospinal disorders[32]. These defects are also likely to be experienced after neurosurgical practice as they have the potential to cause severe postoperative issues. According to them, dural tears are categorized as acute or chronic, and primary or secondary, and may either happen during surgery or happen by accident[33].Deliberate exposures of the dura are normally done in neurosurgical or spinal surgery to diagnose or treat a condition like tumor removal, lumbar puncture, intradural biopsy, or the placement of a shunt. Conversely, traumatic brain or spinal cord injuries cause accidental tears the most frequently[34]. There is clinical evidence that lumbar surgeries correlate with increased incidences of dural rupture as opposed to other neurosurgical procedures. Irrespective of etiology, dural compromise may have disastrous outcomes, such as CSF leakage, intracranial or spinal infection, meningitis, pseudo meningocele, epilepsy, seizure, and brain swelling. Such complications lead to a high risk of morbidity and mortality and thus urgent watertight dural closure is a dire need[35]. Small dural lacerations can be normally treated using direct suture. Nonetheless, sometimes it is necessary to resort to direct repair in case of larger defects, and dural substitutes must be used. These substances are used to maintain the watertight space between the dura as well as to curb the injury extension to the adjacent tissues[36]. A perfect dural substitute should be constructed to interlace with native tissue and to degrade to the same rate as the natural dura mater regeneration, thus facilitating successful healing and functional long-term recovery[37].

1.5 Classical Approaches to Dural Closure

Watertight dura mater closure is essential for preventing CSF leaks. Sealants, hydrogels, sutures, and dural replacements are among the several repair methods for dural material that have been used up to this point[38].

1.5.1 Sealants:

Sealants are used to guarantee watertight dural closure either following primary closure or in combination with dural replacements[39]. However, recent systematic reviews have

found that the incidence of CSF leaking after cranial and spinal surgery is not reduced by realistically used sealants. An ex vivo model was created to assess the effectiveness of majority of clinically administered sealants scientifically and methodically. This concept states that majority of current sealants either detach from dura mater under long-term physiological conditions or are unable to tolerate the intercranial pressure of the human brain (16 mmHg). Consequently, to prevent CSF leaks, a trustworthy dural sealant is needed[40].

1.5.2 Hydrogels:

Gelatin, collagen, and egg white sponges are examples of biological hydrogel materials that are occasionally utilized for dural sealings; however, they also have disadvantages, such as poor adherence in significant inflammation, rapid breakdown, a fluid environment, and prolonged preparation[41].

1.5.3 Sutures:

Direct suture was the most frequently utilized dural closure approach during CNS surgery; but conceptually, it was challenging to ensure watertight closure because of minute pinholes created by suture needles, and sewing the dura thereafter is extremely difficult[42].

Leakage of CSF fluid during anterior cervical treatments. Furthermore, if a dural tear or defect develops at the nerve root branch or on the ventral dural side, suturing might not be an option. Sutureless dural defects seemed promising because they could drastically cut down on operation time, surgical risks, and difficulties associated with sutural pinholes without requiring time-consuming, labor-intensive suturing procedures. This was due to the widespread prevalence of dural defects and the high demand for immediate waterproof closure during CNS surgery[43].

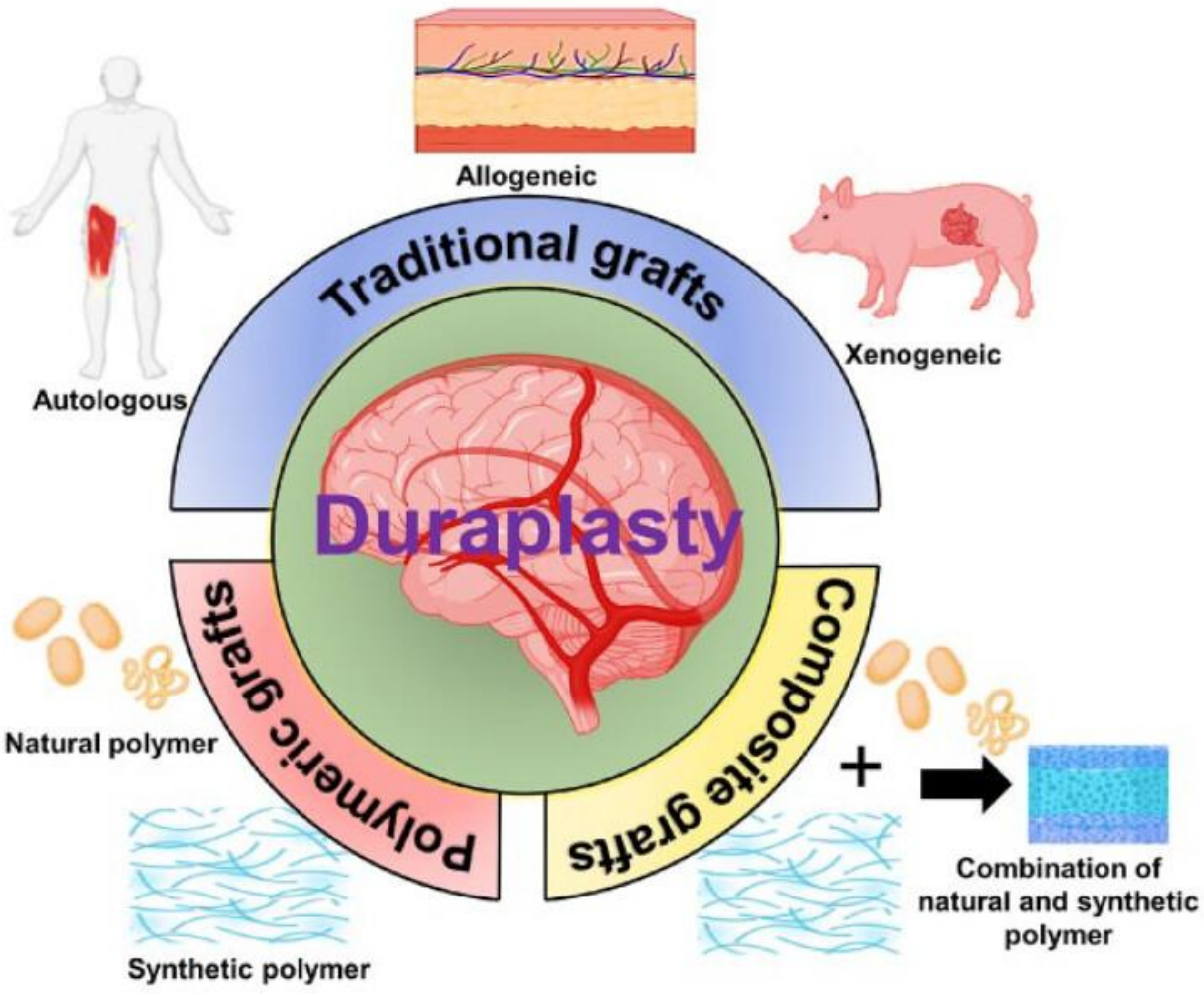

Figure 1. 3 Classical Approaches to Dural Closure [45]

1.6 Categories of Dural Repair Materials:

The main types of dural repair materials accessible nowadays are:

(1) homologous, (2) acellular, (3) natural, (4) synthetic, and (5) composite.

1.6.1 Homologous materials:

Due to their biocompatibility and resemblance to native dura mater, autografts and allografts collectively referred to as homologous materials which are frequently utilized

for dural repair[44]. Because autografts are non-toxic, non-immunogenic, and integrate well with host tissue, they are regarded as perfect replacements. Examples of these include fascia lata and pericranium[45]. Although it necessitates further surgery and may result in donor-site difficulties, fascia lata is the most frequently employed because of its flexibility, vascularization, and efficacy in preventing CSF leakage[46]. Although the pericranium has the benefit of being harvested during craniotomy, which shortens the surgical time, its applicability for big abnormalities is limited by its small size and poor handling characteristics. The amniotic membrane (AM), one of the allografts, has acquired popularity recently due to its anti-inflammatory properties, non-immunogenicity, and capacity to stimulate collagen remodeling and epithelial cell proliferation[47]. According to clinical research, AM successfully reduces scarring, stops CSF leaking, and blends in well with the native dura without any negative side effects[48]. Although more extensive clinical research is required to validate these results, comparative results indicate that AM may offer better dural closure and lower complication rates when compared to conventional autografts[49].

1.6.2 Acellular materials:

Acellular materials are good dural substitutes since they retain the biological composition and natural 3D morphology of tissues produced through the process of decellularization, crosslinking, or freezing-drying[50]. The pericardium, dermis, and small intestine submucosa (SIS) are common donors and are recognized for their mechanical strength, bioactivity, and biocompatibility with native dura mater. Although glutaraldehyde treatment resulted in calcification, the bovine pericardium was the first FDA-approved acellular graft, leading to improved non-processed variants[51]. Acellular dermal matrices, such as AlloDerm, integrate well with natural dura and promote collagen production, cell adhesion, and migration. Similarly, SIS speeds up tissue healing by encouraging collagen deposition and fibrocyte proliferation[52].

1.6. 3 Natural materials:

1.6.3.1 Collagen

Since collagen-based materials are highly biocompatible and have minimal antigenicity, they are among the best natural alternatives for dural repair[53]. Collagen sponges were

originally used therapeutically by James in 1978, and their effectiveness has been confirmed by numerous experimental and clinical trials. Commercially available products such as DuraGen, TissuDura, and Durepair are produced from horse or bovine origins. Because it is flexible and has mechanical qualities similar to human dura, durepair which is derived from fetal bovine dermis is valued for use in high cerebrospinal fluid (CSF) pressure areas[54]. Although irregular CSF leakage has been reported, DuraGen, which is made from the type I collagen of the bovine Achilles tendon, works as a "onlay" graft that makes application easier. Because of its lamellar, nonporous structure, TissuDura which is made from equine collagen displays exceptional elasticity, adhesion, and watertightness and is safe for clinical usage[55]. Recent developments concentrate on hybrid collagen systems that improve hemostasis and watertight closure in neurosurgical applications, such as TachoSil, a collagen fleece coated in fibrin.

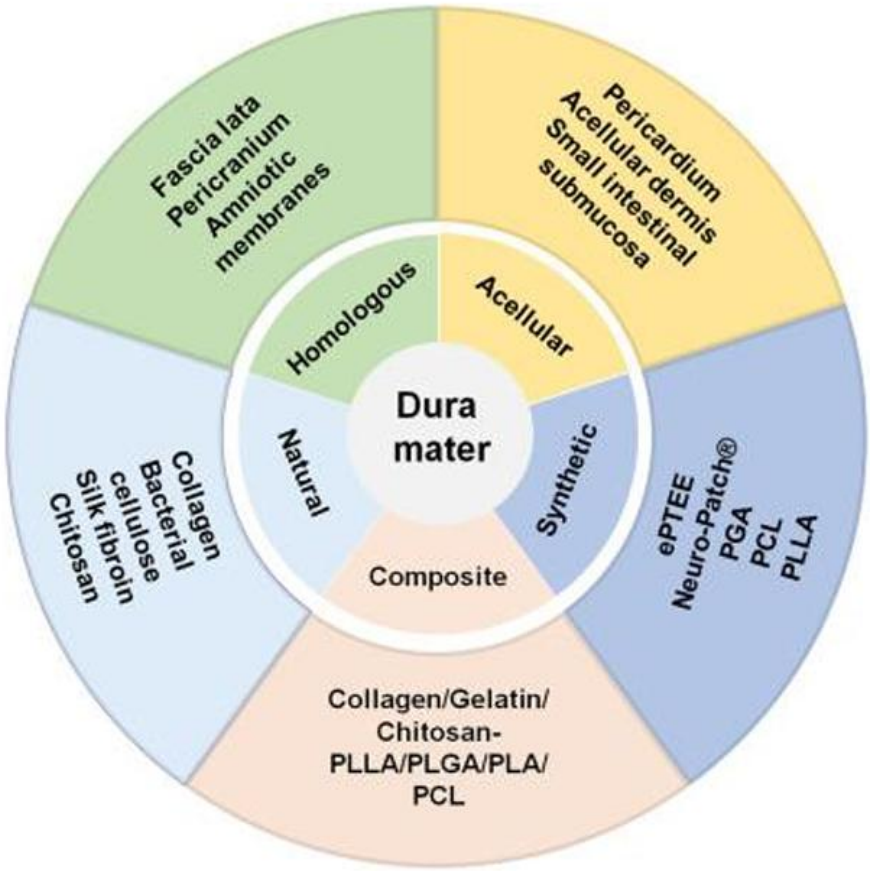

Figure 1. 4 Classification of materials used for dural repair [57]

1.6.3.2 Other natural materials:

A few natural polymers have shown promise as dural repair materials because of their mechanical qualities and biocompatibility[56]. Due to their great biocompatibility, cost-effective manufacturing, and exceptional strength in damp environments, bacterial cellulose (BC) membranes are feasible choices for dural replacements. Animal models like rats have demonstrated that silk fibroin (SF), which is well-known for its regulated degradability and mechanical behavior similar to that of natural dura mater, can tolerate high CSF pressures while reducing cytotoxicity and inflammation[57]. The biodegradability and antimicrobial qualities of chitosan (CS) have drawn attention to applications involving the central nervous system. Researchers have found that bilayer chitosan scaffolds (BChS) can achieve watertight dural closure without CSF leaking, inhibit microbial growth, encourage fibroblast regeneration, and degrade at the right rates[58].

1.6.4 Synthetic materials:

Disadvantages of most naturally occurring materials include intra-production batch variability, rapid exponential degradation, and a lack of mechanical strength[59]. This increases the demand of synthetic versions which are easy to fabricate, can be shaped to different forms and provide controllable mechanical and degradation characteristics. Besides, such synthetic materials tend to be more affordable compared to the natural ones. They are categorized into two broad groups, namely non-biodegradable and biodegradable materials based on the capacity to degrade in the body[60].

1.6.4.1 non-biodegradable materials:

Contaminated bags: These bags contain non-biodegradable materials that cannot be recycled or disposed of, thus producing pollution. These bags have non-biodegradable materials that cannot be reused or discarded, creating pollution. Expanded polytetrafluoroethylene (ePTFE) and polyethylene (PE) are used commonly as non-absorbable synthetic materials in the process of dural reconstruction since they are highly inert and biocompatible and can be worked under mild conditions that do not harm the cellular environment[61]. It has been established through clinical examinations after decompressive craniectomy that the ePTFE is effective in restoring dural structural

integrity and curbing the leakage of cerebrospinal fluid (CSF) as well as not causing any unwanted tissue reactions[62]. On the same note, PE has good structural stability and degradation resistance, hence, long-term stability in dural repair procedures[63]. This drawback can be addressed by modifying the surface and/or by incorporating bioactive nanocomposites like MOFs conjugated with PCL to improve biocompatibility, cellular response, as well as regenerative capacity in general[64].

1.6.4.2 Biodegradable materials:

Three major biodegradable polymers polyglycolic acid (PGA), [65]polycaprolactone (PCL) and poly (L-lactic acid) (PLLA) are typically used to repair damaged dura mater[66]. One of them, PGA mesh, has been widely used in the Japanese clinical practice in repairing the dural defects following the spine surgery and is recognized as a human synthetic dural substitute. Nevertheless, it still has questionable clinical performance[67]. Although there are studies which prove that PGA shows high tensile strength and prevents cerebrospinal fluid (CSF) leakage without causing inflammatory/adhesive reactions, there are other clinical results which also prove that PGA results in complications like infection, granuloma formation and postoperative CSF leakage. Thus, additional long-term research is to be conducted to determine the safety and efficacy of PGA-based materials to the full extent[68]. Polycaprolactone (PCL), however, is a biodegradable semicrystalline polyester that is FDA approved, and has been known to exhibit strong biocompatibility, regulated degradation, and positive mechanical characteristics[69]. It has been demonstrated in experiments that the dural fibroblasts grown on PCL membranes can synthesize type I collagen, and the grafts made of PCL can be used in dural reconstruction without inflammation and scarring. Though synthetic polymers which include PCL and PLLA demonstrated encouraging outcomes in earlier experiments, they usually do not have enough biological stimuli to comprehensively direct and improve the natural regeneration of the dural tissue[70].

1.6.5 Composite materials:

The drawbacks that are involved in the application of single-component materials can be overcome successfully by the creation of composite materials[71]. These composites are prepared by a meticulous mixing of two or more constituents to maximize the composition

and structural properties leading to enhanced dural tissue regeneration and remodeling. In most cases, these materials combine the favorable properties of natural and synthetic polymers[72]. In this regard, Ti-Ce-based metal-organic frameworks (MOFs) coupled with polycaprolactone (PCL) are one of the potentially successful composite systems[73]. It is the constructive interaction of these components structurally and chemically that improves the mechanical integrity and also biological functionality which results into better dural tissue regeneration and remodeling. Ti-Ce MOFs in such composites add a high level of mechanical strength, surface activity and ion release control, capable of inducing cell differentiation and tissue mineralization, alongside PCL providing better biocompatibility, biodegradability and biomimicking of native dura mater mechanical properties[74]. Such hybrid system offers an apt environment to fibroblast adhesion, growth and collagen production that is essential to the healing success of the dural. In addition, the Ti-Ce MOF/PCL composite has shown the possibility of maintaining water tight closure, reduce cerebrospinal fluid (CSF) leakage and inflammatory or immune response thus a safe and long term integration of the tissue[75]. The promising outlook to this novel combination, despite ongoing preclinical experiments is that this next generation biomimetic dural substitute has a high potential of not only being a mechanical durable material but a bioactive regenerative one as well[76].

1.7 Tissue Engineering:

Tissue engineering is a high technology biomedical technology which is used in repairing, regenerating and replacement of spoilt or diseased tissues and organs [77]. It has demonstrated amazing success in healing soft and hard tissues including those of the heart, skin, and bone, and it has been used to repair congenital defects. It is a discipline that integrates knowledge and science in medicine, biology, and engineering into an interdisciplinary model to repair or improve the functional capability of tissues [78]. To ensure the best outcomes of tissue engineering, the constructs developed should be able to integrate cells, scaffold and bioactive molecules (growth factors) [79]. These elements collaborate to produce biomimetic environment promoting cellular growth, differentiation and tissue regeneration which eventually becomes or replaces the native tissue. There are three principal strategies to therapeutic process in tissue engineering[80]. Scaffolds or

growth factors are placed directly over the area of injury in situ tissue regeneration to activate the natural repair processes in the body. Cell implantation whereby cultured cells are implanted in the injured area to enhance healing. Tissue construct implantation, in which a ready-made scaffold load with cells is implanted to replace the area that has been damaged. Early intervention in the first phase with the use of bioactive scaffolds or growth factors is important in that it promotes the growth of native cells, stimulates repair mechanisms, and regenerates functional tissue [81].

1.7.1 Scaffolds for Tissue Engineering:

A major approach in the manipulation of artificial tissues and organs has been to construct in vitro cell cultures on a three-dimensional (3D) scaffold that recapitulates the structure and function of the extracellular matrix (ECM) present in natural tissues [82]. Over the years, a number of methods of fabrication have been developed in order to make 3D scaffolds which are important in sustaining cell adhesion, migration, growth and differentiation. The perfect scaffold must be mechanically stable enough to support its structure throughout the formation of new tissues, in addition to enabling cell attachment, proliferation and survival[83]. It should also support the differentiation of the cell as well as provide a microenvironment that resembles the physiological conditions required to develop native tissues. The degradation of the scaffold upon regeneration should occur in a controlled fashion, as the new tissue is developing, so that by the time that the tissue is fully formed, it is able to substitute the artificial structure smoothly [84].

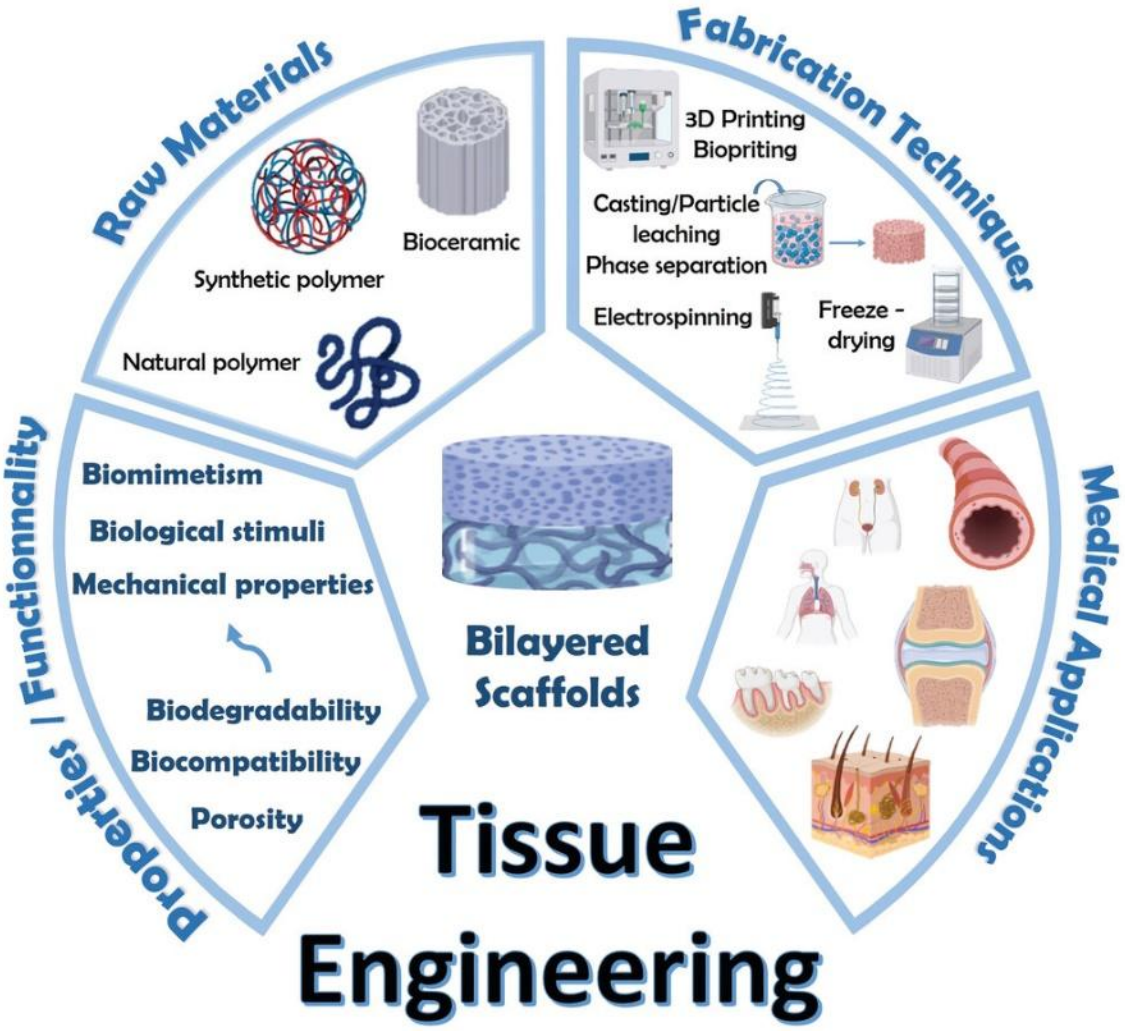

Figure 1. 5 Bilayered Scaffold with tissue engineering [86]

1.7.2 Physiochemical and biochemical properties of Tissue Engineering Scaffolds:

It is also important to note that scaffold is necessary to offer mechanical stability as well as create a good biological environment that supports cell growth and functioning [85]. They guarantee a sufficient provision of oxygen and nutrients, the elimination of waste and the maintenance of the conditions that preserve the viability of cells and the organization of tissues [86]. The 3-dimensional (3D) structure of the scaffolds is required to enable the cells to adhere, proliferate and develop into structured tissue frameworks. Ideally, the cells

in question should synthesize the extracellular matrix (ECM), which then will proceed to biodegrade the scaffold, and create an effective 3D microarchitecture within the regenerating tissue [87]. The choice and functionality of scaffolds materials are dependent on a number of factors that include composition, fabrication method, and the use of the material in the tissue [88]. A perfect scaffold must have a high level of biocompatibility, controlled biodegradability, and mechanical strength, high porosity, high surface area, neutral pH, and physicochemical properties to support cellular activities and tissue remodeling. These properties are directly influenced [89]. An example is that electrospinning can be a very efficient method of making scaffolds of fine fibrous networks, high flexibility, high surface area and cellular interconnecting pores, it is especially useful in soft tissue regeneration like repair of the dura mater [90]. Conversely, freeze-drying has the benefit of producing highly porous and homogenous structures through the sublimation of ice crystals of frozen polymer solutions and this forms a light weight biocompatible matrix that can be used in soft and hard tissue applications [91].

1.7.3 Biomaterials for Scaffold Fabrication:

The scaffold material is bio-compatible tissue and can be grown in the desired shape under desired bio-environment (Clugston, 2004). Researchers over the years have been working tirelessly to ensure that a clear and universally acceptable definition of biomaterials is attained [92]. Since that time various interpretations have developed to develop this concept [93]. Williams was the first to give one of the most broad definitions of a biomaterial, defining it as a substance that has been designed and manipulated to a particular form that either acting alone or as a part of a larger system, interacts with the biological components to guide the path of a therapeutic or diagnostic process in humans or animals [94]. Generally, biomaterials can be divided into two major groups: bioinert materials which are not degraded when placed in the body and biodegradable materials which are supposed to break down and be replaced by the natural tissue in the process of healing [95].

1.7.3.1 Bioinert Materials:

Bioinert materials do not degrade and do not have a radical chemical reaction with the surrounding tissues after implantation preserving their structural stability [96].

1.7.3.2 Biodegradable Materials:

On the contrary, biodegradable biomaterials decompose slowly into metabolic by-products upon exposure to biological fluids during tissue repair [97]. The products of this degradation can be readily metabolized and removed by the body enabling the body to gradually substitute the implanted material [98].

1.7.3.3 Bioactive Materials:

The third group is called bioactive materials, which are aimed at active interaction between the biological systems and the material. Active or inert type of material is determined by the type of clinical use. The use of bioactive scaffolds has become a subject of attention in the recent past due to the ability to induce numerous biochemical and biophysical reactions at the implant-host tissue interface. These scaffolds can be improved and fastened by adding growth factors and other biological agents that can improve and speed up tissue regeneration [99]. In case bioactive materials met blood and other body fluids, they trigger certain immune and cellular reactions. Proteins, carbohydrates or even enzymes can be attached to their surfaces, which allows this biological activity to be controlled to allow a controlled host reaction [100]. The knowledge of how physical and chemical properties of biomaterials affect biological organization on the differing levels of molecules to tissues is an important scientific challenge. In order to overcome this, studies in the area usually take three major directions [101].Looking into the connection between the biological structure and functionality of biomaterials. Integrating empirical and theoretical research to understand the physical and chemical processes behind this relation and use them to materials science and engineering. The creation of biomimetic materials that can mimic natural biological processes and at the same time be scientifically feasible and cost effective. There are three major approaches to bioactive biomaterials engineering[102]. Altering the surface of the material using components like extracellular matrix molecules, bio adhesive macromolecules or certain binding components. Designing and uniformity of the material on the nanoscale so it can be more reminiscent of natural biological designs.

Scaffolds may be fabricated using a few fabrication methods including solvent casting, freeze drying, freeze gelation, particle leaching, gas foaming, thermally induced phase separation, stereolithography and rapid prototyping[103].

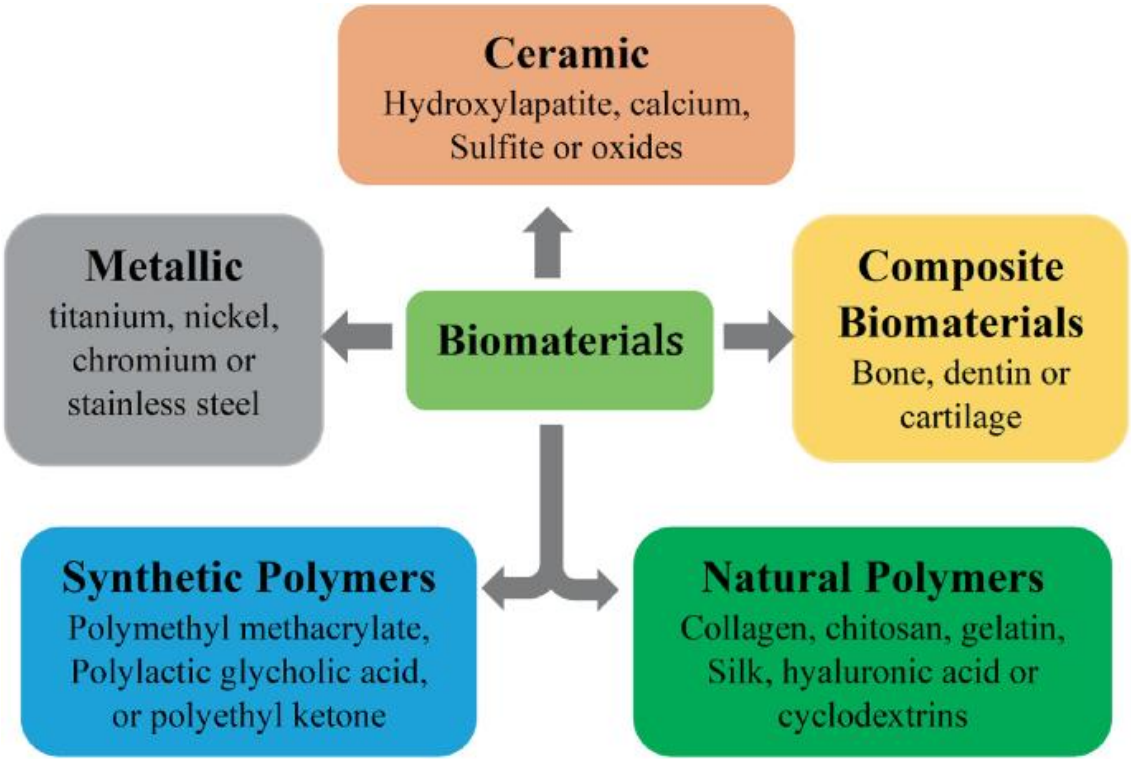

Figure 1. 6 Biomaterials with tissue engineering [104]

1.8 Scaffold Manufacturing Techniques:

All these ways have certain limitations. Electrospinning is an alternative to the traditional methods since technology has made it superior to other methods because of its capacity to produce fibers that are highly flexible, adaptive and cost-effective[104].

i)1.8.1 Electrospinning:

Electrospinning is a universal methodology of forming an incessant nanofiber with a diameter between the submicron and the nanometer by utilizing a voltage electric field[104, 105]. This has made the resulting e-spun (e-spun) fibers and their respective nonwoven mats of great interest because of their outstanding properties namely: high porosity, small fiber diameter, good pore connectivity and high surface-area-to-volume ratio. Due to these favorable characteristics, a great variety of natural and synthetic single and mixed polymers

have been successfully Electrospun into single fibers with diverse uses. In the electrospinning technique, a high electric field is employed on a melt or a solution of a polymer, and the solutions turn into nanoscale fibers [107]. This process, therefore, enhances better cell attachment, growth, specialization, and movement. Proteins, drugs and DNA can be introduced through bioactive agents in an environment which facilitates effective exchange of oxygen and nutrients and at the same time allows elimination of metabolic wastes[108]. These have uses in the areas of filtration, thermal insulation, protective fabrics, sensors, conductor materials, wound dressings, and tissue engineering scaffolds[109].

Figure 1. 7 Electrospinning setup

1.8.1.1 Fundamental principle of Electro spinning:

Electrospinning entails applying high voltage on a polymer solution or melt between a pair of oppositely charged electrodes such that an electric field is created, which extends the polymer to fine fibers. The system normally consists of (i) power source, (ii)syringe pump, (iii)metallic nozzle, and collector. When the polymer droplet with electric charge develops a Taylor cone, the electrostatic forces are stronger than the surface tension and a thin jet of the droplet will be thrown out, extending itself by whipping movements. As the solvent evaporates, the polymer casts itself in the form of continuous fibers on the collector when the solvent is in the air. The structure of the final fiber is variable to parameters like the strength of the electric field, flow rate and the properties of the solution[110].

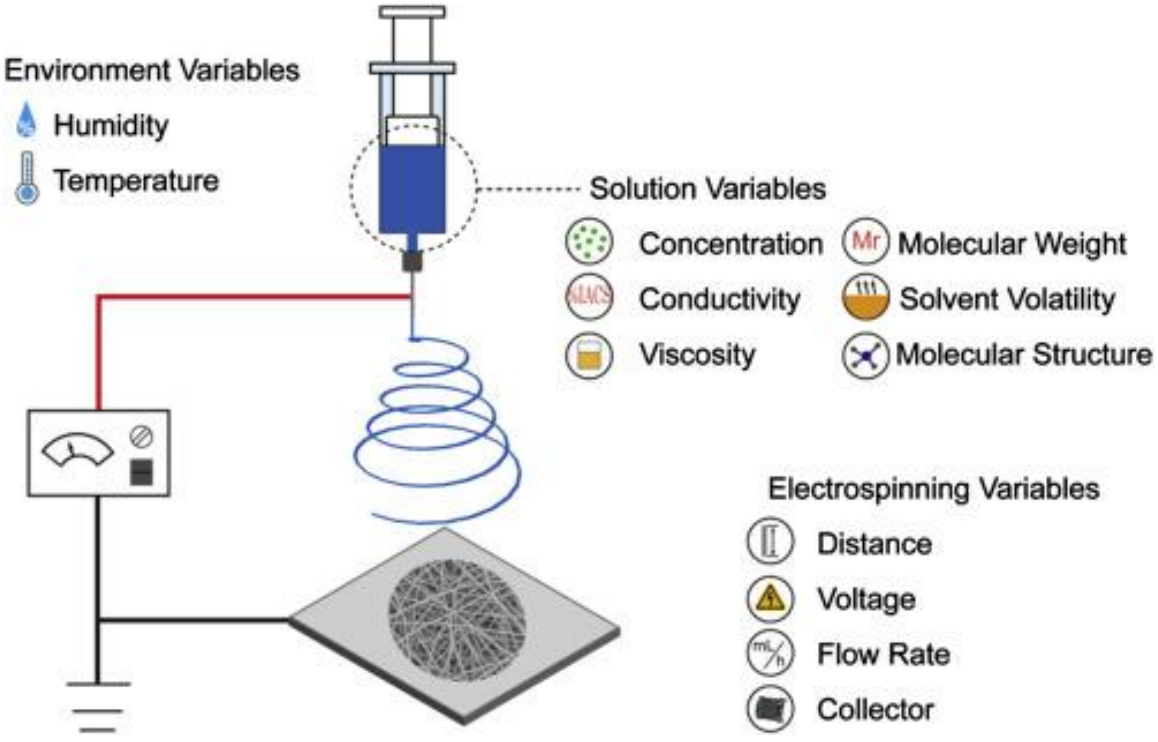

Figure 1. 8 Electrospinning set up with parameters [112]

ii) 1.8.2 Freeze drying:

Freeze-drying is the process includes freezing the substance, reducing the pressure around the substance and then freezing the water by transferring it through the process of sublimation in which the ice turns into vapor without passing through liquid states[111]. This technology is very common in the biomedical industry as it prolongs the life of products and does not harm their structural and functional properties. It is mainly useful in the stabilization of compounds like proteins, peptides, antibiotics, vaccines and liposomes[112]. In addition, freeze-drying has emerged as one of the most common methods of preparing the modern drug delivery systems such as polymeric nanoparticles, liposomes and microspheres and in preparation of highly porous 3D scaffolds that find application in tissue engineering[113].

Figure 1. 9 Freeze drying Setup

1.8.2.1 Fundamental Principle of freeze drying:

Freeze-drying is a process that is multi-step, comprising of freezing: (i) primary drying ii) and secondary drying, and each of them is a critical determinant of the quality and structure of the product. At the freezing stage, the material is cooled to a lower temperature than its freezing point to cause the ice to start solidifying and crystals to develop. This step defines the interior design of the commodity. Freezing at low temperatures under the eutectic temperature (in crystalline systems) or glass transition temperature (in amorphous systems) is necessary to prevent any freezing of the solution[114]. Cooling rate, supercooling and ice nucleation temperature are some of the factors that have a great impact on the rapid freezing of ice because, ice crystal size is highly determined by the rate of freezing, fast freezing forms small crystals with fine structure, and slow freezing forms large crystals with porous structure. Such methods as annealing, during which the material is clamped between glass and eutectic temperatures, are implemented to improve crystal uniformity and accelerate the process of further drying. In primary drying, a low pressure is used to sublimate frozen water as heat is supplied in a gentle manner. It is important to ensure that the structure of the product is not destroyed; the product temperature is kept at temperatures lower than the collapse temperature (Tc) [114]. This step is important to optimize because it will greatly influence the drying time and energy consumption because increasing the temperature of the product by a few degrees can reduce the process by up to 13 percent. Secondary drying stage is the stage in which it removes the bound or adsorbed water by the process known as desorption, and the drying stage typically has a higher shelf temperature than the first stage. This phase is determined by the rate of drying which is affected by the surface area and the remaining moisture content of the material. This aims at producing a product that has a low water content that is below 1 per cent so that it is stable and structurally sound. Briefly, the porosity, mechanical strength, and preservation quality of the final material of freeze-drying depends on good control of the freezing, sublimation, and desorption conditions during the process[115].

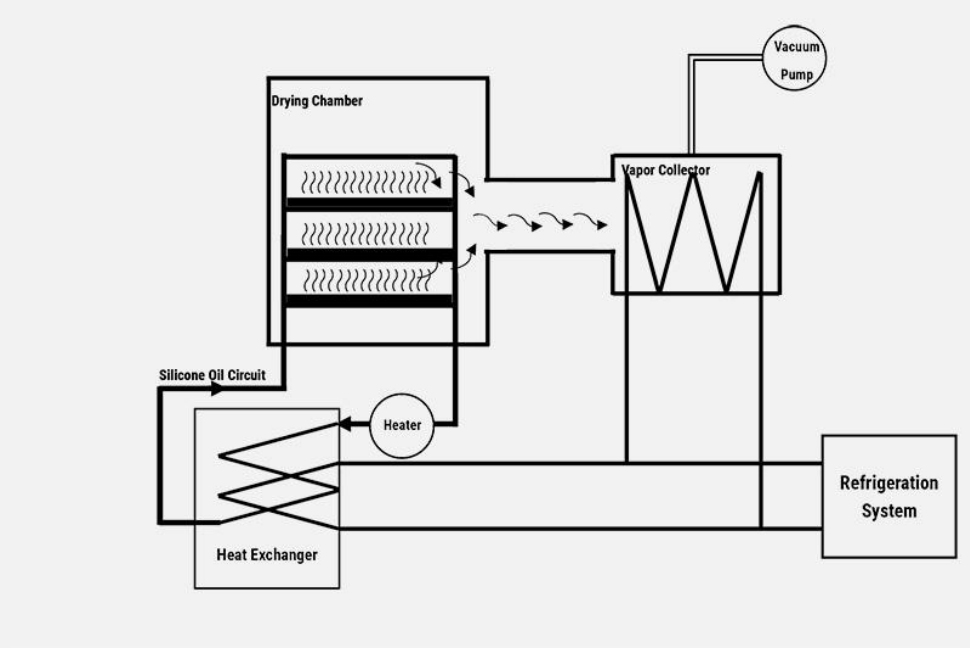

Figure 1. 10 Freeze drying Theory [118]

1.9 Fabrication materials for bi-layered scaffolds:

Some of the biomaterials that have been selected to be fabricated scaffold are; Silk Fibroin (SF), Polycaprolactone (PCL), Metal Organic Frameworks (MOFs), Calcium Magnesium Silicates (CMS).

1.9.1 Silk -A natural Polymer:

Silk is a natural protein polymer, the larvae of different insects, silkworms, mites, spiders, scorpions and fly are used to create silk. It has a significant difference in structure, composition, functional properties, and applications based on the source. Of these, Bombyx mori silk has been the most widely used in biomedical use because of its excellent mechanical strength, high biocompatibility, controlled rate of degradation, and because of its low immunogenicity. Recent studies on silk have found that the main structural element of silk fibroin, which has the following desirable properties that include; optimal water and oxygen permeability, good blood compatibility and the capacity to promote collagen formation and human fibroblast proliferation[116]. Due to these characteristics, silk fibroin

has found a variety of applications in biomedical materials that encompass cell culture platforms, tissue scaffolds, drug delivery platforms, and enzyme immobilization platforms to support cell growth and tissue regeneration[117].

Figure 1. 11 Silk Cocoons from Bombyx mori

1.9.2 Silk: Structural and Chemical Composition

The natural silk fibers are made by the cocoons of the Bombyx mori and it has two primary proteins namely fibroin and sericin. The silk cocoon is usually 75 percent (w/w) fibroin and 25 percent (w/w) sericin. In the silkworm, silk fibroin was produced in the posterior silk glands which produce and store it in the lumen of the middle gland. Epithelial cells of the gland produce sericin, which is a binding agent[118]. The fiber-spinning is a process of obtaining fibroin through the anterior silk gland with the help of the two spinnerets used by the silkworm, that is, the aqueous solution is extruded into the filament in a two-core process. This filament is then covered with sericin, a protein-like substance of glue, which holds the fibers. Silk fibers are of different lengths depending on the strain of B. mori,

which are usually between 1000 and 1500 meters with an average diameter of 10- 20 micrometers (Laoate)[119].

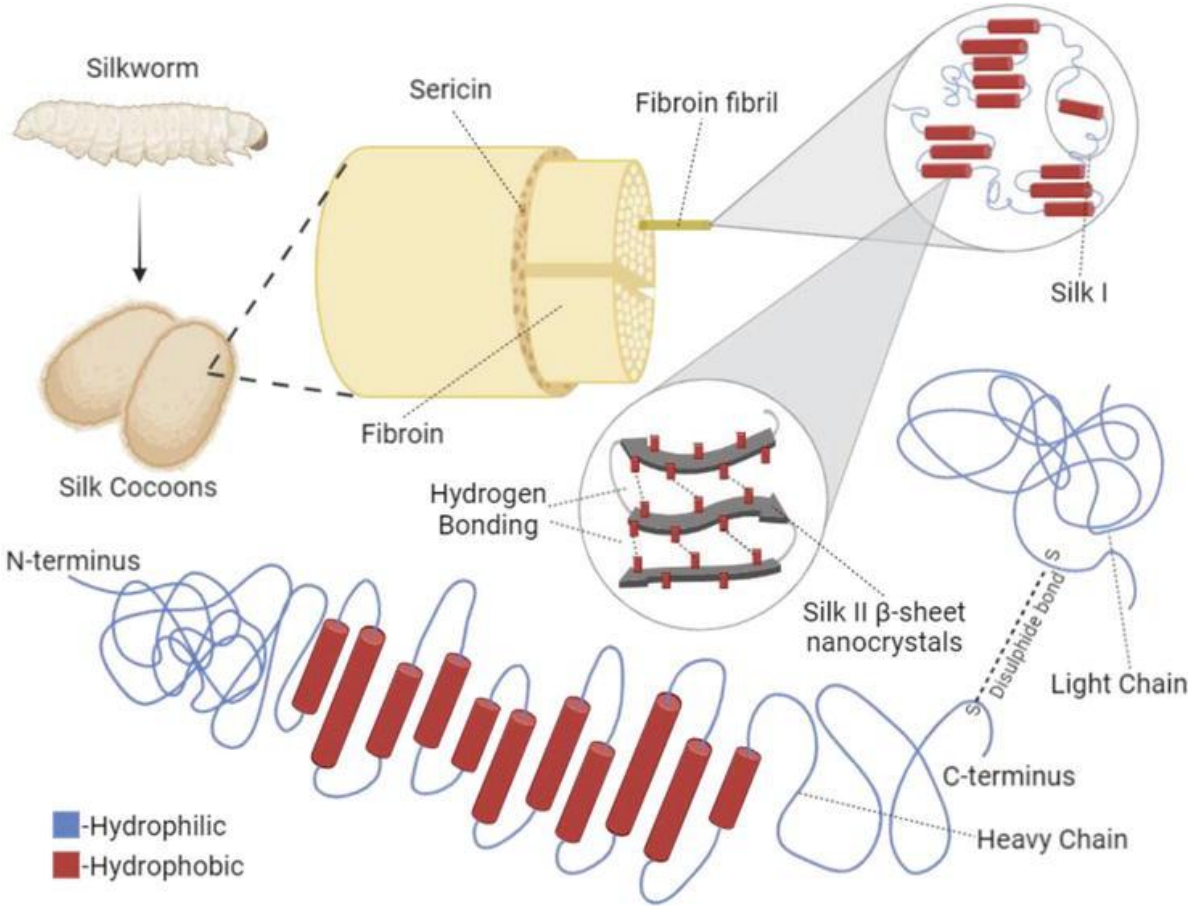

Figure 1. 12 Structure of Silkworm thread [121]

1.9.3 Fibroin Protein:

The Bombyx mori silk fibroin is primarily made up of glycine (43%), alanine (30%), and serine (12%). Fibroin heavy chain has 12 domains with each domain comprising the crystalline areas of silk fiber. These sequences consist of repeating Gly-X repeats with the X being either alanine, serine, threonine or valine. Short repeating units, which make the crystalline parts of silk, like GAGAGS, GAGAGY, and GAGAGA, help to strengthen silk and stabilize it. Interspersed between these crystalline domains are non-repetitive linker regions comprising 42 -44 amino acids, in which the charged residues render them less ordered. The structure of fibroin is hydrophobic and is similar to that of a natural block

copolymer, which assists in making strong and stable fibers. While a disulfide bond connects the heavy and light fibroin chains, this is necessary to make the secretion and formation of silk possible. In the absence of this bond, as in some genetic mutations of B. mori, the cocoon includes a low level of fibroin less than 0.3% and the process of silk production is severely influenced[120].

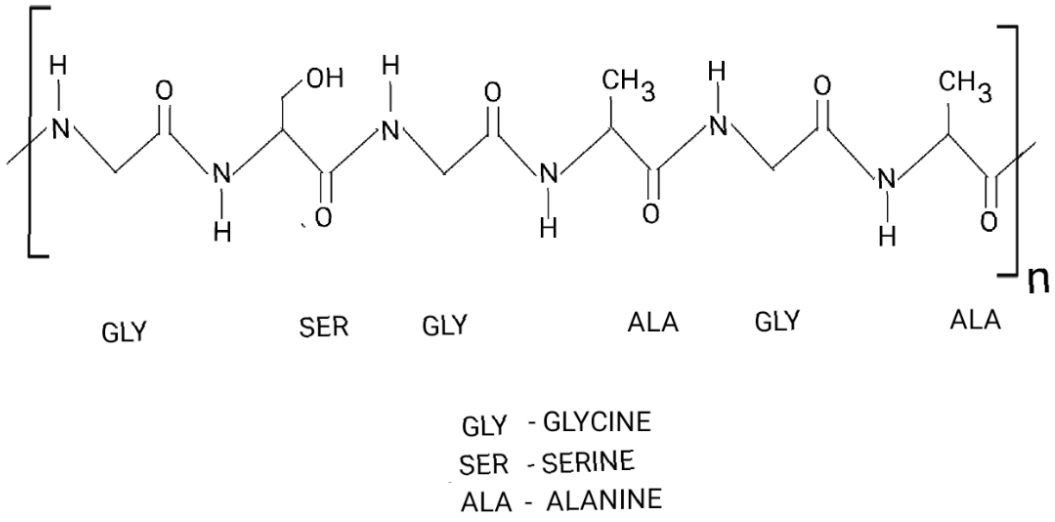

Figure 1. 13 Structure of Silk Fibroin [122]

Fibroin has three structural forms which include amide I, amide II and amide III. The amide-I that I produce is the natural structure of fibroin, obtained naturally as a byproduct of the silk glands of the Bombyx mori. The amide II type has increased tensile strength and is therefore mostly applicable in industry and commercial application[121].In the meantime, the amide III structure is a novel structure, which is mainly produced at the interface of the silk solution during processing. Silk is a material that has a superior mechanical strength and thus it would be a good candidate to be used as a substitute material in tissue engineering. Its ultimate tensile strength ranges from 610 to 690 MPa, which is significantly higher than that of other biopolymers such as collagen (0.9–7.4 MPa) and PLA (28–50 MPa). Similarly, the modulus of silk fibers lies between 15 and 17 GPa, far surpassing that of collagen (0.0018–0.046 GPa) and PLA (1.2–3.0 GPa)[122].

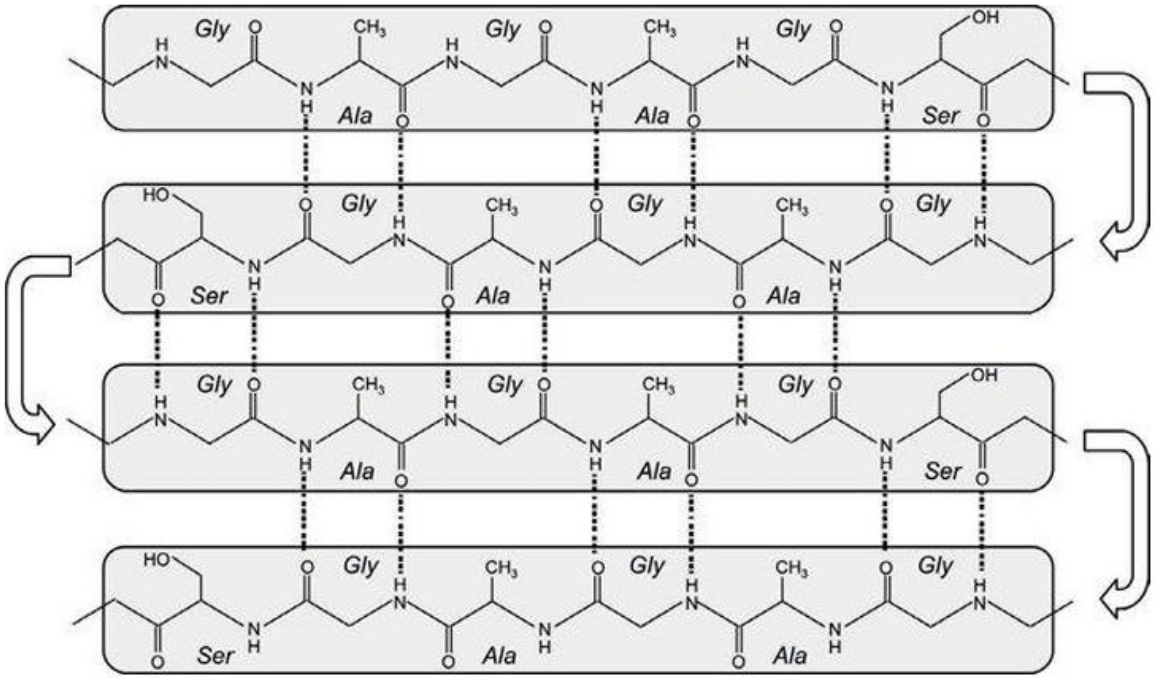

Figure 1. 14 Molecular Crystalline structure of Silk Fibroin [124]

1.9.4 Sericin Protein:

Sericin, the second major glue-like protein found in silk, has a molecular weight ranging from 23 to 400 kDa and belongs to the serine-rich polypeptide family. Variations in the molecular weights of sericin and fibroin arise due to differences in gene expression and post-translational modifications[123]. Sericin is composed of 15 amino acids, with serine (28%), aspartic acid (18%), and glycine (16%) being the most abundant. Based on its location within the middle silk gland of the silkworm, sericin is categorized into three main types[124]:

- Sericin A (≈400 kDa), produced in the anterior region,
- Sericin M (≈250 kDa), secreted in the middle region, and
- Sericin P (≈150 kDa), released from the posterior region.

Additionally, the gland can secrete two smaller sericin variants with molecular weights of approximately 80 kDa and 310 kDa, and in some cases, an even smaller 924 kDa sericin has also been reported[125].

1.9.5 Essential properties of silk fibroin as biomaterial:

Silk has gained significant attention among natural biopolymers due to its remarkable mechanical strength. In addition to this, it offers several other advantages such as controlled biodegradability, ease of processing, excellent biocompatibility, and the presence of reactive chemical groups that allow functional modification. These distinctive properties ensure that silk is better than other allogeneic or xenogeneic biomaterials that are based on proteins, which tend to pose such challenges as increased risks of infection, possible disease transmission, it is not always available, protein separation can be difficult, and purification and processing can be quite costly[126]. Silk has been mostly known as a proven textile fabric and production per year is around 1000 metric tons. Nevertheless, silk constituents have been demonstrated in diverse studies to cause chronic inflammation in vivo and in vitro. To solve this, a process of de-gumming is carried out on sericin, and in most cases the method used is either alkaline or enzymatic depending on the mode used to extract the sericin. Due to the economical conventional methods of processing and its massive scale production, silk has now emerged as a material of clinical research applications that are economical[127]. Solution and fibrous forms of silk fibroin find application in the biomedical field because of its excellent biocompatibility, high mechanical strength and low immunogenicity. The research has shown that different types of cells such as mesenchymal stem cells can be attached, propagated and differentiated on scaffolds composed of silk fibroin, so that they can be utilized in both soft tissue and hard tissue engineering. Slow degradation rate of silk fibroin renders it especially favorable to the regeneration of slow growing tissues, this being one of the reasons why it is considered as being appropriate as a bioresorbable material. Secondly, silk has been approved by the U.S. Food and Drug Administration (FDA) to be used in certain biomedical devices. Since it is amphiphilic and has a versatile processing trait, silk fibroin can be produced in various forms of material including scaffolds, fibers, films, sponges, and hydrogels, which would expand its application in tissue engineering. In the current research, Bombyx mori silk

fibroin was used as a protein-based biopolymer to obtain desirable characteristics, such as low levels of inflammation, low immune response and high biocompatibility[[128].

1.9.6 Poly-ε-caprolactone (PCL)

Poly-caprolactone (PCL) is a biodegradable polyester that was developed by the ring-opening polymerization of 1,5-caprolactone. This polymerization may be done through anionic, cationic, coordination or radical, depending on the catalyst of interest, usually stannous octoate or aluminum alkoxides. The molecular weight and polydispersity of PCL are highly dependent on reaction conditions including temperature, time, concentration of catalysts, and solvent ratio, which has an impact on its mechanical strength and degradation profile. [129].

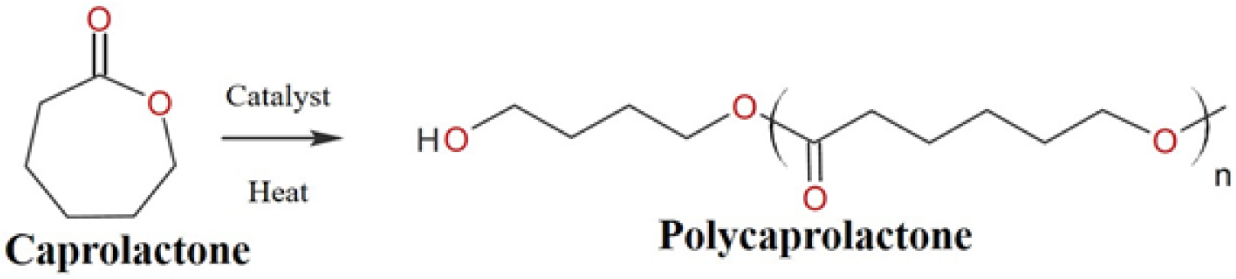

Figure 1.15 Formation of polycaprolactone [131]

PCL is soluble in organic solvents including chloroform, toluene, and dichloromethane, but insoluble in water and alcohols. It is a semicrystalline polymer at both room and body temperature with a temperature of -60˚C at the glass transition temperature and a melting point of approximately 60˚C. The amorphous parts are rubbery at physiological temperature permitting the molecular mobility and increased permeability to metabolites in application to biological systems [130]. The rate at which scaffold materials degrade is also very vital in tissue engineering and must match with the new tissue formation. Compared to polylactides, PCL is less susceptible to degradation due to the presence of fewer ester groups that allow this group to form the molecular structure of the polymer per unit of monomer. Physiological conditions can result in the degradation process, which mainly involves enzymatic hydrolysis by lipase enzymes in the interstitial fluids, and is possible in 23. The degradation rate is affected by factors like molecular weight, geometry, residual monomer content and pH where higher pH yields a higher degradation rate[131].

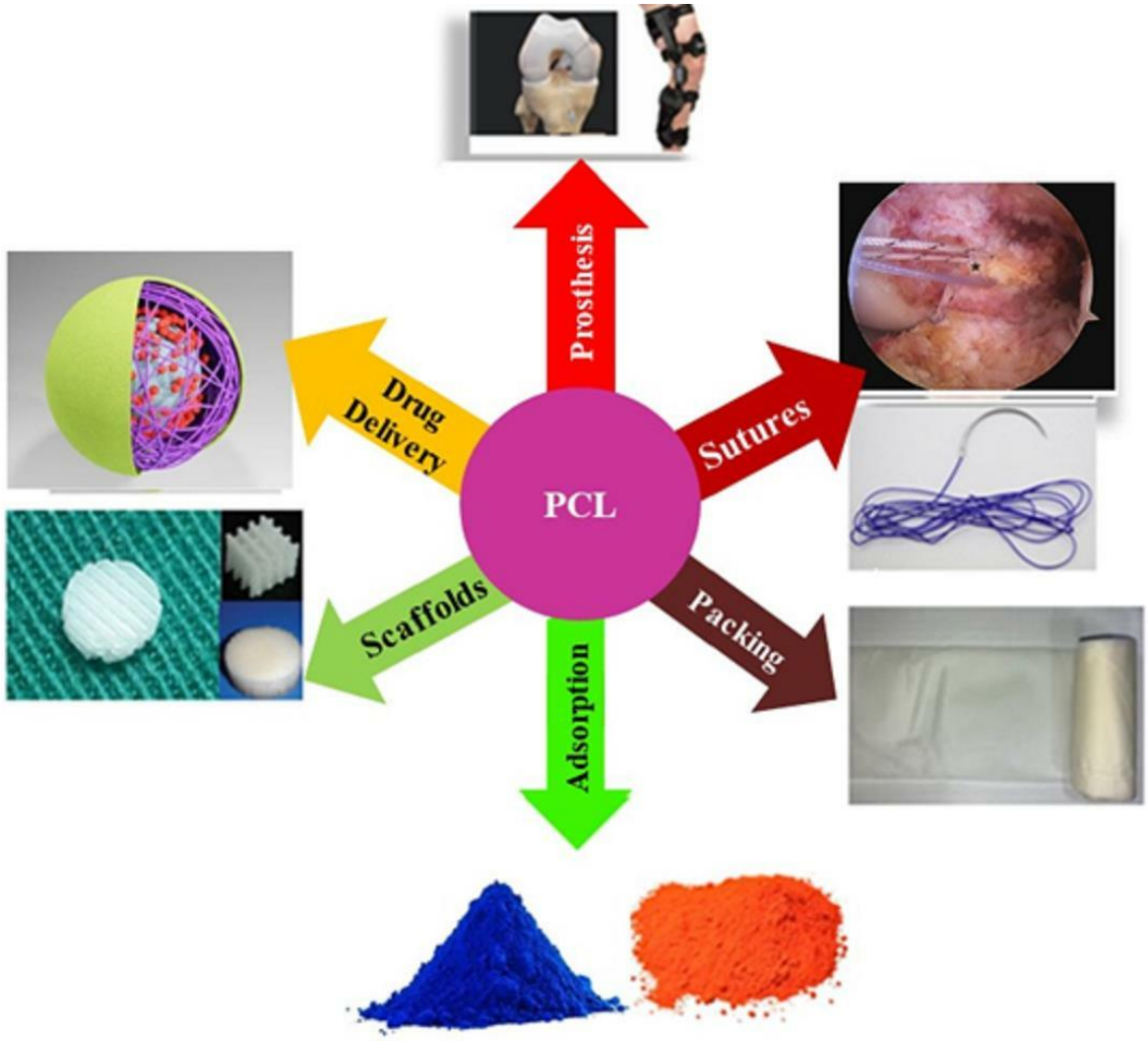

Figure 1.16 Polycaprolactone Composites/Blends and Their Applications [134]

The primary degradation product, 6-hydroxycaproic acid, is processed by means of 6-hydroxycaproic acid by 8-hydroxycaproic acid into acetyl-CoA and excreted through the normal metabolic routes without blocking up in the body. Although intrinsically biocompatibility is relatively low, PCL is praised due to its flexibility, biodegradability which can be fine-tuned, as well as the ability to form blends, composites, and copolymer. These attributes render very applicable in biomedical applications like scaffolds in tissue engineering, bone regeneration, sutures, and drug delivery systems. It is also possible to modify its properties on the surface to increase cell attachment and integration. PCL scaffolds facilitate the growth of mesenchymal stem cells, osteoconduction and new blood

vessel development as well as reduce immune responses in the process of guided tissue regeneration. As an example, the bone regeneration and selective degradation of PCL composites with hydroxyapatite (HA), polyethylene glycol, (PEG) or growth factors like BMP-2 have been improved[132].

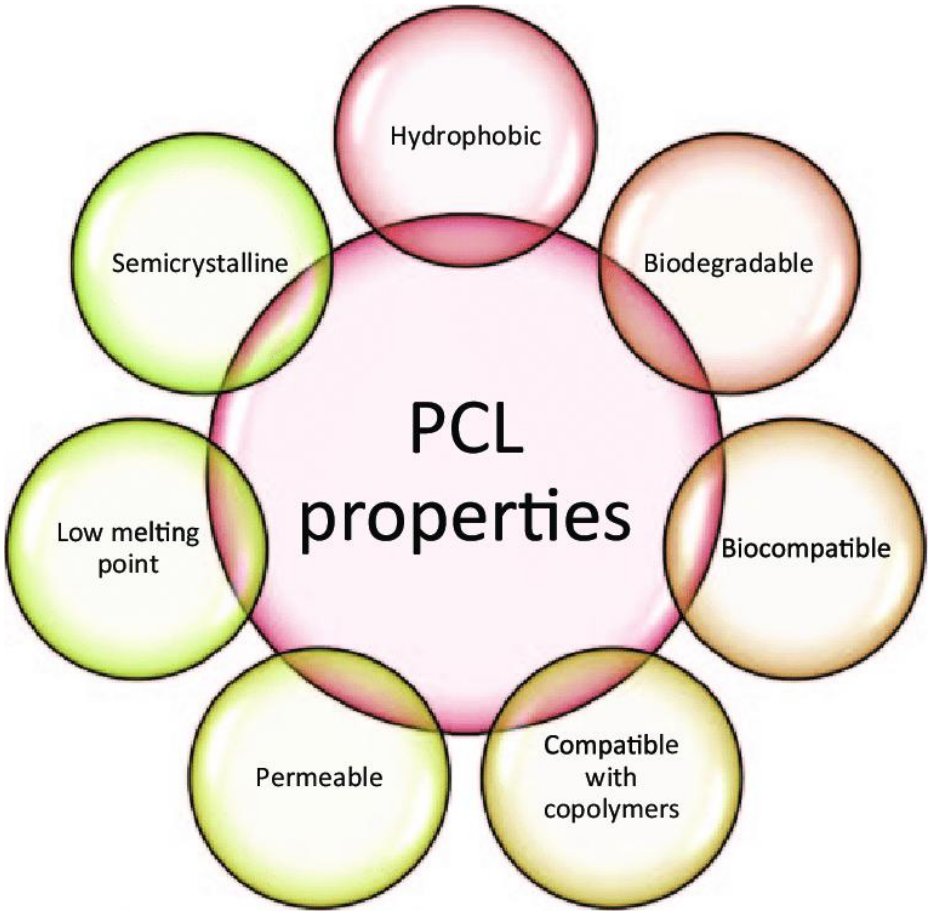

Figure 1. 17 Key Properties of PCL [134]

Altogether, the ability to control slow degradation, flexible nature of processing, mechanical stability and functional flexibility of PCL make it a highly studied and approved FDA biomaterial, best suited to long-term scaffold uses in bone and cartilage, vascular and nerve scaffold use, and soft tissue scaffold use. One of the strengths of PCL is its ability to be fabricated by a range of technologies, including electrospinning, solvent casting, 3D printing, and particulate leaching, and therefore the precise control of scaffold architecture, pore size, and fiber orientation[133].

1.9.7 Metal-Organic Framework (MOFs):

Metal-organic frameworks (MOFs) or porous coordination polymers (PCPs) are hybrid materials that are constructed by linking inorganic metal centers with organic linkers. These designs have gained a lot of scientific attention due to the exceptional physicochemical characteristics[134].

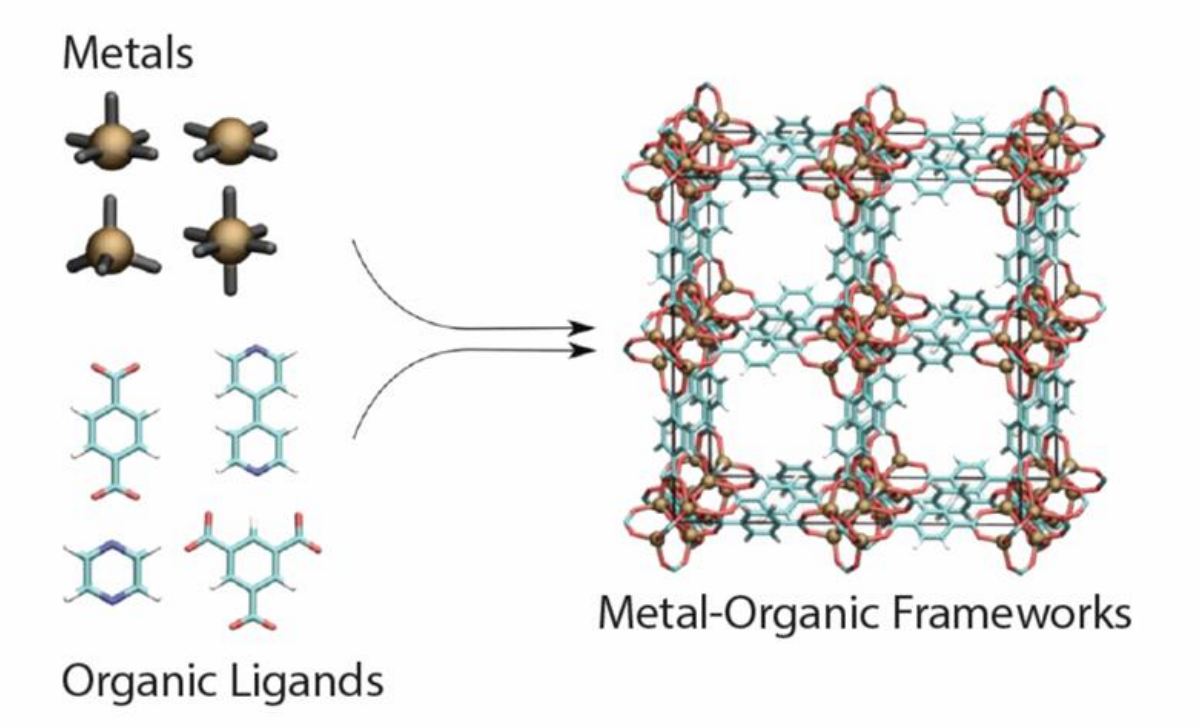

Figure 1.18 Representation of Metal-Organic Frameworks [136]

Although examples of coordination polymers with guest molecules inside the cavities were reported back in the 1950s, it was not clear whether the cavities would be able to maintain the porosity when the guest species was removed, or whether the cavities could be used to adsorb its own molecules without structural integrity being lost. A significant improvement in the understanding of MOFs was proposed by Yaghi and Li in the 1990s, which resulted in a modern understanding of MOFs. This was later independently proven by Kitagawa and Yaghi, who, in their efforts to study gas adsorption, established that it was possible to have a combination of crystallinity and permanent porosity in a singular coordination

network. This breakthrough set a fast-growing sphere of studies that has increased manifold within the last several decades[135].

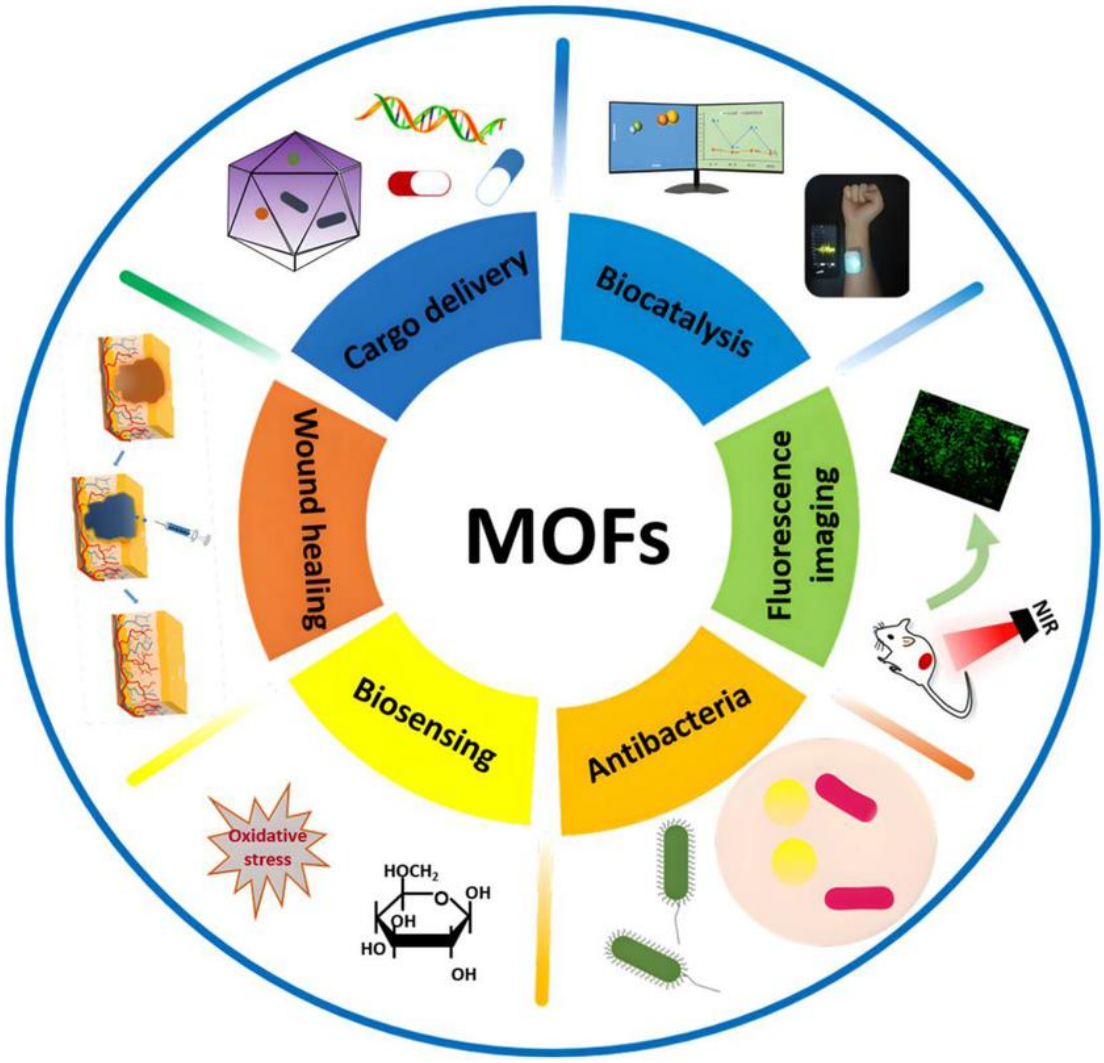

Figure 1. 19 Applications of MOFs in the biomedical field [137]

The current state of MOFs is that they have been identified as having numerous potential applications such as storing and separating gases, chemical sensing, heterogeneous catalysis, energy storage and conversion, and multiple applications in the field of biomedicine. The structural properties of MOFs in particular, their composition, topology, and architecture have a direct connection with their overall performance. In turn, MOFs functionality can be optimized by intentional design and careful structural optimization to

ensure that these materials suit various technological and scientific purposes. The metalorganic frameworks (MOFs) are a special type of hybrid substances, consisting of metal ions or clusters with the help of organic ligands[136]. The versatility in their sizes, large surface area, chemical adaptability, excellent biocompatibility, and possible ability to stimulate bone growth makes them very promising to use in bone tissue engineering and the curing of bone-related diseases. This has led to an increased interest in the use of MOFs in osteogenic studies and drug delivery within the last few years. This review gives a broad account of the application of MOFs and their composites in bone regeneration and treatment of diseases[137]. It starts with an overview of the different approaches to synthetically making MOFs, and the corresponding advantages and disadvantages of each approach. The next discussion is on the biological behaviors of MOFs, which are the basis of interactions of MOFs in biological systems. Moreover, the mechanisms and different biomedical uses of MOFs in bone tissue engineering and bone pathology are well discussed. Finally, the review does not omit the future outlook, which involves the investigation of MOFs as a novel treatment option to bone-related diseases and the extent to which this technology can be broadened to other biomedical fields[138].

1.9.7.1 Titanium-based MOFs

Metal-organic frameworks (MOFs) are hybrid materials which are inorganic-organic materials and have gained considerable scientific interest due to the broad fields of application that it can be used in. Although MOFs are no new to a range of different fields, their application in terms of biological and medical social domains is a rather recent and fast-growing research field. Titanium-based metal organic frameworks (Ti-MOFs) are among them with their unique structural and functional features such as nanoscale size of particles, high surface area, high biocompatibility and excellent photocatalytic and oxidative catalytic activity. The review identifies the recent achievements of the biomedical applications of Ti-MOFs with reference to their applications in the antibacterial therapy, cancer therapy, anti-inflammatory responses, and repairing bone tissues. These advancements demonstrate the enormous opportunities of Ti-MOFs in clinical practice. Cerium-based metal-organic frameworks (Ce-MOFs) are the recently observed (and thus gaining more and more popularity in biomedical studies) type of MOFs due to their promising redox characteristics, biocompatibility, and structural versatility [139].

1.9.7.2 Cerium-based MOFs

Cerium has enzyme-mimetic antioxidant activity due to its capacity to have a cerium-based reversible cycle (Ce^{+3} to Ce^{+4}) and thus scavenge reactive oxygen species (ROS), a process that is especially useful in the treatment of oxidative stress-associated diseases. Moreover, therapeutic agents, such as drugs, genes and biomolecules, can be loaded and released by Ce-MOFs due to its high surface area and porous structure. Their modifiable organic linkers and chemical stability allow surface functionalization to enhance target performance and cellular internalization and reduce cytotoxicity. Consequently, Ce-MOFs have proven potential in versatile applications of drug delivery, cancer therapy, bioimaging, antibacterial therapy, and tissue engineering.

Ce-MOFs have high surface area, tunable porosity and well-defined pore structure besides the antioxidant capability; hence, they are ideal in loading and regulated release of therapeutic agents, such as drugs, genes, and biomolecules. The porous structure enables the easy encapsulation, whereas the chemical stability of Ce-MOFs possesses structural stability at the conditions of the human organism. Moreover, functionalization of the surface can be achieved by modifiable organic linkers, and can be modified to enhance biocompatibility, cellular uptake, targeted delivery and reduce cytotoxicity. Thanks to such multifunctional properties, Ce-MOFs have already shown a very promising application in a large variety of biomedical uses, such as drug delivery technology, cancer treatment, bioimaging, antibacterial therapy, and tissue engineering. The synergistic antioxidant activity, large loading capacity, and versatile surface of Ce-MOFs make them promising sources of the synthesis of novel therapeutic and regenerative biomaterial.[140].

1.9.8 Calcium Magnesium Silicates (CMS)

Bone is a naturally powered and highly complicated structural tissue that ensures mechanical stability and other necessary functions in the human body. As the number of bone fractures, bone infections, bone-related diseases like osteoporosis continue to rise, there is a growing necessity to come up with effective biomaterials that would be used as bone substitutes. The ideal material to be used to do this is still a challenge because it should have excellent bioactivity in the formation of apatite and should have the right amount of dissolution and resorption, great mechanical properties, and the high

antibacterial effect. Even though synthetic hydroxyapatite has been extensively studied, it does not entirely mimic the dahlite phase the mineral composition of natural bone. Consequently, silicate materials have also been considered as a prospective choice to replace the bone grafts. Nevertheless, not every silicate has the appropriate qualities of bone regeneration as their properties differ according to their composition and the way that they are manufactured. Certain factors like calcium, magnesium and silicon are also very significant because they play a very important role in bone mineralization and metabolic event in the process of forming bones[141]. Among various bio ceramics, calcium magnesium silicates have gained recognition as having extraordinary osteoinductive potential, mechanical stability, and outstanding osteoconductive as well as angiogenic features that transpire through the regulated discharge of silicon, calcium, and magnesium ions. Nevertheless, irrespective of these interesting advantages, differences in their constructions still require the enhancement of both mechanical and biological activities to maximize their application in biomedical use. The bio ceramics have been found to be quite appropriate material to be used in biomedical needs because of their high biocompatibility that enables their safe incorporation into the human body[142].There are also certain forms of bioceramics with bioactive behavior, which are able to develop strong and stable connections with bone tissue and the surrounding biological structures. The calcium-based silicate bioceramics have been reported to possess more potential to promote cell growth and differentiation compared to most calcium phosphate materials. This enhanced biological reaction has been largely due to the discharge of silicon (Si) and calcium (Ca) ions which have been known to trigger osteoblasts activity and bone production. Calcium-magnesium silicates are the only subclass of silicate compounds that manifestly contribute to bone regeneration, and its advantageous effect is mainly attributed to the positive influence of magnesium (Mg). Their dissolution rate is comparatively lower than other calcium silicates and bioactive glasses because the replacement of CaO bonds with MgO bonds of higher stability enhance their structural stability. This enhanced stability also explains their higher strength of mechanical force and their elevated level of crystallinity. The most common calcium magnesium silicate compounds that have been in focus over the past few years include; akermanite($Ca_2MgSi_2O_7$), diopside ($CaMgSi_2O_6$), bredigite

($Ca_7MgSi_4O_{16}$) and monticellite ($CaMgSiO_4$) which have all proved to be very biocompatible and bioactive [143].

1.10 Theoretically (Software and Computational studies)

Theoretical study of MOF interactions with poly(epsilon-caprolactone) (PCL) The theoretical interactions between MOFs and poly(epsilon-caprolactone) (PCL) were investigated using the gaussian 16 Rev program, molecular models were created and visualized using Gauss View 6.1.1.Representative MOF cluster models and short PCL oligomers were constructed in Gauss View 6.1.1, followed by geometric optimization using density functional theory (DFT) built in Gauss View 6.1.1, followed by geometry optimization using Density Functional Theory (DFT)[144]. Interaction energies were calculated to evaluate the affinity between PCL functional groups and MOF active sites, particularly carbonyl–metal coordination and hydrogen bonding interactions. Gaussian 16 Rev was then used to analyze the optimized structures, charge distribution, and noncovalent interactions, thereby providing atomistic-level insight into the interfacial stabilization of MOF-PCL systems further used to analyze optimized structures, charge distribution, and non-covalent interactions, providing atomistic-level insight into the interfacial stabilization of MOF–PCL systems[145].

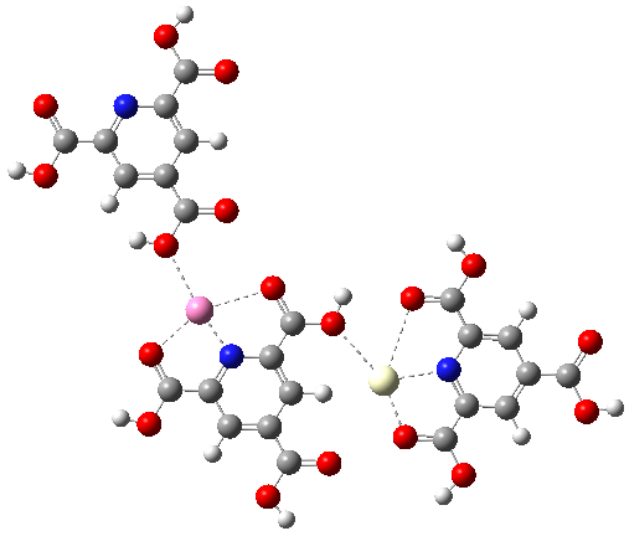

Figure 1. 20 Input structure of Ti-Ce Pyridine-2,4,6-tricarboxylic acid MOFs

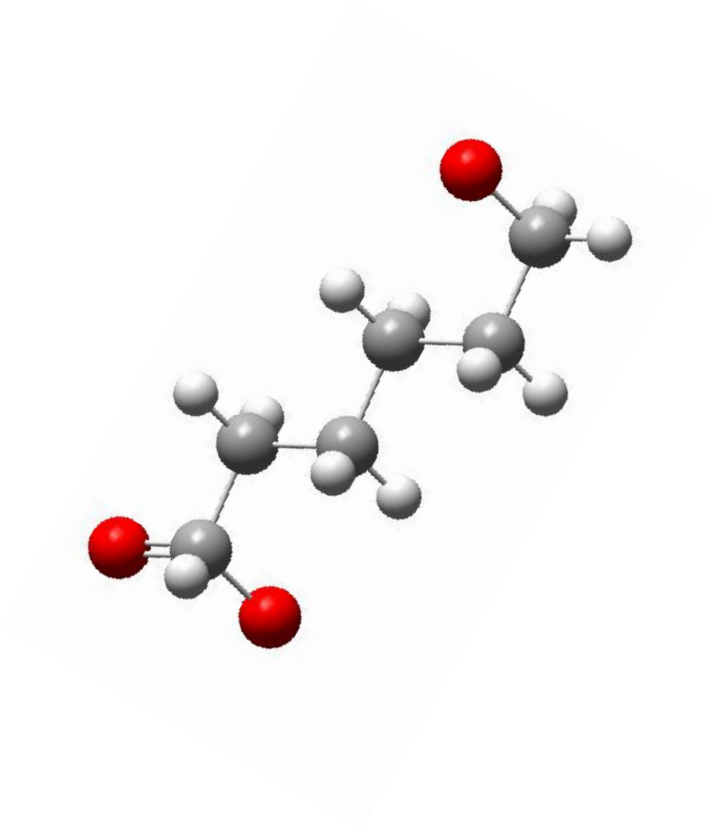

Figure 1. 21 Input structure of PCL (polycaprolactone)

Chapter 02

Literature review

In 1895, Abbe was the first one who reported that using rubber patches to repair dura mater. Because of the intricate anatomy, functions, and essential magnitude dural abnormalities, neurosurgery for dural repairs is the most difficult and demanding goal, although it is still regarded as an unmet medical need. Up to now, many alternatives with appropriate biodegradability and biocompatibility have been created and described. Numerous studies on their mechanical and structural characteristics have been published. The first report on the restoration of the dura mater using animal-derived materials was published in 1905 by Craig and Ellis. During the process, Cargile membrane, a replacement for dura was extracted from the periosteum of cows[146]. Zhu et al. have reported that a high-efficacy hydrogel for suture-less dural closure by combining tetra-PEG-NH2 and tetra-PEG-SS in PBS. The synthetic hydrogel was created to have features like increased safety, ease of use, and operation, good mechanical strength, strong tissue adhesion, quick set time, and ease of injection for effective dural healing during neurosurgery. Surprisingly, they discovered that their prepared hydrogel could prevent or stop CSF leakage during surgery, bind to uneven tissues even in moist environments, and induce water-tight dural healing in patients undergoing neurosurgery for dural regrowth or suture-less dural repair[147]. In 2021, Deng et al. reported that a bilayer membrane as a dural substitute that was made up of two layers: a dense layer that was constructed of bacterial cellulose and glutaraldehyde and citric acid crosslinked carboxymethyl chitin of chitosan and bacterial cellulose. Their research focused on creating a structure that could replicate human dura. They analyzed their material for this purpose and concluded that the porous layer had porous connectivity in the appropriate range (90-200μm), and the synthetic alternative demonstrated good mechanical strength and appropriate swelling. Furthermore, cell studies were conducted to assess the toxicity, which showed no damage on NIH/3T3 and enhanced cell proliferation and reduced inflammation[148]. Jin *et al*. reported several methods to create a unique double layer dural replacement synthesis. The solution casting method was employed to

prepare Dichloromethane (DCM) was used to dissolve poly (caprolactone co-lactide) film. The purpose of this layer was to offer good mechanical properties and an enclosed environment to newly emerging dura plants. Silk fibroin was used to prepare spongy layer of the substitute via freeze drying method. Spongy layer was made hydrophilic to give suitable water absorbing properties to the scaffold. Degradation and toxicity were assessed by an in vitro investigation that revealed material's suitable biocompatibility and biodegradation while also offering the damages tissues with the necessary mechanical support[149]. Yan Xu reported that Silk fibroin (SF) is a fibrillar protein derived from silk degumming. Its secondary conformation includes random coil, α-helix, and β-sheet. Under the impact of external conditions including temperature, concentration, pH value, stress, and ions, random coil unstable structure can convert secondary structure into β-sheet stable structure[150]. Hamad Khalid at el. in 2020 reported that Silk fibroin (SF) is a natural protein which is isolated from Bombyx mori and is certified as a safe biological material by the FDA It has been used in sutures for a very long time due to its outstanding biocompatibility, low immunogenicity, flexible biodegradability and high mechanical strength[151]. M. Asadniaye Fardjahromi.et.al in 2022 reported that recent advances in the fabrication of metal-organic framework scaffolds have provided great opportunities to boost up the properties of scaffold in bone healing. These scaffolds create three-dimensional network that simulate the extracellular matrix, improving cell survival, adhesion, growth and migration while sustaining the structural framework of regenerated tissues in vivo[152]. Xiang Li.et.al in 2023 reported that good porous structure and mechanical property of MOFs are advantageous in cell differentiation, nutrient transfer and biochemical waste secretion. Several types of MOFs based synthetic bone grafts are employed such as Zn, Ca, Ti, Ce, ZIF-8 etc. They all have bioactive and biocompatible properties. Among all these, combination of bimetallic Ti-Ce (MOFs) stands out for having potential characteristics which will enhance the extracellular matrix mineralization, secrete a high amount of collagen, and elevate the osteogenic genes and osteogenesis process[153]. Jiaxin Wu.et al in 2023 reported that biocompatibility and osteointegration are widely required in orthopedic and dental applications. There are some advantages of MOFS application in composite materials against bacterial infections in orthopedics. This paper discusses the prospective potential of MOFs coating with osteogenic activity in bone tissue

engineering. The role of Ti will be highly effective in the bone healing process because of its potential characteristics like low toxicity, Earth's abundance, and tetravalency. For example, a new multifunctional smart drug release system called CEL@ZIF-8 was fabricated for the systematic treatment of osteomyelitis. In addition, MOFs-based composites may be designed to respond at certain environmental stimuli that exists in the site of infection[154]. Javanbakht et al. reported utilized electrospinning technique to build up the composite scaffold. These electrospun scaffolds include magnesium gallate MOFs (MgGA) and dicalcium phosphate dihydrate (DCPD) having high porosity and huge surface area. In addition, the even distribution of Ca, Mg, P in the resulting scaffold confirms the integration of (MgGA) and (DCPD) for the possible application of bone regeneration[155]. Wang and Yeung et al reported that PCL is one of the non-toxic polyesters produced by ring-opening polymerization of ε-caprolactone monomers, which can proceed by anionic, cationic, coordination or radical polymerization methods. At room temperature and body temperature, PCL is semicrystalline. Its Tg is about −60 °Cand Tm is about 60 °C. At ambient temperatures amorphous chains are in rubbery form which allows PCL chains unlimited mobility at the body temperature and consequently increases its porosity for the body by products when transported into the body. Due to its mechanical flexibility, gradually degradation, and simplicity of electrospinning make it an ideal base for long-term help in acute bone deficiencies[156]. Lingfei Xiao at el. in 2021 reported that PCL (Polycaprolactone) is a highly efficient degradable polyester recognized for its biocompatibility, highly mechanical strength and extraordinary moldability its slow rate of degradation serves as appropriate for tissue scaffolding and copolymerization can modify its mechanical properties resulting in it more suitable for various kinds of application. PCL is a beneficial material in the fabrication of regenerative scaffolds because of its good compatibility with cell and tissues which also promotes cell adhesion and cell growth to enhance scaffold bioactivity, natural polymers like gelatin, collagen, chitosan and silk fibroin have been explored[157]. Xi et al in 2020 reported that Polycaprolactone is hydrophobic, semicrystalline and synthetic polymer with appropriate fiber forming properties Although , the main problem with nanofibers is their shortened strength due to their tiny dimensions which blocks their applications According to the literatures, the biological and mechanical properties of polymeric nanofibers can be enhanced by the

addition of various chemical materials like metal-oxides ,carbon-nanotube ,and metal-organic framework (MOFs)[158]. Leus.et.al reported that MOFs high porosity and structural capacity are the main sources of their prospects. MOFs in the biological area have been frequently used as medication delivery method. Due to their low cytotoxicity and biocompatibility some MOFs, like Fe-and Zn-carboxylates are now close to the preclinic phase of development. H.E. Emam et al. discussed the development of Cu-BTC/fabric hybrids as antimicrobial hybrid and nano MIL (Ti, In)/ natural textiles as anti-UVR fabrics[159]. Shin et al.in 2012 reported that Electrospinning is a standard approach to fabricate nanofibers from natural and synthetic polymers with unique properties that includes large surface area, high porosity and high permeable properties. The nanofibrous structures fabricated by electrospinning technology provides extra cellular matrix parameters for the cell movement, retention and differentiation of tissue cells, especially those which are involved in hard tissue regeneration. Electrospinning scaffold materials have been adequately proven too closely resemble the nanofibrillar elements of the ECM. The technique employs a high-voltage electrical field to create solid fibers from a polymeric fluid jet emitted through millimeter-scale nanofibrils. The electrospinning conditions (i.e., voltage, feed rate, needle tip to collector distance) can be manipulated in a way to obtain nanofibers with complicated and distinctive three-dimensional morphologies[160]. Shaheed et al. reported that the fabrication of Cu-BTC/CNC (Copper-benzene-1,3,tricarboxylate/ Cellulose Nanocrystals) and Cu-BTC/NFC (Nanofibrilliated Cellulose) composites by a direct mixing method, in which Cu-BTC powder was incorporating into the liquid precursor solution, followed by gelation and then freeze-drying, opening new possibilities for the production of purified materials. Nevertheless, it is important to note that this method can provide limited degree of control over the size, shape, and dispersion of the MOFs form during the composite material[161]. R. Semino et.al reported that interfacial nanoarchitectures of a family of metal-organic framework/polymer composites comprising the Zr-based UiO-66 with various polymers are comprehensively investigated by using a computational framework that combines the density functional theory (DFT) and force field-based molecular dynamics. Experimental results are correlated with these predictions to have an insight into the association between structure and compatibility of the MOF/polymer pairs.[162]

Chapter 03

Materials and Methodology

3.1 Materials:

Silk cocoons were obtained from Changa Manga Jungle located in Punjab, Pakistan. Calcium Magnesium Silicates (CMS) and Metal-Organic framework (bimetallic Ti-Ce MOFs) were provided by bone regeneration group IRCBM, COMSATS University Islamabad Lahore Campus. Chemicals and Materials are used in synthesis and in-vitro cell studies are listed below:

Table1.1 List of Chemicals

Sr. No	Chemicals	Abbreviation	Suppliers
01	Lithium Bromide Anhydrous	LiBr	SAMCHUN
02	Dichloromethane	DCM	Merck, Germany
03	Absolute Ethanol	EtOH	Merck, Germany
04	Sodium Bicarbonate	$NaHCO_3$	Scharlau
05	Silver Nitrate	$AgNO_3$	Sigma Aldrich
06	Phosphate Buffer Slime tablets	PBS	bio-WORLD
07	Polycaprolactone	PCL	Sigma Aldrich
08	Agar		Millipore
09	Broth		BHI

Instruments Used:

- Weighing Balance
- Magnetic Stirring Hot Plate

- Drying Oven
- Centrifuge Machine
- Freeze dryer
- Electrospinning Machine
- FTIR
- XRD
- Zeta Potential
- Scanning Electron Microscope
- Autoclave
- Incubator

3.2 Computational Methodology

All the calculations were performed by density functional theory (DFT). The B3LYP technique was used to obtain the optimal shapes of the molecules and to determine the frequencies of their vibrations. To the metal atoms (Ti and Ce) we performed our calculations with the LANL2DZ basis set and to the non-metal atoms, we performed our calculations with the 6-31G(d,p) basis set. We computed frequencies to ensure that the shapes we obtained are real minima on the energy surface. We optimized used to compute the strength with which TiO_2-Ce bimetallic MOFs attach to the polymer poly (ε - caprolactone) (PCL). The calculations were done using the Gaussian 16 (B.01) code, and the shape of the molecules was represented using Gauss View 6.1.1.

3.3 Experimental Methodology

3.3.1 Fabrication of Silk Fibroin Scaffold

Bombyx mori silk cocoons were degummed to extract sericin because this protein can cause an immunogenic reaction when employed in human biomaterials. Silk was degummed in accordance with the procedure described by Rockwood et al. to extract and purify it. Titanium scissors were used to cut the cocoons into tiny bits. After heating one liter of deionized water to a boil, 0.02 M (4.24g) Na_2CO_3 was added. After a few minutes,

2.0g of cut cocoons were added, and the boiling water containing Na_2CO_3 was continuously stirred for precisely 30 minutes. To get rid of any remaining sericin, the degummed silk was rinsed three times with deionized water. The obtained silk fibroin was spread out on filter paper and allowed to dry for a full day at room temperature.

3.3.2 Dissolution of Silk Fibroin

To obtain the silk fibroin solution, it was dissolved in a ternary solvent system consisting of LiBr was exactly weighed to 13.11g and dissolved into 16.24 ml distilled water. Subsequently, 2g of degummed silk was introduced into this prepared solution. Gentle stirring was used to dissolve the LiBr solution. The solution was continuously heating using a heating gun for dissolution of silk fibroin. Mix degummed silk fibers into the solution vigorously until the solution turns into water like consistency. The solution was then put in an oven at 70ºC for 3 hours to ensure the entire solubility of any residual fiber groups of silk. After this, Dialysis was carried out in distilled water using a cellulose dialysis membrane (MWCO 12400kDa) for 72 hrs. To prevent the solidification of silk fibroin, the process of dialysis was further continued 3 days in refrigerator. Water changes were every 30 minutes during the first 8 hours and adjusted next to 1, 4, 8, 16 and 24 hours. The success of dialysis was verified by placing crystal of $AgNO_3$ in the dialyzing water; a crystal-clear solution was the sign of elimination of LiBr salt. The dialyzed silk fibroin was centrifuged at 2000 rpm for 10 minutes to remove residual impurities. Surprenant was obtained and debris was discarded. Finally, the pure silk fibroin was obtained. The concentration of the solution was calculated using the dried solution of 1mL of the collected supernatant in an oven at 70ºC until complete removal of water. The yield obtained was 6% and then diluted to set the concentration at 4%. The desired scaffolds were synthesized using this concentration. Before freeze drying, which took place for 72 hours, the solution was frozen in a petri dish at -25°C for 24 hours.

3.3.3 Freeze drying of Silk Fibroin

Prepared three petri plates of silk fibroin solution containing 20ml in each plate. The yield obtained was 6% and then diluted to the concentration at 4%. The required concentration of freeze drying is 4%. (which means 0.8g silk is present in 4% solution). Before freeze drying, all the petri plates were placed in refrigerator at -25°C for 24 hours and covered

with aluminum foil. After 24 hours, when they become completely frozen, took place into freeze dryer for 72 hrs. Set the temperature and pressure carefully -40 degree and 00012pa respectively.

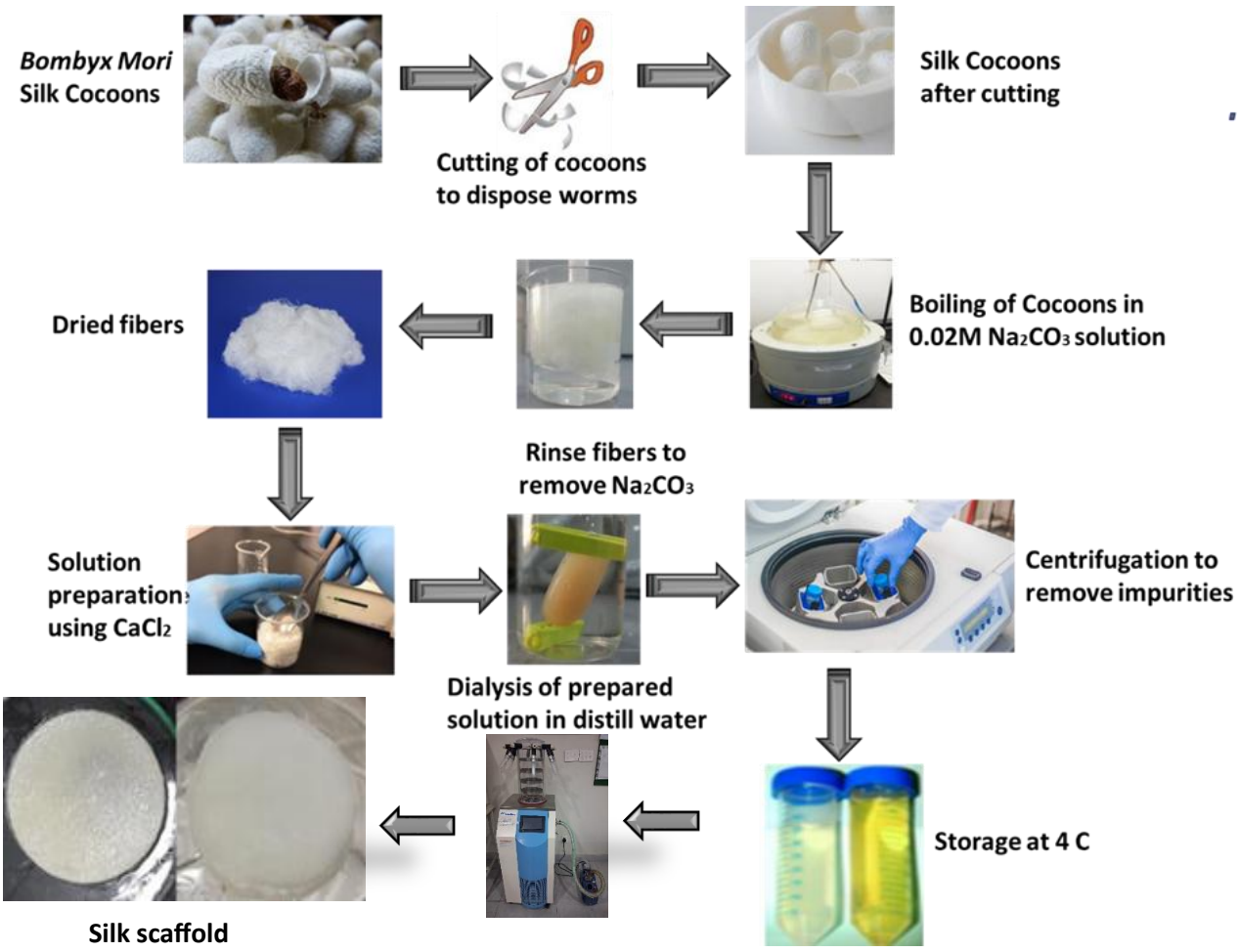

Figure 3. 1 Fabrication of Silk scaffold

3.3.4 Fabrication of SF+CMS Scaffolds:

3.3.4.1 Preparation of Silk+CMS Solution

We took the prepared Calcium Magnesium Silicates (CMS) powder from bone regeneration group by IRCBM. To obtain the SILK+CMS suspension solution, we took the 20ml of 4% silk solution in a clean beaker. In literature required concentration of CMS in

bone regeneration is about 40%. According to the calculations of silk solution we add 40% CMS (0.32g) into the silk solution. After adding this, ultrasonicate for 15 minutes. CMS particles were suspended in silk solution. Added magnetic stirrer and stirring this solution at magnetic hot plate. After a few minutes of stirring, a homogeneous suspension of SILK+CMS was obtained.

3.3.4.2 Freeze drying of SILK+CMS scaffolds:

Prepared three petri plates of SILK+CMS solution containing 20ml in each plate. Before freeze drying, the plates were kept in a refrigerator at -25°C for 24 hours to ensure complete freezing. After 24 hours of freezing, the samples were completely frozen and then placed in a freeze dryer for 72 hours.

3.3.4.3 Electrospinning of PCL

The electrospun membrane of PCL was fabricated, procured from Sigma Aldrich, USA was used having molecular weight of 80,000g/mol. The solution was prepared by dissolving 20% PCL in 40 mL DCM. PCL crystals were added in the solution slowly to the solvent under the constant magnetic stirring at 75rpm with room temperature. The solution was stirred for 3 to 4 hours to obtain a crystal-clear solution. Prior to electrospinning, PCL/DCM solution was loaded into 20mL syringe and the 18-gauge needle for the smooth ejection of fibers from its tip. Electrospinning was done by supplying the voltage power of 18kV and keeping the distance between the tip of the needle and the drum collector 15cm. To obtain highly aligned fibers, feed rate was fixed to 0.5 mL, and drum speed was increased to 5000 rpm. The synthesized fibrous scaffold sheets were carefully collected from the aluminum foil, and the formation of fibers was collected from the aluminum foil, and the formation of fibers was confirmed by observing them under an optical microscope.

3.3.4.4 Electrospinning of PCL+MOF

For the preparation of electrospun membrane of PCL+MOFs, known concentration of MOF was added to the PCL solution.5% MOFs with respect to the quantity of PCL was acquired for the synthesis of PCL+MOFs electrospun membrane. MOFs were incorporated into the prepared PCL solution under continuous magnetic stirring, followed by ultrasonication to ensure uniform dispersion. Since MOFs did not completely dissolve in the polymer solution, a stable solution was obtained. Following the same parameters that

were used for the electrospinning of PCL membrane. Desired, uniform and smooth fibers were successfully obtained on the aluminum foil covered on the drum collector.

3.3.5 Fabrication of Bi-layered Scaffold:

The preparation of novel bi-layered scaffold SF+CMS and PCL+MOF composite scaffold was carried out that made up of two layers. The upper layer is composed of freeze-dried SF+CMS and lower layer is made up of electrospun membrane of PCL.

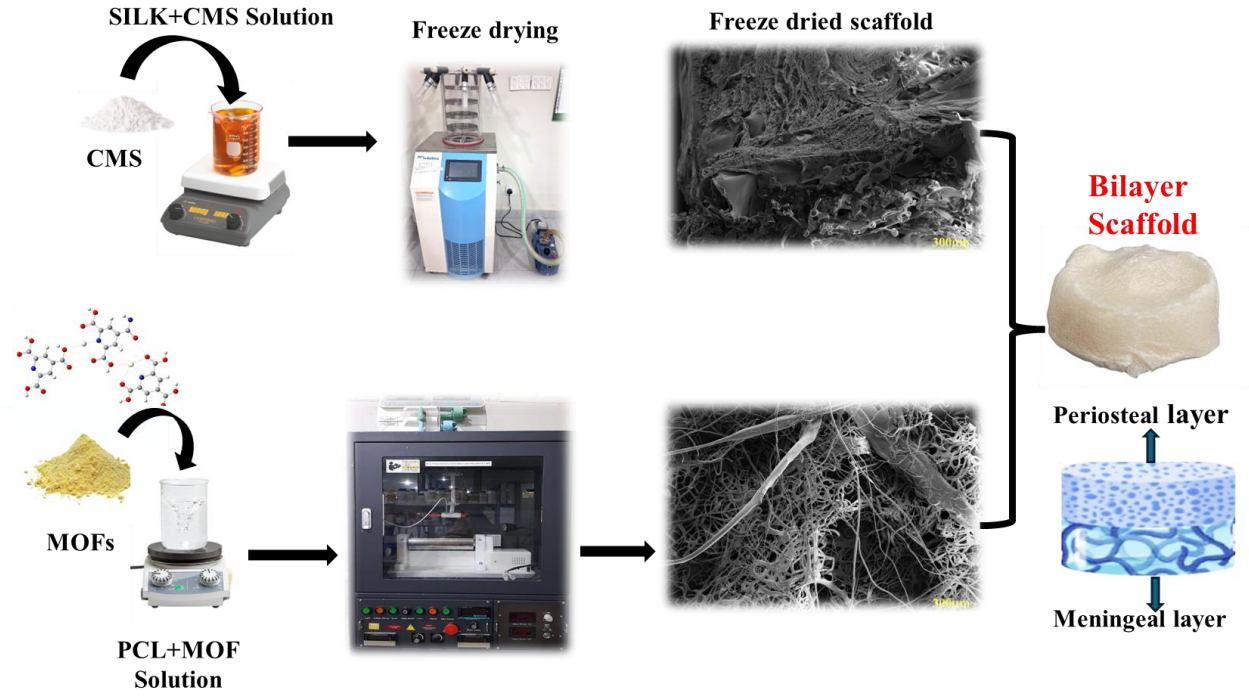

Figure 3. 2 Fabrication of Bilayer Scaffold

3.4 Characterization techniques

In the initial phases of materials exploration characterization techniques are crucial for identifying the distinctive properties of synthetic materials, chemical compounds and composites. By applying these analytical techniques, the physiochemical and mechanical properties of the synthetic materials are investigated. Physical shape, pore size, chemical composition and mechanical properties are some of these traits. These traits method must be used to define synthetic materials prior to their use in practical scientific settings. Several approaches are used to characterize biomedical scaffolds, some of which are given below:

- Fourier transform-infrared spectroscopy (FT-IR)
- Scanning electron microscopy (SEM)
- X-rays Diffraction (XRD)
- Contact Angle
- Swelling ratio measurement
- Porosity measurement
- Density measurement
- In vitro degradation studies

3.4.1 Fourier transform-infrared spectroscopy (FT-IR)

FTIR spectra of SF, CMS, SF+CMS, PCL, PCL+MOF and BL were acquired in the IR range of 4 cm^{-1} using smart iTR diamond Attenuated total reflection (ATR) mode of Thermo Nicolet Scientific 6700 FTIR, USA. All the materials spectra were obtained using the scan range of $8cm^{-1}$ and total 256 runs were carried out to determine the specific functional groups versus characteristics peaks of the spectra.

Figure 3. 3 Thermo Nicolet Scientific 6700 FTIR, USA

3.4.2 Scanning Electron Microscope (SEM)

Scanning electron microscope is one of the most promising techniques for assessing and thoroughly investigating the scaffold morphology. To investigate the surface morphology, fibers alignment and composition of the composite scaffolds, samples were cut into dimensions having clean surface. This experiment was carried out at room temperature using it. SE (topography) and BSE (phase contrast) modes were used to do the study a 5kV with a magnification range of 1000x- 1000,000x. Using a TESCAN Vega LMU-Variable Scanning Electron Microscope, all samples were coated with gold to capture images of scaffolds having porous, fibrous and nanostructure properties.

Figure 3. 4 Thermo Fisher SCIENTIFIC Electron Microscope 1142267

3.4.3 Contact Angle (Biolin Scientific Attention Theta Measurement)

The capacity of resin surfaces to wet was tested using the contact angle approach, which is an extremely precise method. The scaffolds that were created were meticulously trimmed into a 2x2 size and evaluated for their hydrophobic and hydrophilic qualities using Young-Laplace analytical technique. The solvent, deionized water, was sprayed onto the scaffold surfaces using an automated dispenser with a 300 µL tip. A drop size 4 µL was used in the investigation. The contact angle was measured in ten seconds by the tangent method in which the scaffolds were in contact with the water. To examine the drop profile, a telescope goniometer was used, whereas an instrument with associated software was used to record images.

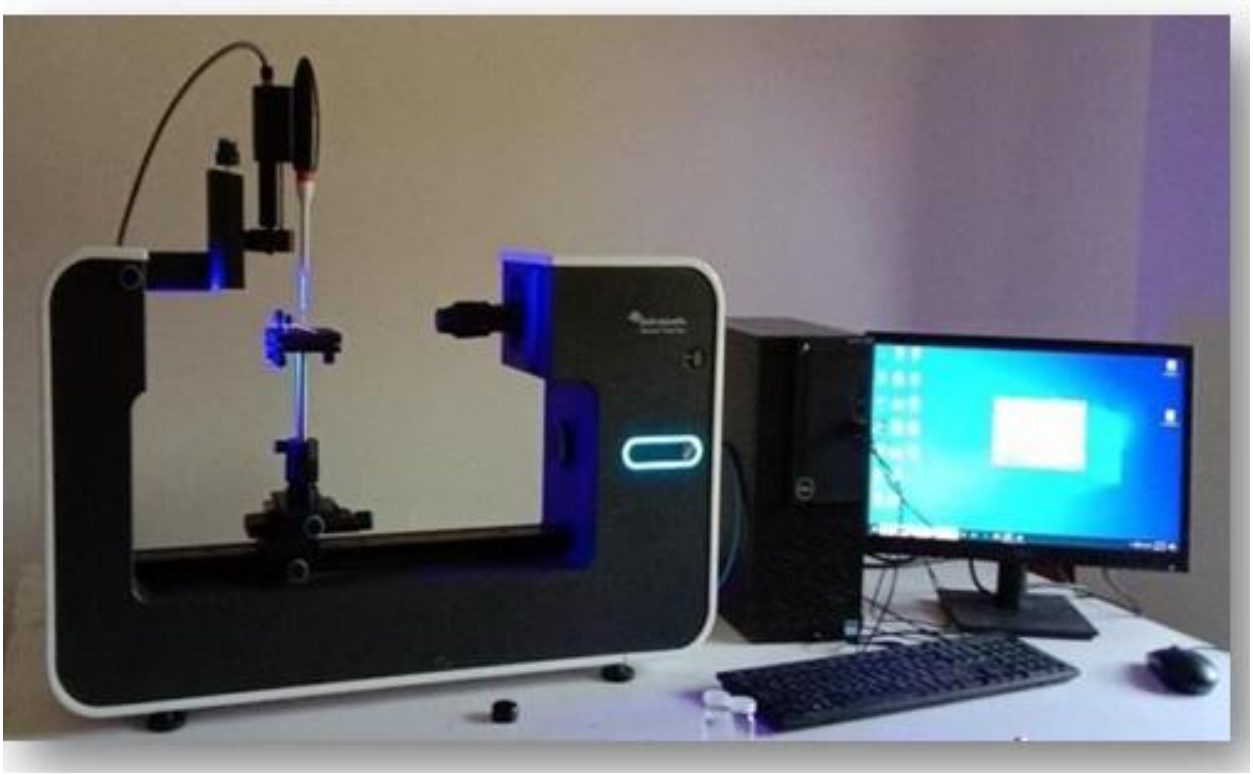

Figure 3. 5 Biolin Scientific Attention Theta Measurement

3.4.4 X-rays Diffraction (XRD)

Powder X-ray diffraction (PXRD) was employed to analyze the crystalline structure and phase composition of carboxymethyl silk (CMS) and metal–organic framework (MOF)–based samples. PXRD is a fast method of analysis that is non-destructive and is based on the diffraction of X-rays by randomly oriented crystallites to produce characteristic diffraction peaks at interplanar (d) spacings in accordance with the Bragg law. The diffraction patterns obtained gave a good understanding of the extent of crystallinity and structure organization of the polymeric and inorganic components. The fact that the crystalline MOF structure was incorporated and maintained in the CMS matrix was proven by the distinct MOF diffraction peaks and the variation in the intensity, expansion, or minor shift of the peak manifested the physical interactions between the polymer chains and the MOFs and the potential change in the crystallite size and the lattice strain. The fact that the MOF peaks in the composite samples were reduced or covered by the other peaks showed

a homogeneous dispersion of MOFs in the polymer matrix as well. The purity of the phases of the materials in PXRD were also confirmed, and no secondary crystalline phases or undesired impurities were observed, which indicates the structural appropriateness of the prepared composites to further biological and functional testing.

Figure 3.6 Rigaku MiniFlex XRD Measurement

3.4.5 Migration Assay

To determine the migration of NIH-3T3 fibroblast cells in response to membranes, an in vitro test related to wound healing was performed. This technique that is commonly used illuminates cell mobility. The porosity of the fabricated scaffolds is particularly useful in evaluating the effects of biomaterials on cellular migration, which is central to wound healing and tissue regeneration. To encourage ideal development and adhesion, NIH-3T3 fibroblasts were initially cultivated under carefully monitored circumstances. The cells

were cultured in (DMEM) Dulbecco Modified Eagle Medium, inoculated with 10% (v/v) (FBS) fetal bovine serum to provide the required nutrients. and growth factors. To prevent bacterial contamination, 1% (v/v) penicillin- streptomycin. solution was introduced in the culture medium. Seed was then grown in Cell suspensions. culture of 6-well tissue culture plates at a predetermined density (2×10^4 cells per square) centimeter. The reason that this density was chosen was that a uniform may be formed. monolayer within a reasonable time interval of incubation, which ensures uniformity in the experimental. conditions across all wells. The plates were then incubated at 37˚C in a humidified plate. 5% CO_2 environment to recreate physiological conditions. Cell growth occasionally examined using a light microscope until the monolayers attained. approximately 90% confluence. Here the cells were gaped tightly together but had not yet. 49 was placed on the surface and this made it ideal to perform the scratch assay because it is clear. cell migration into the wound area can be visualized without its interference overcrowding. A linear mechanical injury was when the confluency desired was achieved. incorporated in every single cell monolayer through a 200 μL micropipette tip that was sterile. This tip was pulled down the middle part of the well to cause a visible, cell-free scratch or wound, that was the zone of reference to assess cell migration. Efforts were made to ensure all wells had a uniform scratch width and direction. reducing variation in later measurements. By Adhering to the formation of the wound, very careful aspiration of the culture media was done to remove attached cells and debris. produced as the scratching occurred. Adding fresh media was then carefully introduced to the well. In experimental groups previously sterilized and preconditioned samples were used. located on the periphery of the scratching. This localized position tried to simulate. directional stimuli and monitor whether the existence of membrane materials influenced. movement of fibroblast cells towards the material. An observation on time-lapse was started. after the formation of the scratch (time point 0 h). Digital images were imaged with the inverted phase-contrast microscope (Olympus IX-53 model) to record cell set-up and width of the original wound. The plates were then set back. to the incubator so that it can migrate cells within 24 hours. A second incubation follows this incubation. group of photos was captured in the same spots as the original ones to compare it with the changes. throughout the wound site and measure cell migration. During the experiment, aseptic was observed. procedures were followed to ensure sterility and avoid exogenous

contamination, which otherwise may affect cell behavior or subvert image quality. The experiment was also independently repeated at least thrice. events to guarantee reproducibility and statistical reliability. For each experiment, there were triplicate wells per condition, control and treatment, giving one a total of two. at least nine items in each group. This method assisted in explaining away. biological variability and gave adequate data on significant quantitative. analysis. Image processing software was then used to analyses the image. determine the percentage of wound closure. The 0-hour open wound area was calculated and compared to the rest of the uncovered area after 24 hours. A higher percentage, a higher rate of wound closure after 24 hours, showed an increase in cell migration, and a restricted one. closure implied lesser cell movement, probably because of material cytotoxicity or physical impairment of migration pathways.

3.4.6 Swelling ratio measurement

According to the procedure described by Liuyun et al., swelling investigations of all the samples were conducted by submerging them in freshly made PBS solution (7.4 pH) in a shaker with a temperature set at 37˚C. To determine the swelling behavior of the sample scaffolds, the study was conducted in triplicate for 24 and 48 hours after all the samples were cut into similar shapes with equivalent weights. The materials were dried to a constant dry weight, denoted as W_d, prior to the experiment's started. Following the earlier period, the dried materials were put in 15 mL falcons filled with PBS solutions. The samples were taken out of the solution at each specified time point, gently tapped on filter paper to remove excess water, and their weights were recorded as wet weights and noted as W_s. The mean values of the samples were computed by averaging the triplicates, and the swelling ratio was calculated using the following equation:

$$\text{Swelling ratio (\%)} = [W_S – W_d/W_d] \times 100$$

3.4.7 Porosity measurement:

The methods described by Deng et al. were modified to measure the porosity of the sample scaffolds. Every sample was dried to a consistent weight of W_1. Triplicates of the study took place. After dipping the sample scaffolds in 100% ethanol for an hour, the samples' wet weight was recorded as W_2.

The porosity was determined by the following formula:

$$\text{Porosity (\%)} = [W_2 – W_1 / W_2] \times 100$$

3.4.8 Density measurement:

Electrospun membrane density, freeze dried scaffold density influences porosity and pore size of the scaffold which in turn. infiltration by control cells, proliferation and viability. To determine the density of sample, 20mg samples of Electrospun membranes and freeze dried scaffold were cut in triplicates and then immersed in ethanol an hour. Samples were cut out and density was obtained by means of the formula.

3.4.9 *In Vitro* Degradation studies

The development of new tissues depends on the composite scaffold degrading at an acceptable and controlled rate. The implanted material's degradation time should match the target tissue's growth pace. The time periods of the degradation research were 1, 7, 14, and 28days, and triplicate samples were taken. The average value of the weights was calculated by their mean value. All scaffolds had the same sample weight, which was recorded as W_O. The samples were soaked into 3mL PBS solution, with a pH of 7.4 and incubated at 37°C in an incubator. To eliminate any chance of salt ions being absorbed on the sample surface, the scaffolds were cleaned with distilled water on the day the study was completed. To remove the moisture, the samples were dried in vacuum drying oven, and their dry weight was recorded as W_t. The % degradation was calculated using the following equation:

$$\text{Degradation (\%)} = (W^o – W_t / W^o) \times 100$$

Chapter 04

Results and discussion

4.1 Theory Results and Discussion

4.1.2 Geometry optimization

Gauss View was used to create the initial molecular geometries of all species such as Ti-Ce bimetallic MOFs and poly-caprolactone (PCL). Optimization was then fully performed on the structures with the B3LYP functional and LANL2DZ basis set of metal atoms Ti and Ce and 6-31G (d, p) of non- metal atoms. Calculations of frequency were done on the optimized structures to ensure that they represent true minima as represented by the absence of imaginary frequencies. The interaction complexes of the MOFs with PCL were also evaluated by the same optimization and frequency analysis to determine their binding and interaction energy.

4.1.3 Interaction Energies

We determined the interaction energies when Ti-Ce bimetallic MOFs react with the polymer PCL. Negative numbers imply that the interaction is positive and complexes are stable. The best systems that we considered were the complex with Ti and the oxygen of PCL, with an energy of -0.0331 Hartree (-0.90 eV). The interaction between the complex with the oxygen of Ce and PCL was weaker of -0.0129Hartree (-0.35 eV). All interaction energies had been in the range of -0.35 -0.90 eV with Ti bonding PCL stronger than Ce. Ti is more attractive to PCL and therefore, Ti-Ce MOFs provides a better stability of polymer composites and Ti is the one that contributes the overall strength of the interaction. These results can make us realize that some metal centers are more effective in MOFs polymer systems and can be used to create more efficient hybrid materials. The more powerful attraction of Ti to the PCL monomer is due to the electronic and chemical factors. Ti^{+4} is a hard Lewis acid and is strongly attracted to the carbonyl oxygen of the PCL, and a covalent nature to the Ti–O bond is further contributed by the presence of Ti 3d orbitals and O 2p lone pairs. DFT charge analysis reveals that an increase in the charge volume of the polymer oxygens to Ti is the reason why the Ti O bond is more stable. Ce in contrast does

not interact strongly since its 4f orbitals are localized such that the Ce-O bond is predominantly electrostatic and has reduced charge transfer. In that way, the interaction energies and bond distance of complexes with Ce are smaller, indicating that the role of Ce in the bimetallic framework is different, and not a drawback.

Table 4.1: Interaction Energies

Interaction energies	**Hartree**	**eV**
Ti-O(PCL)	−0.0331	−0.90
Ce-O(PCL)	−0.0129	−0.35

4.2 Experimental Results and Discussion

4.2.1 Functional Group Detection-FTIR Spectroscopy

FTIR spectroscopy was done using Thermo Fisher Scientific (Nicolet 6700TM) machine. FTIR analysis was performed to identify the characteristic functional groups and chemical interactions of Silk, CMS, PCL, MOFs as well as their respective composite materials. . The FTIR spectrum of CMS shows typical absorption bands at the area of about 3200 3400 cm^{-1}, which is in the stretching vibration of hydroxyl (-OH) groups and this indicates the hydrophilic character of the polysaccharide backbone. The near C-H stretch at about 2920 cm^{-1} is attributed to C-H stretching vibrations of groups that are aliphatic. A major absorption peak around -1600-1650cm^{-1} is attributed to the asymmetric replacement of carboxylate (-COO) and the one close to -1400 -1450cm^{-1} is attributed to the symmetric carboxylate replacement, which verifies the carboxymethyl replacement in CMS. There are also peaks around 1000-1100 cm^{-1}, which are linked to Si-O-Si and C-O vibrations, which are reflected in the glycosidic linkages. FTIR spectrum of silk exhibits clear amide bands, which are characteristic of materials based on protein. The high absorption at a relatively low wavelength of around 1650 cm^{-1} (amide I) is the most likely to be the result of the C=O stretching vibrations of the peptide backbone whereas the band at 1530-1550 cm^{-1} (amide II) may be ascribed to the N-H bending and C-N stretching. The amide III band at that was observed at around 1230 1260 cm^{-1} is yet another indication of 1230 1260 cm^{-1} presence of 1230 1260 cm -1 structure of silk fibroin. The extensive absorption in the -32003400 cm^{-1} region is attributed to the N-H and O-H vibrations, which indicate the existence of hydrogen bonding in the silk structure. All the typical peaks of the silk and CMS are preserved in the composite of the Silk+CMS, which means that they are blended successfully without any chemical degradation. Nevertheless, observable alterations in the strength of the peptide and slight variations, especially in the -OH/ -NH region and the amide I band, indicate that the hydrogen bonding interactions occur between the hydroxyl and carboxyl groups of CMS and the amide groups of silk. These interactions show that the two components have a good interfacial compatibility.

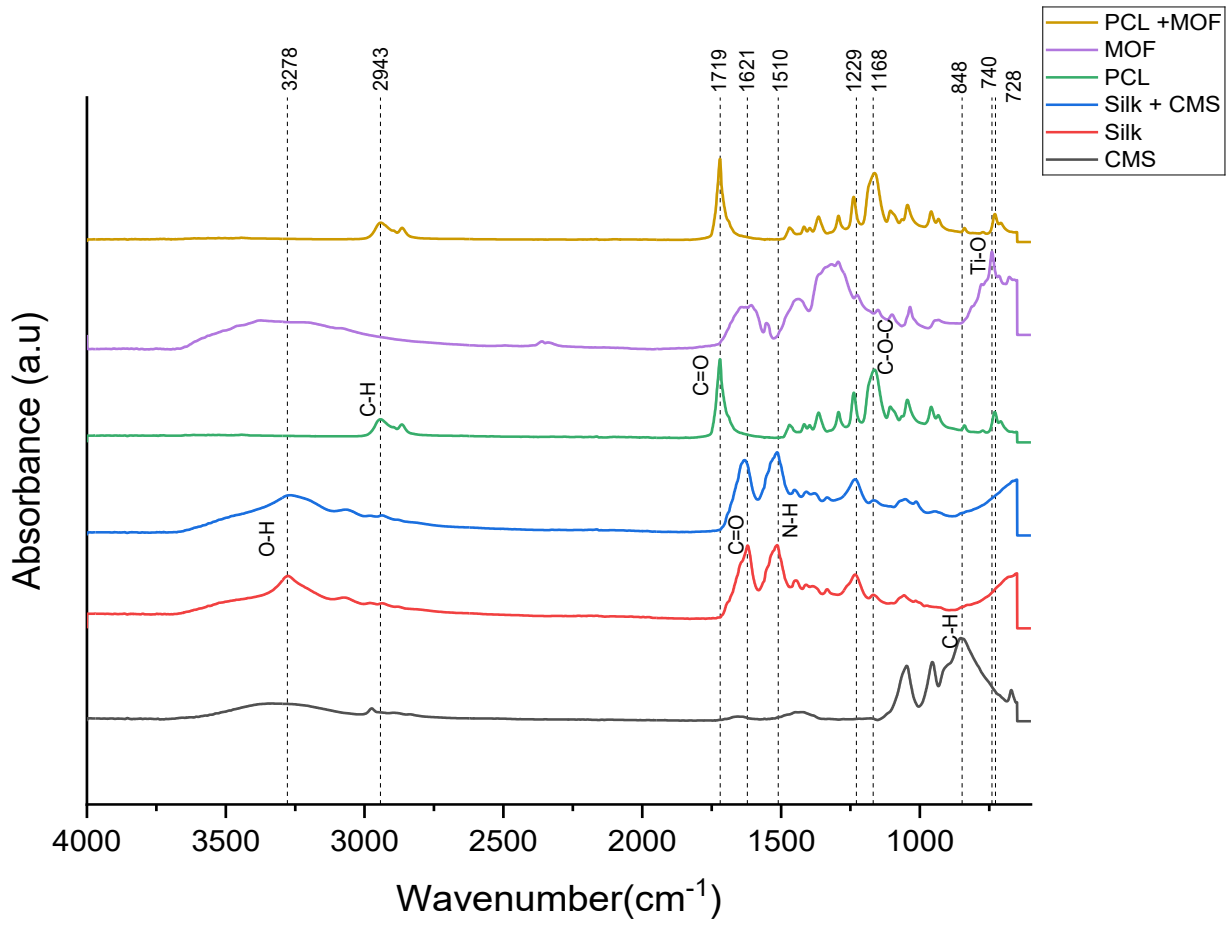

Figure 4. 1 FTIR Analysis of CMS, SF, SF+CMS, PCL, MOF, PCL+MOF

The FTIR spectrum of pure PCL shows typical absorption peaks at 2940 and 2860 cm^{-1} that are associated with asymmetric and symmetric vibrations of the -CH_2 groups of PCL. The presence of a robust and sharp peak of absorption at a wavelength of about 1720-1730 cm^{-1} is recognized to the carbonyl of the ester (C=O) vibration that is characteristic of PCL. Additional bands observed close to 1290 to 1160 cm^{-1} ,corresponding to C-O and C-O-C stretching of ester linkages further confirmed semi-crystalline nature of polyester PCL.The vibrations The MOF spectrum has peculiar peaks linked with organic linker vibration and coordination between metals and ligands. Bands in the region of 1500-1600 min are attributed to C=C aromatic stretching vibrations of the organic linker, whereas bands in the region of 1350-1450 cm^{-1} are attributed to carboxylate symmetric and asymmetric stretching of the coordinated group. The appearance of bands lower than 800 cm^{-1} is due to the presence of metal oxygen (M-O) vibrations and thus it verifies that metal ions and

organic ligands are coordinated successfully in the MOF structure. The typical PCL ester carbonyl peak of PCL is still present in the PCL + MOF composite, which implies that the polymer backbone is not lost when MOF is added. Nevertheless, both changes in the peak intensity and slight changes in the C N O and carbonyl stretching regions indicate the physical interactions between PCL chains and the MOF network, including hydrogen bonding or dipole-dipole interactions. The fact that the main MOF-related peaks were retained also proves the effective integration and structural stability of the MOF into the PCL matrix.

Table 4.2 Characteristics peaks for the functional groups of scaffolds

Sr. No	Wavenumber	Functional Groups	Materials
01	3200-3400	–OH stretching	SF+CMS
02	1000-1100	Si–O–Si/C–O (glycosidic linkages)	CMS
03	1650	Amide I (C=O) Amide II (N-H)	SF+CMS
04	1720-1730	C=O stretching (ester)	PCL
05	1290-1160	C-O-C	Semi-crystalline PCL
06	<800	M-O	Metal-Ligand Coordination

4.2.2 X-ray Diffraction (XRD)

To discuss the phase characteristics and crystalline structure of CMS and the synthesized Ce–Ti MOF, the X-ray diffraction (XRD) analysis was performed. The pattern of XRD of CMS shows that the polymeric structure is semi-crystalline and has several diffraction peaks at the 2 theta of about 27.72˚, 29.98 ˚, 3 1.31 ˚, 35.12 ˚ and 35.76 ˚. The acuity and strength of these peaks indicate some level of organization due to the uniform arrangement of polysaccharide chains, whereas the existence of a wide-spread background indicates the amorphousness of the CMS matrix. This crystalline/amorphous mixture is characteristic of chemically modified cellulose derivatives, and it is a testament to the fact that CMS was formed successfully without the entire loss of structural order. Conversely, the XRD pattern of the Ce–Ti MOF has a set of sharp and strong diffraction peaks at 2-theta around 23.49, 29.18, 31.23, 32.27, 34.63, 36.29, 37.79, 38.83 and 40.18 which indicate that it is highly crystalline. The existence of many sharp reflections shows that the structure is long-range periodic, and this fact confirms that the structure was formed using well-ordered metal-organic frameworks. These diffraction peaks are ascribed to the coordination of centers of cerium and titanium metal with organic ligands, leading to stable crystalline lattice. The lack of wide amorphous humps as well as the high peak intensity is also an affirmation that the synthesized Ce-Ti MOF is pure and intact, as far as its structure is concerned. In general, XRD findings apparently differentiate the semi-crystalline nature of CMS and the highly crystalline structure of the Ce-Ti MOF.

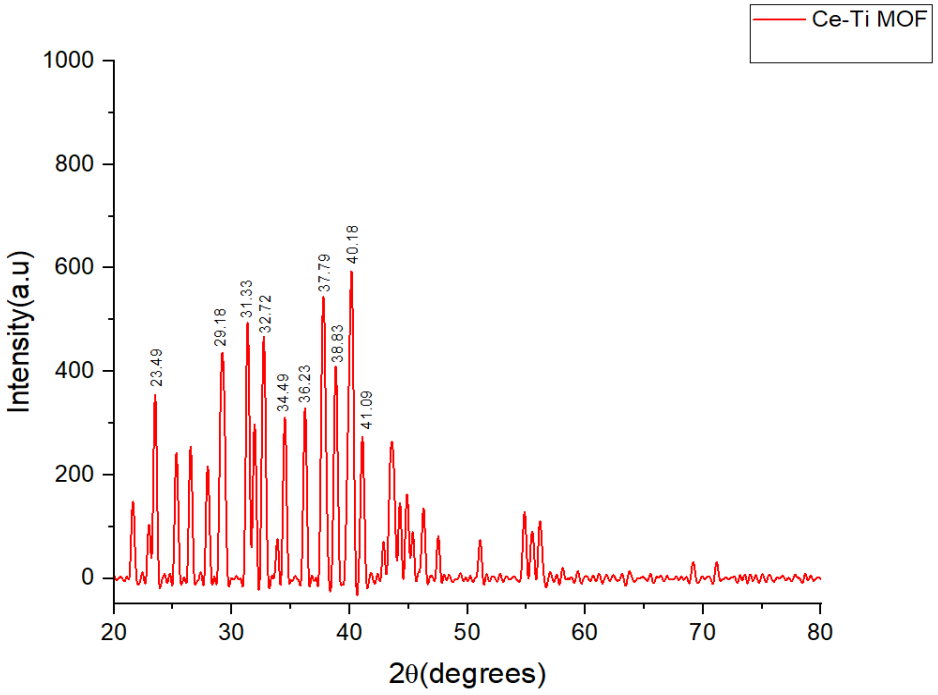

(a)

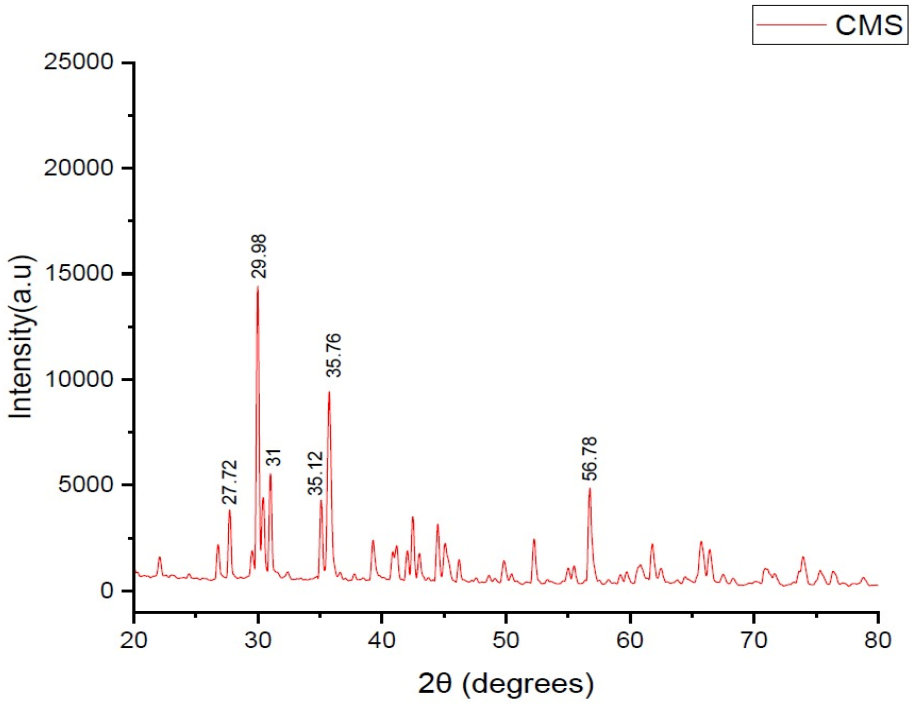

(b)

Figure 4.2 XRD Analysis of (a) Ce-Ti MOF (b) CMS

4.2.3 Scanning Electron Microscopy (SEM)

To investigate the surface morphology and microstructural features and pore architecture of SF, SF+CMS, PCL, PCL+MOF, and bilayer (BL) scaffolds, the authors used the Field Emission Scanning Electron Microscopy (FESEM) presented in Figure 4.3. FESEM micrographs of pure silk fibroin (SF) scaffold show the existence of fibrous and interconnected network with the relatively smooth surface of the fibers and randomly oriented fibers. Pores at micro- to nanoscale are also present all over the structure; this is a sign of porous morphology that is desirable in cell infiltration and nutrition diffusion. Another aspect, though, is that there are regions that seem to be compact, indicating some part of the fibers fusing in the processing. In the SF+CMS composite scaffold a significant alteration in the surface morphology is recorded relative to pure SF. CMS integration results in the roughness of the surface, as well as the development of irregular porous structures. The scaffold shows more porous structure due to interactions between hydroxyl and carboxyl groups of CMS. These interactions enhance integrity between two phases which improve hydrophilicity and promote better cell-material attachment. FESEM images of pure PCL scaffolds reveal that they are smooth and continuous and even have a uniform diameter and morphology like semi-crystalline polymeric materials. The fibers are packed tightly with a relatively low surface roughness, and the pore structure is largely influenced by the arrangement of fibers and not by their intrinsic porosity. This relatively low morphology indicates the hydrophobic character of PCL and its smooth surface may limit initial cell attachment. When MOF is incorporated into the PCL matrix, morphological changes are observed to be significant in the PCL+MOF scaffold.

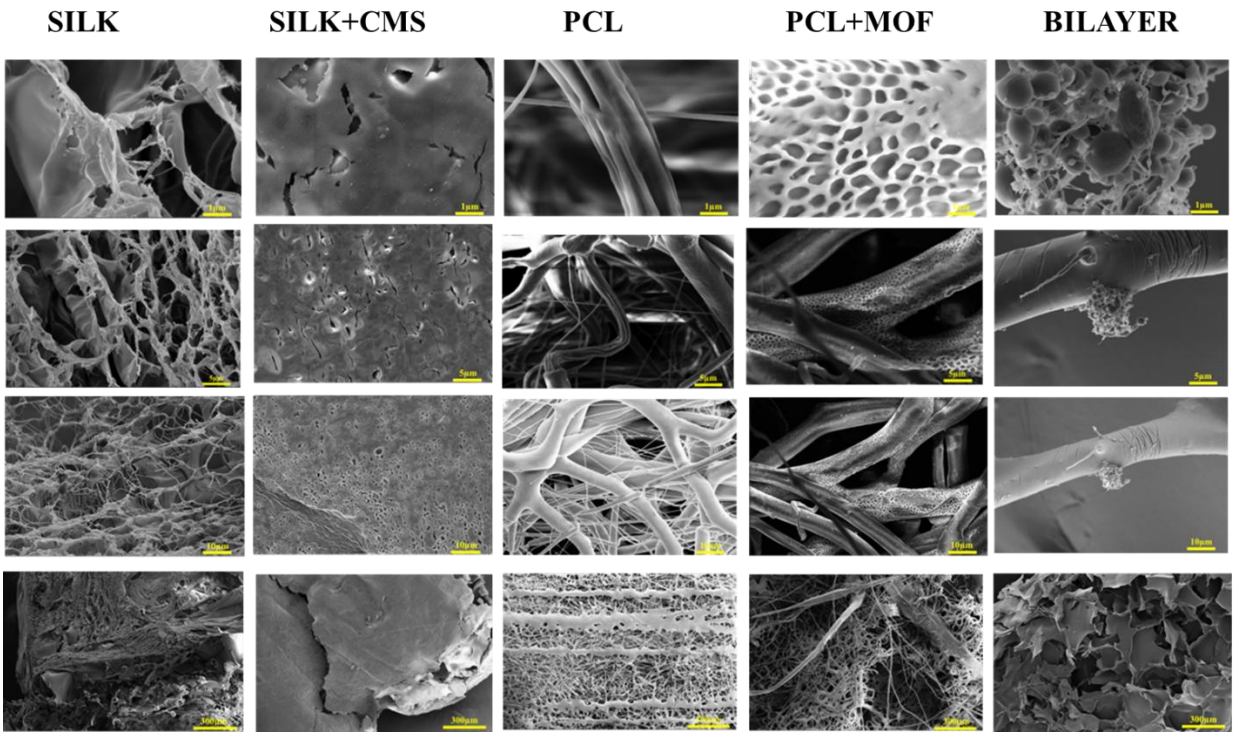

Figure 4. 3 FESEM Analysis of SF, SF+CMS, PCL, PCL+MOF and BL SCAFFOLD

The fiber surfaces are seen to become more pronounced and discrete particles of MOF are seen to be well dispersed along the fiber and embedded in them. This roughness on the surface area doubles the area and suggests high strength of interfacial adhesion between the PCL matrix and the MOF particles. MOF also helps in formation of micro and nano scale pores, which may make them bioactive and allow better cell adhesion. The bilayer (BL) scaffold has a unique layered structure which is a combination of morphological properties of the SF-based and PCL-based layers. The upper layer is porous and fibrous in nature and highly interconnected whereas the bottom layer is denser with smoother fibers which give structural support. The successful bilayer fabrication by the two layers is ensured by the transparent interface between the two layers. The porosity that is hierarchically distributed at various length scales indicates that the BL scaffold can be used to maintain mechanical stability and biological functionality at the same time. In general, FESEM analysis proves that the morphology of the scaffolds is largely dependent on the

material composition. The CMS and MOF incorporation increase surface roughness, porosity, and micro-structure complexities whereas bilayer design provides a versatile architecture that can be used in tissue engineering. These morphological characteristics will have a positive effect on cell adhesion, proliferation and tissue regeneration.

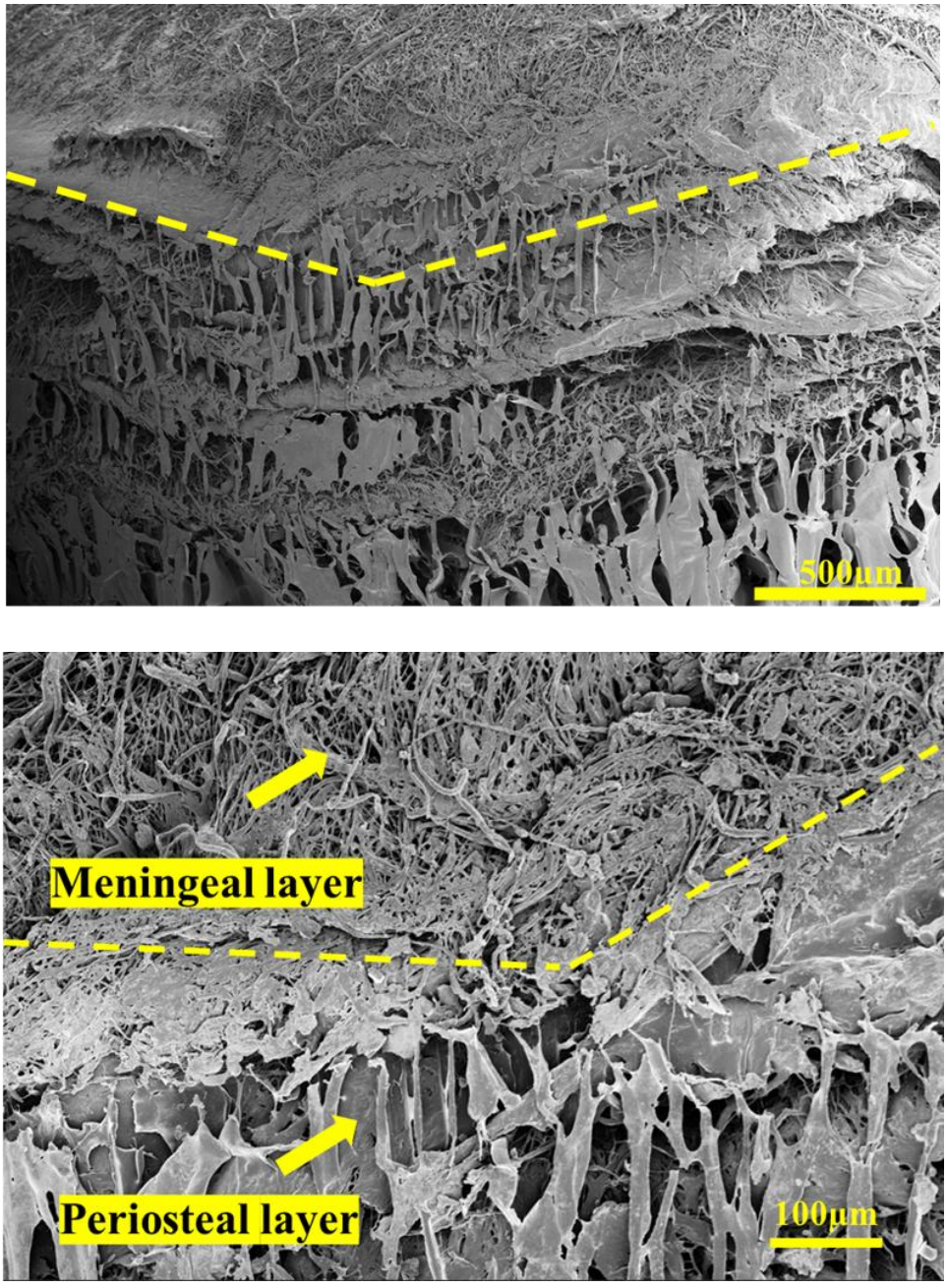

Figure 4.4 FE-SEM Cross-Section Area of BL Scaffold

4.2.5 Contact Angle

The contact angle tests were performed to determine the extent to which water spreads on the respective parts and the bilayer scaffold.

Table 4.3 Contact angle of the scaffolds

Sr.no	Contact Angle	Materials
1	55.66˚	SF
2	91.66˚	SF+CMS
3	106.6˚	PCL
4	111.38˚	PCL+MOF
5	52˚	BL(SF)
6	99˚	BL(PCL)

The whole issue that concerns the cells is their wettability that allows them to adhere and the material to prevent fluids. Pure silk was found to have a 55.66˚ contact angle implying that it was hydrophilic. This is because it contains polar groups that enable water to spread and stick to the cells. The contact angle was 91.66˚with the addition of calcium-magnesium silicates. This makes CMS alter the surface chemistry and roughness of silk they appear as having moderate wettability yet good in biology. Pure PCL possesses a high contact angle of 106.6˚ and displays that it is a hydrophobic material as its chains are not polar. The inclusion of metal-organic frameworks increased the angle of contact to 111.38˚ that is more hydrophobic, suitable to a water-resistant barrier. The bilayer scaffold is of wettability difference on either side. The contact angle of the silk side is 52˚ which is highly hydrophilic and that is suitable to cell attachment on the skull side. The contact angle of PCL side is 99˚ and it is hydrophobic that prevents the leakage of fluid on the brain surface. Anyway, the findings indicate that the bilayer scaffold exhibits variable wettability on both sides, as is the case with actual dura mater, and may be useful as a dural replacement.

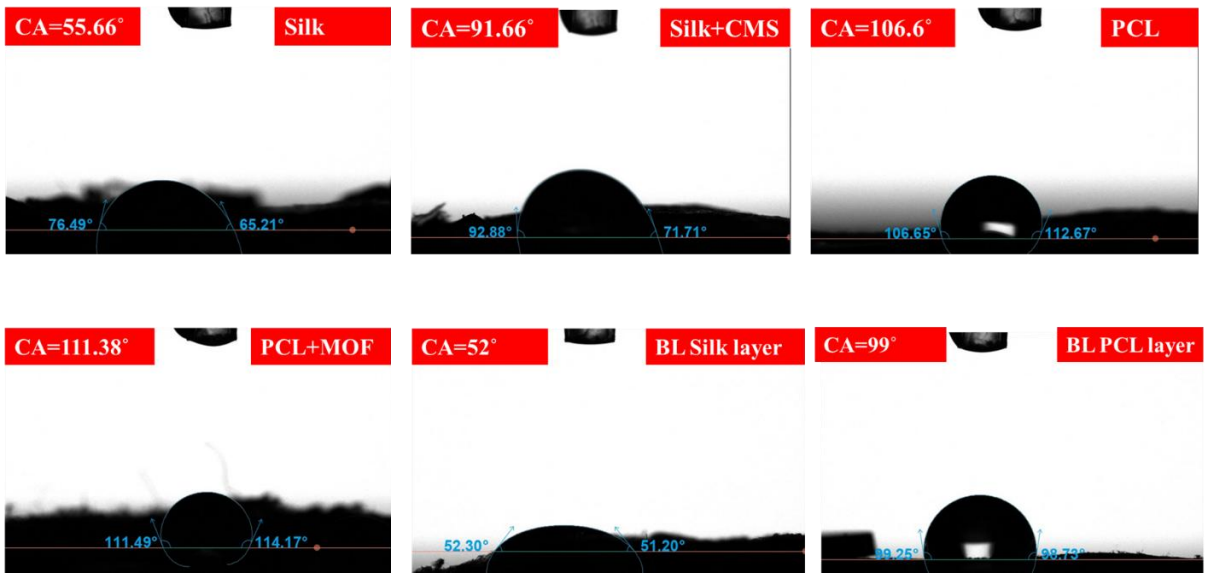

Figure 4. 5 Contact angle of SF, SF+CMS, PCL, PCL+MOF and BL SCAFFOLDS

4.2.6 Swelling ratio measurement

Swelling pattern of Silk, Silk+CMS, PCL, PCL +MOF and bilayer (BL) scaffold was studied based on the swelling ratio of the scaffold at varying time (2, 4, 8, and 24 hrs) as demonstrated in Figure 4.5. Swelling ratio of silk and Silk+CMS scaffold was remarkably higher than that of PCL based scaffold, which implied that both are hydrophilic. The Silk+ CMS scaffold showed the highest swelling at 24 hours, this increased swelling is due to hydrophilic hydroxyl and carboxyl groups in CMS, which increased water absorption. Pure silk too exhibited large swelling as it has porous structure and polar functional groups. Conversely, PCL and PCL+MOF scaffolds exhibited comparatively low swelling ratios during the research period indicating their hydrophobic nature and water absorption. Integration of MOF slightly enhanced the swelling ratio of PCL, probably because of enhanced roughness and micro-porosity on the surface. The bilayer scaffold had intermediate swelling characteristics with high water absorption capacity of the silk-based layer with the structural stability of the PCL-based layer. The statistical analysis revealed that there are significant differences between the groups ($p < 0.05$ to $***p < 0.0001$), which proves that the composition of scaffolds has a strong impact on swelling behavior.

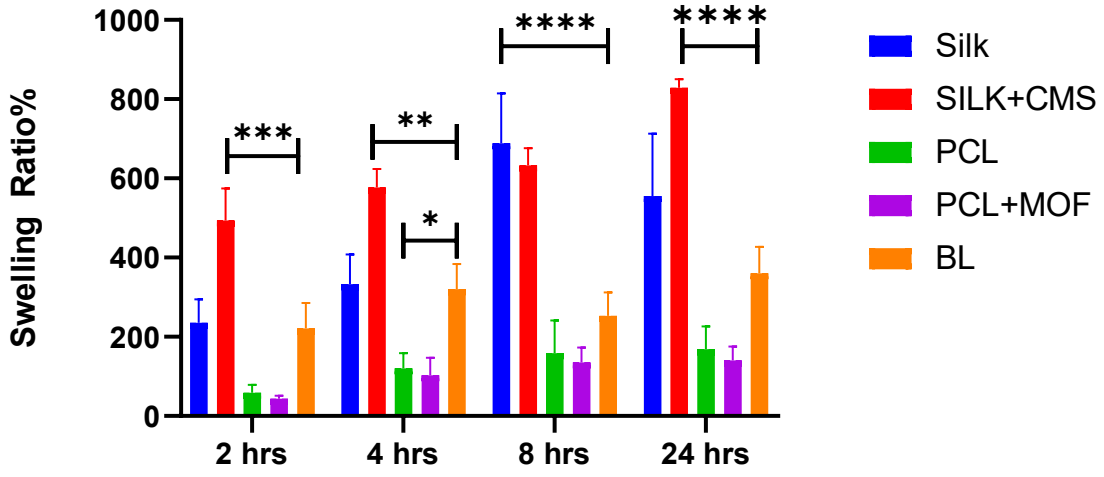

Figure 4.6 %Swelling measurement of SF, SF+CMS, PCL, PCL+MOF and BL scaffolds

4.2.7 Porosity Measurement

The porosity of the fabricated scaffolds is also important in tissue engineering practice because it directly affects nutrient diffusion, cell infiltration, waste removal, and overall vascularization potential. Figure 4.6 shows the percentage porosity of the various materials tested by means of the liquid displacement method. The findings show that the silk fibroin control, was the most porous with a porosity value of approximately 93 percent due to the high interconnection porous structure formed during freeze-drying of pure silk fibroin solutions. The addition of calcium-magnesium silicates (CMS) to silk fibroin, denoted as SILK +CMS caused a slight decrease in porosity to approximately 91. This is due to the higher viscosity and pore filling by hydrophilic CMS. However, open pore structure of the scaffold remained high porosity. On the other hand, the polycaprolactone (PCL) control scaffold had a much lower porosity of about 88 with the higher density of the microstructure typical of electrospun or solvent-cast PCL scaffolds, which tend to have smaller and less connected porosity. When the metal-organic framework (MOF) particles were added to the PCL, that is, PCL+MOF, the reduction to approximately 87 was minimal, which may be attributed to the fact that the MOF fillers are dense in nature and could fill the pore spaces or change the packing of the polymer chains during the fabrication process.

The bilayer scaffold (BL) composed of layers of the silk fibroin-based and PCL-based materials exhibited the lowest porosity in the groups studied at about 85 percent. The porosity decreased primarily because the two layers are fitted closer and because of inclusion of PCL. Naturally, PCL is less porous, and the entire structure becomes denser. Despite these modifications, porosity in all the scaffolds remained above 85 which is within the appropriate range of over 80 to allow cell migration and tissue growth in regenerative medicine. These findings indicate that scaffolds made of silk fibroin are more porous and that a bilayer structure and proper mixing of the two components can provide a good way to balance the mechanical properties and the biological functions of the pore by varying the pore properties.

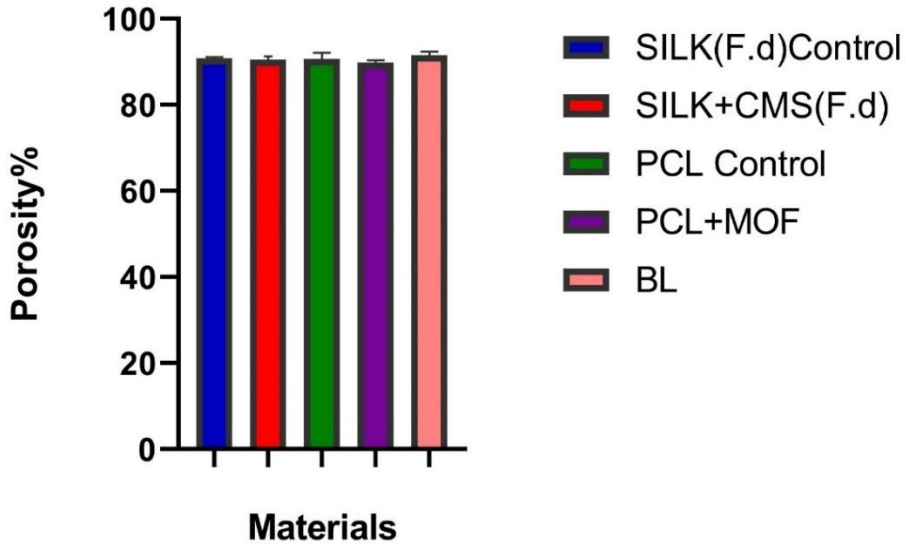

Figure 4. 7 %Porosity measurements of SF, SF+CMS, PCL, PCL+MOF, BL in absolute ethanol

4.2.8 Density Measurement

Another parameter of significance with regards to tissue engineering is apparent density of the scaffolds, which indicates the compactness of the material structure and is inversely related to porosity, which may affect mechanical properties, degradation rate, and the overall applicability of the scaffold to load-bearing applications or soft tissue applications. The density (in g/cm^3) of the prepared scaffolds is shown in Figure 4.7 obtained by the

standard mass-volume method. The freeze-dried silk fibroin control scaffold, SILK Control, was found to have the lowest density of about 0.14 g/cm^3, and its high density is attributed to its highly porous and lightweight structure created by the freeze-drying process with consequent low solid fraction and high volume. When calcium magnesium silicates were added to silk fibroin (SILK+CMS) ,the density enhanced significantly to about 0.17g/cm^3 which is enhanced by the addition of solid material(the hydrophilic CMS),leading to a densor scaffold structure. The PCL control scaffold was densely populated at a value of approximately 0.15 g/cm^3, a little greater than the pure silk fibroin control, which is indicative of the tighter microstructure of polycaprolactone-based materials produced through technologies like electrospinning or solvent casting. A further decrease in density by the incorporation of metal-organic framework (MOF) particles, denoted as PCL+MOF, to about 0.13 g/cm^3 may be due to the porosity of the incorporated MOF structures or changes in polymer packing that may create additional micro-voids. Silk fibroin-based and PCL-based bilayer scaffold (BL) exhibited the lowest density among the PCL-containing samples, approximately 0.12 g/cm^3,which helps the combined effect of the lighter silk layer with small gaps between two layers.. In sum, the scaffolds were all low densities (0.12-0.17 g/cm^3) which is beneficial to recapitulate the low densities of the native extracellular matrix and ease of manipulation during implantation. These findings are the opposite of porosity data, which proves that the higher the porosity, the lower the density, and illustrates that compositional variations and fabrication techniques allow controlling the scaffold density accordingly.

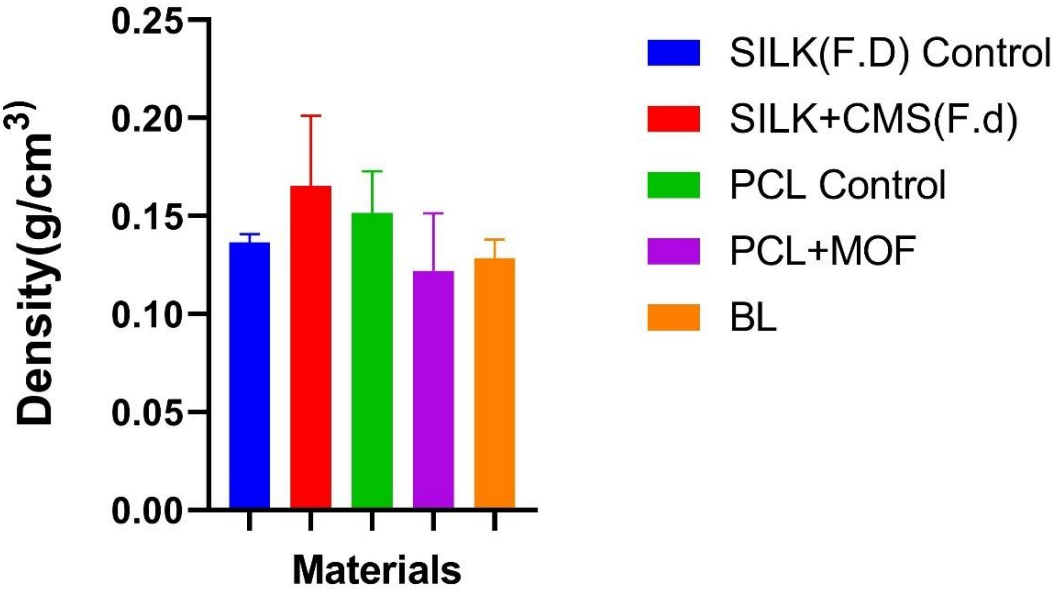

Figure 4.8: Density measurement of SF, SF+CMS, PCL, PCL+MOF and BL scaffolds

4.2.9 *In vitro*-Degradation studies

In vitro degradation of the scaffolds was determined by determining the percentage weight loss in 28 days in PBS (pH 7.4) at 37˚C, which mimicked the physiological conditions. Figure 4.8 gives the profiles of degradation of all groups, and the statistical significance is indicated ($p = 0.05$, $p = 0.001$). On day 01, initially all scaffolds shows minimal amount of degradation. Among all these samples, silk fibroin showed the highest weight loss about 7% while bilayer scaffold showed lowest weight loss about 3%. This results indicates that bilayer scaffold is more stable having the combined layers PCL+MOF. On day 07, SILK+CMS had the greatest weight loss (~11%), which was due to an increase in water intake by hydrophilic CMS. PCL scaffolds (PCL Control and PCL + MOF) were stable (~4-5%), which is consistent with the slow hydrolysis of PCL. Silk-based scaffolds degraded much quicker at day 14 and day 28; SILK attained a value of approximately 22% and SILK+CMS attained a value of approximately 14% by day 28 ($p < 0.001$).On day 28, However, PCL control (~9%), PCL+MOF (~7%), and BL (~10%) exhibited significantly lower degradation indicating PCL resistance to hydrolysis. These findings show that PCL-

based scaffolds are more stable, whereas fibroin-based, in the form of silk scaffolds, achieve relatively rapid degradation, which is appropriate in early-stage tissue remodeling. The bilayer scaffold provides an intermediate, balanced degradation profile and thus has potential usage in applications where staged tissue regeneration is needed.

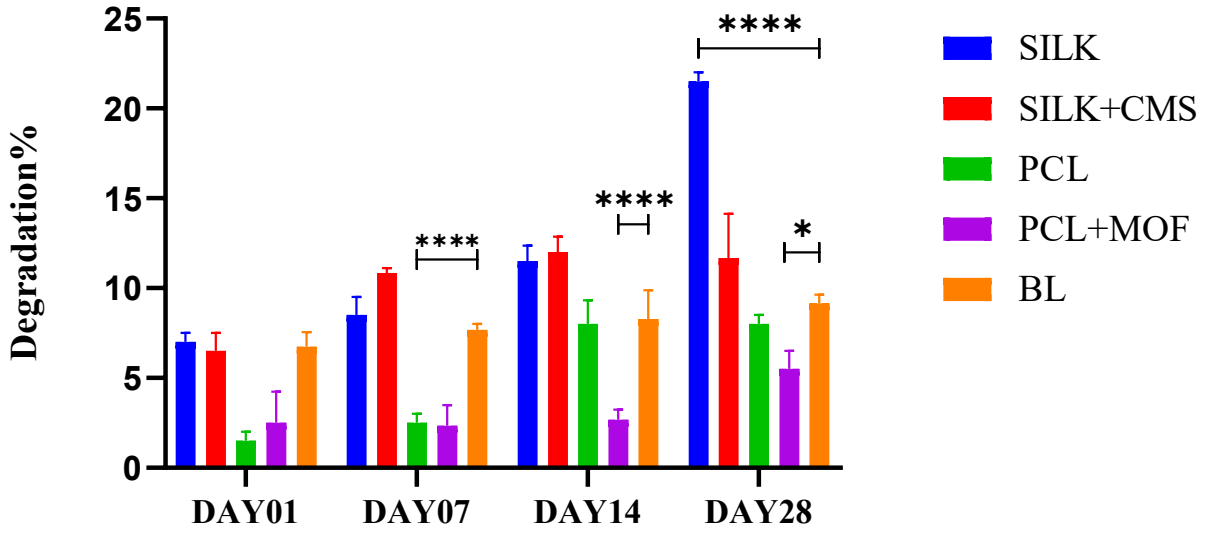

Figure 4. 9: %Degradation profile of scaffolds after 1, 7, 14 and 28 days

4.2.10 Cell Migration Study

Migration of cells is an important process of wound healing. It takes healing cells to the injured area allowing new tissue and blood vessels to grow. In the scaffold guided healing, the scaffold should assist cells in proper movements to blend properly with the tissue. This experiment was an examination of cell motion on various types of scaffolds by a scratching test. We cultured fibroblast cells on silk fibroin (SF), silk fibroin plus calcium magnesium silicates (SF+CMS), polycaprolactone (PCL) and polycaprolactone plus MOF (PCL+MOF) and bilayer scaffold (BL) respectively. Fig:10 indicated that scaffolds healed wounds within 24 hours, however, rates and degree of movement differed with scaffold. The most effective was SF with regards to cell movement. Cells became adherent, dispersed, extended and migrated towards the wound. PCL cells were slower, less spread and the wound closed later, and this could be since PCL is water repelling and inactive in

terms of bioactivity. The addition of CMS to silk enhanced movement. The wound of SF+CMS was also repaired more evenly and faster than SF due to the sticky property of the proteins and cell interaction of the new hydrophilic groups. In the same context, PCL+MOF was superior to plain PCL since MOF raised the activity of the surface and provided increased signals to cells to attach and migrate. The most successful scaffold was the bilayer scaffold (BL) with the most successful cell movement. Cells on BL plugged the wound out, regenerated the scratch and demonstrated active directed migration. The reason behind this is that the layer of silk is very attractive and distributes cells whereas the layer of PCL is supportive but not resistant to movement. The combination of them provides a setting in which cells can move optimally and in an organized manner. To conclude, cell movement is regulated by the scaffold material and the surface variations. Bilayer scaffold is an excellent wound healing design since the cells can enter fast and move together, which is essential in effective tissue repair and healing of the wound.

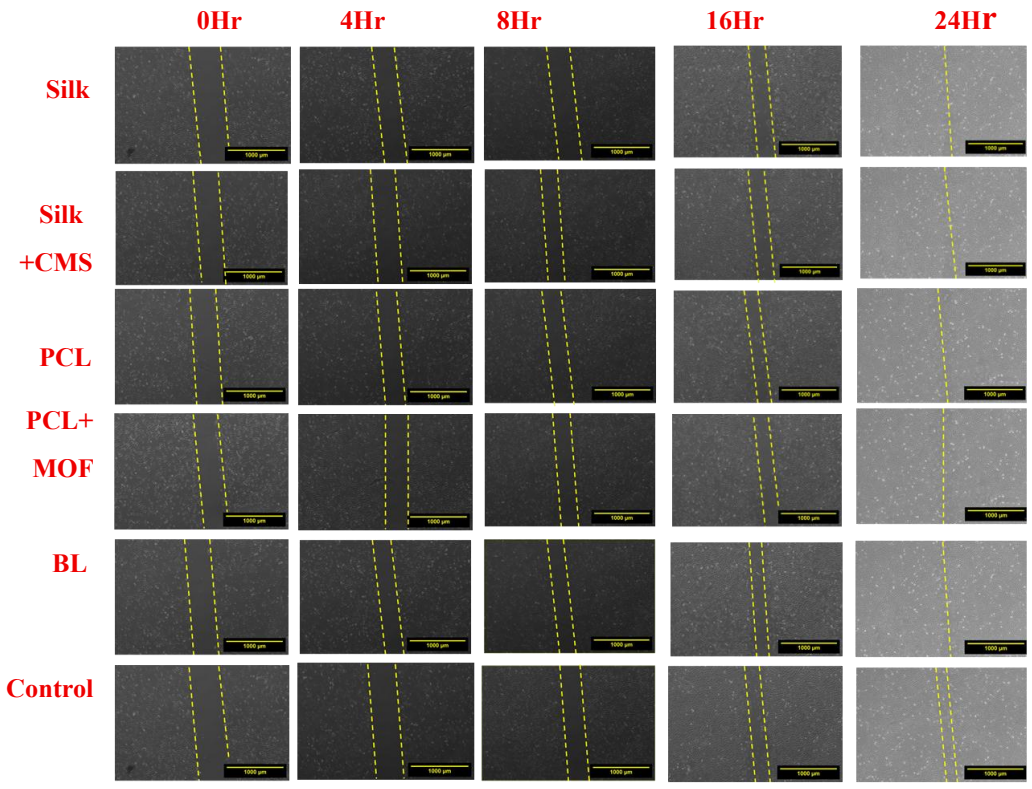

Figure 4. 10: Migration Assay of SF, SF+CMS, PCL, PCL+MOF, BL and Control scaffolds

Chapter 05

Conclusion

Dura mater regeneration Bilayered scaffolds were successfully prepared using an electrospinning method with silk, silk-carboxymethyl silk (silk+CMS), poly(ε-caprolactone) (PCL), and PCL+metal-organic (PCL+MOF). Such bilayer structure was aimed at bringing together the positive biological characteristics of natural polymers and mechanical stability and controlled degradation of synthetic polymers and satisfy the functional needs of dura mater repair. The FTIR analysis showed that all components had characteristic functional groups and there was slight difference in intensity which appeared to correspond to the physical interaction between the polymers. The bilayer scaffolds were optimally hydrophilic and interconnected porous, which allowed cell adhesion, cell proliferation, nutrient diffusion, and tissue integration. SEM showed a homogenous fibrous structure and oriented fibers and homogeneous distribution of MOFs which is like the extracellular matrix of the dura mater as it is. The porosity, swelling, density, and degradation analysis indicated that the scaffolds had adequate structural strength and degradation characteristic that is in tandem with dura mater healing needs. In vitro cell research validated the observation and cell experiments of great cytocompatibility, high cell viability and low cytotoxicity, and MOF-based scaffolds exhibited superior cellular activity and migration. All in all, the produced silk/PCL-based bilayer scaffolds offer a low-cost, biocompatible, and structurally suitable platform, and it is possible to emphasize that they have a great future potential in the realm of dura mater repairs, but additional ex vivo and in vivo experiments would have to be conducted to prove that these materials can be utilized in clinical practice.

References

1. De Kegel, D., et al., *Biomechanical characterization of human dura mater.* Journal of the mechanical behavior of biomedical materials, 2018. **79**: p. 122-134.
2. Bi, X., et al., *Applications of materials for dural reconstruction in pre-clinical and clinical studies: advantages and drawbacks, efficacy, and selections.* Materials Science and Engineering: C, 2020. **117**: p. 111326.
3. Zhu, T., et al., *High efficacy of tetra-PEG hydrogel sealants for sutureless dural closure.* Bioactive materials, 2022. **8**: p. 12-19.
4. Cohen-Gadol, A.A., et al., *Surgical anatomy of dural defects in spontaneous spinal cerebrospinal fluid leaks.* Operative Neurosurgery, 2006. **58**(4): p. ONS-238-ONS-245.
5. Harvey, R.J., et al., *Endoscopic skull base reconstruction of large dural defects: a systematic review of published evidence.* The Laryngoscope, 2012. **122**(2): p. 452-459.
6. Briggs, R. and P.J. Wormald, *Endoscopic transnasal intradural repair of anterior skull base cerebrospinal fluid fistulae.* Journal of Clinical Neuroscience, 2004. **11**(6): p. 597-599.
7. Harvey, R.J., et al., *Intracranial complications before and after endoscopic skull base reconstruction.* American journal of rhinology, 2008. **22**(5): p. 516-521.
8. Wang, E., et al., *ICAR: endoscopic skull-base surgery. Int Forum Allergy Rhinol 9: S145–S365*. 2019.
9. Kassam, A., et al., *Evolution of reconstructive techniques following endoscopic expanded endonasal approaches.* Neurosurgical focus, 2005. **19**(1): p. 1-7.
10. Koutourousiou, M., et al., *Endoscopic endonasal approach for resection of cranial base chordomas: outcomes and learning curve.* Neurosurgery, 2012. **71**(3): p. 614-625.
11. Cavallo, L.M., et al., *Endoscopic endonasal transsphenoidal surgery: history and evolution.* World neurosurgery, 2019. **127**: p. 686-694.
12. Van Calenbergh, F., et al., *The use of Vicryl Collagen® as a dura substitute: A clinical review of 78 surgical cases.* Acta neurochirurgica, 1997. **139**(2): p. 120-123.
13. Ramot, Y., et al., *Local tolerance and biodegradability of a novel artificial dura mater graft following implantation onto a dural defect in rabbits.* Toxicologic Pathology, 2020. **48**(6): p. 738-746.
14. Pogorielov, M., et al., *Experimental evaluation of new chitin–chitosan graft for duraplasty.* Journal of Materials Science: Materials in Medicine, 2017. **28**(2): p. 34.
15. Deb, P., et al., *Scaffold development using biomaterials: a review.* Materials Today: Proceedings, 2018. **5**(5): p. 12909-12919.
16. Fielding, G.A., A. Bandyopadhyay, and S. Bose, *Effects of silica and zinc oxide doping on mechanical and biological properties of 3D printed tricalcium phosphate tissue engineering scaffolds.* Dental materials, 2012. **28**(2): p. 113-122.

17. Jin, S., et al., *A double-layer dura mater based on poly (caprolactone-co-lactide) film and polyurethane sponge: preparation, characterization, and biodegradation study.* Journal of Materials Chemistry B, 2021. **9**(18): p. 3863-3873.
18. Chauvet, D., et al., *Histological and biomechanical study of dura mater applied to the technique of dura splitting decompression in Chiari type I malformation.* Neurosurgical review, 2010. **33**(3): p. 287-295.
19. Barber, S.M., et al., *Cerebrospinal fluid leaks after spine tumor resection: avoidance, recognition and management.* Annals of Translational Medicine, 2019. **7**(10): p. 217.
20. Protasoni, M., et al., *The collagenic architecture of human dura mater.* Journal of neurosurgery, 2011. **114**(6): p. 1723-1730.
21. Dasgupta, K. and J. Jeong, *Developmental biology of the meninges.* genesis, 2019. **57**(5): p. e23288.
22. Nagel, S.J., et al., *Spinal dura mater: biophysical characteristics relevant to medical device development.* Journal of medical engineering & technology, 2018. **42**(2): p. 128-139.
23. Wang, W. and Q. Ao, *Research and application progress on dural substitutes.* Journal of Neurorestoratology, 2019. **7**(4): p. 161-170.
24. Patel, N. and O. Kirmi. *Anatomy and imaging of the normal meninges*. in *Seminars in Ultrasound, CT and MRI*. 2009. Elsevier.
25. Louveau, A., et al., *Structural and functional features of central nervous system lymphatic vessels.* Nature, 2015. **523**(7560): p. 337-341.
26. Kinaci, A., et al., *Histologic comparison of the dura mater among species.* Comparative medicine, 2020. **70**(2): p. 170-175.
27. Komotar, R.J., et al., *Endoscopic endonasal versus open repair of anterior skull base CSF leak, meningocele, and encephalocele: a systematic review of outcomes.* Journal of Neurological Surgery Part A: Central European Neurosurgery, 2013. **74**(04): p. 239-250.
28. Epstein, N.E., *A review article on the diagnosis and treatment of cerebrospinal fluid fistulas and dural tears occurring during spinal surgery.* Surgical Neurology International, 2013. **4**(Suppl 5): p. S301.
29. Jing, Y., et al., *Repair of dural defects with electrospun bacterial cellulose membranes in a rabbit experimental model.* Materials Science and Engineering: C, 2020. **117**: p. 111246.
30. Deng, K., et al., *Evaluation of efficacy and biocompatibility of a new absorbable synthetic substitute as a dural onlay graft in a large animal model.* Neurological Research, 2016. **38**(9): p. 799-808.
31. Laun, A., J. Tonn, and C. Jerusalem, *Comparative study of lyophilized human dura mater and lyophilized bovine pericardium as dural substitutes in neurosurgery.* Acta neurochirurgica, 1990. **107**(1): p. 16-21.
32. Lin, T.-Y., et al., *Postoperative meningitis after spinal surgery: a review of 21 cases from 20,178 patients.* BMC infectious diseases, 2014. **14**(1): p. 220.
33. Yu, F., et al., *Current developments in dural repair: a focused review on new methods and materials.* Front Biosci (Landmark Ed), 2013. **18**(4): p. 1335-1343.

34. Kinaci, A., et al., *Ex vivo evaluation of a multilayered sealant patch for watertight dural closure: cranial and spinal models.* Journal of Materials Science: Materials in Medicine, 2021. **32**(8): p. 85.
35. Huang, Y.-C., et al., *Photo-crosslinked hyaluronic acid/carboxymethyl cellulose composite hydrogel as a dural substitute to prevent post-surgical adhesion.* International journal of molecular sciences, 2022. **23**(11): p. 6177.
36. Louis Jr, R.G., et al., *Harvest of autologous clavipectoral fascia for use in duraplasty: cadaveric feasibility study.* Journal of Craniofacial Surgery, 2013. **24**(2): p. 619-621.
37. Wang, L., et al., *Novel bilayer wound dressing composed of SIS membrane with SIS cryogel enhanced wound healing process.* Materials Science and Engineering: C, 2018. **85**: p. 162-169.
38. Shi, Z., et al., *A new absorbable synthetic substitute with biomimetic design for dural tissue repair.* Artificial organs, 2016. **40**(4): p. 403-413.
39. Xu, Y., et al., *Hierarchical micro/nanofibrous bioscaffolds for structural tissue regeneration.* Advanced healthcare materials, 2017. **6**(13): p. 1601457.
40. Abuzayed, B., et al., *Duraplasty using autologous fascia lata reenforced by on-site pedicled muscle flap.* Journal of craniofacial surgery, 2009. **20**(2): p. 435-438.
41. Pařízek, J., et al., *Detailed evaluation of 2959 allogeneic and xenogeneic dense connective tissue grafts (fascia lata, pericardium, and dura mater) used in the course of 20 years for duraplasty in neurosurgery.* Acta neurochirurgica, 1997. **139**(9): p. 827-838.
42. Eichberg, D.G., et al., *The use of dehydrated amniotic membrane allograft for augmentation of dural closure in craniotomies and endoscopic endonasal transphenoidal surgeries.* British journal of neurosurgery, 2018. **32**(5): p. 516-520.
43. Turchan, A., et al., *Duraplasty using amniotic membrane versus temporal muscle fascia: a clinical comparative study.* Journal of Clinical Neuroscience, 2018. **50**: p. 272-276.
44. Islam, S., et al., *Usefulness of acellular dermal graft as a dural substitute in experimental model.* Surgical neurology, 2004. **61**(3): p. 297-302.
45. He, S.-k., et al., *Efficacy and safety of small intestinal submucosa in dural defect repair in a canine model.* Materials Science and Engineering: C, 2017. **73**: p. 267-274.
46. Neulen, A., et al., *Evaluation of efficacy and biocompatibility of a novel semisynthetic collagen matrix as a dural onlay graft in a large animal model.* Acta neurochirurgica, 2011. **153**(11): p. 2241-2250.
47. Zerris, V.A., et al., *Repair of the dura mater with processed collagen devices.* Journal of Biomedical Materials Research Part B: Applied Biomaterials: An Official Journal of the Society for Biomaterials, the Japanese Society for Biomaterials, and the Australian Society for Biomaterials and the Korean Society for Biomaterials, 2007. **83**(2): p. 580-588.
48. Narotam, P.K., et al., *Collagen matrix (DuraGen) in dural repair: analysis of a new modified technique.* Spine, 2004. **29**(24): p. 2861-2867.

49. Cappabianca, P., et al., *Use of equine collagen foil as dura mater substitute in endoscopic endonasal transsphenoidal surgery.* Surgical neurology, 2006. **65**(2): p. 144-148.
50. So, J., et al., *Sandwich technique using fibrin-coated collagen fleece for sellar reconstruction in large dural defects during transsphenoidal surgery.* Journal of Clinical Neuroscience, 2017. **43**: p. 256-260.
51. Kim, D.W., et al., *A transparent artificial dura mater made of silk fibroin as an inhibitor of inflammation in craniotomized rats.* Journal of neurosurgery, 2011. **114**(2): p. 485-490.
52. Sandoval-Sánchez, J.H., et al., *A new bilayer chitosan scaffolding as a dural substitute: experimental evaluation.* World neurosurgery, 2012. **77**(3-4): p. 577-582.
53. Barbolt, T.A., et al., *Biocompatibility evaluation of dura mater substitutes in an animal model.* Neurological research, 2001. **23**(8): p. 813-820.
54. RAUL, J.-S., et al., *Utilisation du polyester uréthane (Neuro-Patch®) comme substitut dural: Etude prospective sur 70 cas.* Neuro-chirurgie (Paris), 2003. **49**(2-3): p. 83-89.
55. Sugawara, T., et al., *Novel dural closure technique using polyglactin acid sheet prevents cerebrospinal fluid leakage after spinal surgery.* Operative Neurosurgery, 2005. **57**(4): p. 290-294.
56. Mohtaram, N., et al., *Development of a glial cell-derived neurotrophic factor-releasing artificial dura for neural tissue engineering applications.* Journal of Materials Chemistry B, 2015. **3**(40): p. 7974-7985.
57. Wee, J.H., et al., *Stem cell laden nano and micro collagen/PLGA bimodal fibrous patches for myocardial regeneration.* Biomaterials Research, 2022. **26**(1): p. 79.
58. Shi, R., et al., *Fabrication and evaluation of a homogeneous electrospun PCL–gelatin hybrid membrane as an anti-adhesion barrier for craniectomy.* Journal of Materials Chemistry B, 2015. **3**(19): p. 4063-4073.
59. Wang, J., et al., *Biodegradable polymer membranes applied in guided bone/tissue regeneration: a review.* Polymers, 2016. **8**(4): p. 115.
60. Gomes, S., et al., *Evaluation of nanofibrous scaffolds obtained from blends of chitosan, gelatin and polycaprolactone for skin tissue engineering.* International journal of biological macromolecules, 2017. **102**: p. 1174-1185.
61. Huang, Y., et al., *Bilayered antimicrobial nanofiber membranes for wound dressings via in situ cross-linking polymerization and electrospinning.* Industrial & Engineering Chemistry Research, 2018. **57**(50): p. 17048-17057.
62. Şafak, Ş., et al., *In vitro evaluation of electrospun polysaccharide based nanofibrous mats as surgical adhesion barriers.* Textile and Apparel, 2020. **30**(2): p. 99-107.
63. Siracusa, V., G. Maimone, and V. Antonelli, *State-of-art of standard and innovative materials used in cranioplasty.* Polymers, 2021. **13**(9): p. 1452.
64. Yin, G.-Z. and X.-M. Yang, *Biodegradable polymers: a cure for the planet, but a long way to go.* Journal of Polymer Research, 2020. **27**(2): p. 38.
65. Amini, A.R., C.T. Laurencin, and S.P. Nukavarapu, *Bone tissue engineering: recent advances and challenges.* Critical Reviews™ in Biomedical Engineering, 2012. **40**(5).

66. Bai, W., et al., *Application of PLGA/type I collagen/chitosan artificial composite dura mater in the treatment of dural injury.* Journal of Materials Science: Materials in Medicine, 2013. **24**(9): p. 2247-2254.
67. Mabrouk, M., H.H. Beherei, and D.B. Das, *Recent progress in the fabrication techniques of 3D scaffolds for tissue engineering.* Materials Science and Engineering: C, 2020. **110**: p. 110716.
68. Naahidi, S., et al., *Biotechnol. Adv*. 2017.
69. Porter, J.R., T.T. Ruckh, and K.C. Popat, *Bone tissue engineering: a review in bone biomimetics and drug delivery strategies.* Biotechnology progress, 2009. **25**(6): p. 1539-1560.
70. Kumbhar, S. and S. Pawar, *Self-functionalized, oppositely charged chitosan-alginate scaffolds for biomedical applications.* BioTechnology: An Indian Journal, 2017. **13**(2): p. 1-15.
71. Eltom, A., G. Zhong, and A. Muhammad, *Scaffold Techniques and Designs in Tissue Engineering Functions and Purposes: A Review.* Advances in Materials Science and Engineering, 2019. **2019**(1): p. 3429527.
72. Pina, S., et al., *Biofunctional Ionic-Doped Calcium Phosphates: Silk Fibroin Composites for Bone Tissue Engineering Scaffolding.* Cells Tissues Organs, 2017. **204**: p. 150 - 163.
73. Guarino, V., et al., *Design and manufacture of microporous polymeric materials with hierarchal complex structure for biomedical application.* Materials Science and Technology, 2008. **24**(9): p. 1111-1117.
74. Aizenberg, J. and P. Fratzl, *Biological and Biomimetic Materials.* Advanced Materials, 2009. **21**(4): p. 387-388.
75. Freund, R., et al., *The Current Status of MOF and COF Applications.* Angewandte Chemie International Edition, 2021. **60**(45): p. 23975-24001.
76. Liu, C., et al., *MOF-on-MOF hybrids: Synthesis and applications.* Coordination Chemistry Reviews, 2021. **432**: p. 213743.
77. Ikada, Y., *Challenges in tissue engineering.* Journal of the Royal Society Interface, 2006. **3**(10): p. 589-601.
78. Chapekar, M.S., *Tissue engineering: challenges and opportunities.* Journal of Biomedical Materials Research: An Official Journal of The Society for Biomaterials, The Japanese Society for Biomaterials, and The Australian Society for Biomaterials and the Korean Society for Biomaterials, 2000. **53**(6): p. 617-620.
79. Khademhosseini, A., J.P. Vacanti, and R. Langer, *Progress in tissue engineering.* Scientific American, 2009. **300**(5): p. 64-71.
80. Lavik, E. and R. Langer, *Tissue engineering: current state and perspectives.* Applied microbiology and biotechnology, 2004. **65**(1): p. 1-8.
81. Stock, U.A. and J.P. Vacanti, *Tissue engineering: current state and prospects.* Annual review of medicine, 2001. **52**(1): p. 443-451.
82. Shafiee, A. and A. Atala, *Tissue engineering: toward a new era of medicine.* Annual review of medicine, 2017. **68**(1): p. 29-40.
83. Atala, A. and R. Lanza, *Methods of tissue engineering*. 2002: Gulf professional publishing.

84. Vacanti, C.A. and J.P. Vacanti, *The science of tissue engineering.* Orthopedic Clinics, 2000. **31**(3): p. 351-355.
85. Jia, W., et al., *Design and comprehensive assessment of a biomimetic tri-layer tubular scaffold via biodegradable polymers for vascular tissue engineering applications.* Materials Science and Engineering: C, 2020. **110**: p. 110717.
86. Ruan, S.-q., et al., *Preparation of a biphase composite scaffold and its application in tissue engineering for femoral osteochondral defects in rabbits.* International Orthopaedics, 2017. **41**(9): p. 1899-1908.
87. Ambekar, R.S. and B. Kandasubramanian, *Progress in the advancement of porous biopolymer scaffold: tissue engineering application.* Industrial & Engineering Chemistry Research, 2019. **58**(16): p. 6163-6194.
88. Nagam Hanumantharao, S. and S. Rao, *Multi-functional electrospun nanofibers from polymer blends for scaffold tissue engineering.* Fibers, 2019. **7**(7): p. 66.
89. Xu, L., et al., *Bioprinting small diameter blood vessel constructs with an endothelial and smooth muscle cell bilayer in a single step.* Biofabrication, 2020. **12**(4): p. 045012.
90. Pu, J. and K. Komvopoulos, *Mechanical properties of electrospun bilayer fibrous membranes as potential scaffolds for tissue engineering.* Acta Biomaterialia, 2014. **10**(6): p. 2718-2726.
91. Norouzi, S.K. and A. Shamloo, *Bilayered heparinized vascular graft fabricated by combining electrospinning and freeze drying methods.* Materials Science and Engineering: C, 2019. **94**: p. 1067-1076.
92. Melchor-Martínez, E.M., et al., *Modern world applications for nano-bio materials: tissue engineering and COVID-19.* Frontiers in Bioengineering and Biotechnology, 2021. **9**: p. 597958.
93. Basu, B., *Biomaterials science and tissue engineering: principles and methods*. 2017: Cambridge University Press.
94. Silver, F., *Biomaterials, Medical Devices and Tissue Engineering: An Integrated Approach: An Integrated Approach*. 1993: Springer Science & Business Media.
95. CHEN, B., D. WANG, and L. FENG, *Effects of physical and chemical properties of tissue engineered material surface on cell compatibility.* Chinese Journal of Tissue Engineering Research, 2007: p. 197-200.
96. Iwaki, R., et al., *Current status of developing tissue engineering vascular technologies.* Expert Opinion on Biological Therapy, 2022. **22**(3): p. 433-440.
97. Sittinger, M., *Tissue engineering: artificial tissue replacement containing vital components.* Laryngo-Rhino-Otologie, 1995. **74**(11): p. 695-699.
98. Luo, Z., et al., *Welcome to BIO Integration 2025: Embracing a New Era in Biomaterials and Clinical Therapy.* BIO Integration, 2025. **6**(1): p. 995.
99. Duarte Campos, D.F., et al., *Hand-held bioprinting for de novo vascular formation applicable to dental pulp regeneration.* Connective Tissue Research, 2020. **61**(2): p. 205-215.
100. Das, M., et al., *Synergetic reinforcing effect of graphene oxide and nanosilver on carboxymethyl cellulose/sodium alginate nanocomposite films: Assessment of physicochemical and antibacterial properties.* International Journal of Biological Macromolecules, 2023. **239**: p. 124185.

101. Ma, J., et al., *Instability-Driven 3D bioprinting for engineering composite bio-inks.* Engineered Regeneration, 2024. **5**(3): p. 350-360.
102. Boccaccini, A.R. and J.J. Blaker, *Bioactive composite materials for tissue engineering scaffolds.* Expert review of medical devices, 2005. **2**(3): p. 303-317.
103. Makris, E.A., et al., *Repair and tissue engineering techniques for articular cartilage.* Nature Reviews Rheumatology, 2015. **11**(1): p. 21-34.
104. Zulkifli, M.Z.A., et al., *Overview of electrospinning for tissue engineering applications.* Polymers, 2023. **15**(11): p. 2418.
105. Martins, A., R. Reis, and N. Neves, *Electrospinning: processing technique for tissue engineering scaffolding.* International Materials Reviews, 2008. **53**(5): p. 257-274.
106. Lannutti, J., et al., *Electrospinning for tissue engineering scaffolds.* Materials Science and Engineering: C, 2007. **27**(3): p. 504-509.
107. Muthukrishnan, L., *An overview on electrospinning and its advancement toward hard and soft tissue engineering applications.* Colloid and Polymer Science, 2022. **300**(8): p. 875-901.
108. Khorshidi, S., et al., *A review of key challenges of electrospun scaffolds for tissue-engineering applications.* Journal of tissue engineering and regenerative medicine, 2016. **10**(9): p. 715-738.
109. Sill, T.J. and H.A. Von Recum, *Electrospinning: applications in drug delivery and tissue engineering.* Biomaterials, 2008. **29**(13): p. 1989-2006.
110. Hong, J., et al., *Cell-electrospinning and its application for tissue engineering.* International journal of molecular sciences, 2019. **20**(24): p. 6208.
111. Fereshteh, Z., *Freeze-drying technologies for 3D scaffold engineering*, in *Functional 3D tissue engineering scaffolds*. 2018, Elsevier. p. 151-174.
112. Angraini, N., et al., *Advancements in Bone Tissue Engineering: A Comprehensive Review of Biomaterial Scaffolds and Freeze-Drying Techniques From Perspective Global and Future Research.* Artificial Organs, 2025.
113. Sultana, N. and M. Wang, *Fabrication of Tissue Engineering Scaffolds Using the Emulsion Freezing/Freeze-drying Technique and Characteristics of the Scaffolds.* Integrated Biomaterials in Tissue Engineering, 2012: p. 63-89.
114. Lv, Q. and Q. Feng, *Preparation of 3-D regenerated fibroin scaffolds with freeze drying method and freeze drying/foaming technique.* Journal of Materials Science: Materials in Medicine, 2006. **17**(12): p. 1349-1356.
115. Kang, H.-W., Y. Tabata, and Y. Ikada, *Fabrication of porous gelatin scaffolds for tissue engineering.* Biomaterials, 1999. **20**(14): p. 1339-1344.
116. Vepari, C. and D.L. Kaplan, *Silk as a biomaterial.* Progress in polymer science, 2007. **32**(8-9): p. 991-1007.
117. Holland, C., et al., *The biomedical use of silk: past, present, future.* Advanced healthcare materials, 2019. **8**(1): p. 1800465.
118. Asakura, T., S. Kametani, and Y. Suzuki, *Silk.* Encyclopedia of polymer science and technology, 2002: p. 1-19.
119. Schoeser, M., *Silk*. 2007: Yale University Press.
120. Ebrahimi, D., et al., *Silk–its mysteries, how it is made, and how it is used.* ACS biomaterials science & engineering, 2015. **1**(10): p. 864-876.

121. Sahoo, J.K., et al., *Silk chemistry and biomedical material designs.* Nature Reviews Chemistry, 2023. **7**(5): p. 302-318.
122. Wang, C., et al., *Silk-based advanced materials for soft electronics.* Accounts of Chemical Research, 2019. **52**(10): p. 2916-2927.
123. Thurber, A.E., F.G. Omenetto, and D.L. Kaplan, *In vivo bioresponses to silk proteins.* Biomaterials, 2015. **71**: p. 145-157.
124. Omenetto, F.G. and D.L. Kaplan, *A new route for silk.* Nature Photonics, 2008. **2**(11): p. 641-643.
125. Kundu, B., et al., *Silk fibroin biomaterials for tissue regenerations.* Advanced drug delivery reviews, 2013. **65**(4): p. 457-470.
126. Reddy, R.M. and G.V. Prasad, *Silk-the prospective and compatible bio-material for advanced functional applications.* Trends in Applied Sciences Research, 2011. **6**(1): p. 89.
127. Leal-Egaña, A. and T. Scheibel, *Silk-based materials for biomedical applications.* Biotechnology and applied biochemistry, 2010. **55**(3): p. 155-167.
128. Jastrzebska, K., et al., *Silk as an innovative biomaterial for cancer therapy.* Reports of Practical Oncology and Radiotherapy, 2015. **20**(2): p. 87-98.
129. Malikmammadov, E., et al., *PCL and PCL-based materials in biomedical applications.* Journal of Biomaterials science, Polymer edition, 2018. **29**(7-9): p. 863-893.
130. Grann, M., *The PCL–R and gender.* European Journal of Psychological Assessment, 2000. **16**(3): p. 147.
131. Montgomery, S.R., et al., *Surgical management of PCL injuries: indications, techniques, and outcomes.* Current Reviews in Musculoskeletal Medicine, 2013. **6**(2): p. 115-123.
132. Datta, A., et al., *Protocol composition logic (PCL).* Electronic Notes in Theoretical Computer Science, 2007. **172**: p. 311-358.
133. Blanchard, E.B., et al., *Psychometric properties of the PTSD Checklist (PCL).* Behaviour research and therapy, 1996. **34**(8): p. 669-673.
134. Yuan, L., et al., *AS-scheme MOF-on-MOF heterostructure.* Advanced Functional Materials, 2023. **33**(20): p. 2214627.
135. Lee, S., G. Lee, and M. Oh, *MOF-on-MOF growth: inducing naturally nonpreferred MOFs and atypical MOF growth.* Accounts of Chemical Research, 2024. **57**(21): p. 3113-3125.
136. Yang, J. and Y.W. Yang, *Metal–organic frameworks for biomedical applications.* Small, 2020. **16**(10): p. 1906846.
137. Keskin, S. and S. Kızılel, *Biomedical applications of metal organic frameworks.* Industrial & Engineering Chemistry Research, 2011. **50**(4): p. 1799-1812.
138. Zhang, B., et al., *Advances in immunomodulatory MOFs for biomedical applications.* Small, 2024. **20**(11): p. 2307299.
139. Chen, J., et al., *Recent advances in Ti-based MOFs in biomedical applications.* Dalton Transactions, 2022. **51**(39): p. 14817-14832.
140. Jacobsen, J., et al., *The chemistry of Ce-based metal–organic frameworks.* Dalton Transactions, 2020. **49**(46): p. 16551-16586.

141. Venkatraman, S.K. and S. Swamiappan, *Review on calcium-and magnesium-based silicates for bone tissue engineering applications.* Journal of Biomedical Materials Research Part A, 2020. **108**(7): p. 1546-1562.
142. Zadehnajar, P., et al., *Recent advances on akermanite calcium-silicate ceramic for biomedical applications.* International Journal of Applied Ceramic Technology, 2021. **18**(6): p. 1901-1920.
143. Yamada, S., et al., *Osteoblast-like cell responses to ion products released from magnesium-and silicate-containing calcium carbonates.* Bio-Medical Materials and Engineering, 2017. **28**(1): p. 47-56.
144. Wang, C., et al., *Highly selective recovery of Au (III) from wastewater by thioctic acid modified Zr-MOF: Experiment and DFT calculation.* Chemical Engineering Journal, 2020. **380**: p. 122511.
145. Schleder, G.R., et al., *From DFT to machine learning: recent approaches to materials science–a review.* Journal of Physics: Materials, 2019. **2**(3): p. 032001.
146. Danilova, D., et al., *Materials for plastic surgery of the dura mater: History and current state of the problem.* Современные технологии в медицине, 2018. **10**(3 (eng)): p. 194-201.
147. Suh, D.C., *Where did the dura mater come from?* Neurointervention, 2020. **15**(1): p. 2-3.
148. Hammady, M., *Histology of the human Dura mater; a review article.* 2023.
149. Mao, J., et al., *Bioactive electrospun Poly (p-dioxanone)/bioactive glass Hierarchical structured fibrous membrane for enhanced dura mater regeneration and integration.* Journal of Colloid and Interface Science, 2025. **689**: p. 137290.
150. Yan, S., et al., *Biomimetic natural silk nanofibrous microspheres for multifunctional biomedical applications.* ACS nano, 2022. **16**(9): p. 15115-15123.
151. Khalid, H., et al., *Silk fibroin/collagen 3D scaffolds loaded with TiO2 nanoparticles for skin tissue regeneration.* Polymer Bulletin, 2021. **78**(12): p. 7199-7218.
152. Abbasi, A.R. and A. Morsali, *Formation of silver iodide nanoparticles on silk fiber by means of ultrasonic irradiation.* Ultrasonics sonochemistry, 2010. **17**(4): p. 704-710.
153. Li, X., et al., *Preparation and extraction property study of corn cob-like magnetic mosaic carbon materials derived from MOF-on-MOF composites.* Analytica Chimica Acta, 2024. **1287**: p. 342112.
154. Wu, J., et al., *Surface modification of the Ti surface with nanoscale bio-MOF-1 for improving biocompatibility and osteointegration in vitro and in vivo.* Journal of Materials Chemistry B, 2022. **10**(41): p. 8535-8548.
155. Sadrjahani, M., A.A. Gharehaghaji, and M. Javanbakht, *Aligned electrospun sulfonated polyetheretherketone nanofiber based proton exchange membranes for fuel cell applications.* Polymer Engineering & Science, 2017. **57**(8): p. 789-796.
156. Ren, K., et al., *Electrospun PCL/gelatin composite nanofiber structures for effective guided bone regeneration membranes.* Materials Science and Engineering: C, 2017. **78**: p. 324-332.
157. Zong, C., et al., *A novel therapy strategy for bile duct repair using tissue engineering technique: PCL/PLGA bilayered scaffold with hMSCs.* Journal of tissue engineering and regenerative medicine, 2017. **11**(4): p. 966-976.

158. Wong, H.M., et al., *A biodegradable polymer-based coating to control the performance of magnesium alloy orthopaedic implants.* Biomaterials, 2010. **31**(8): p. 2084-2096.
159. Wu, F., et al., *Fabrication and properties of porous scaffold of zein/PCL biocomposite for bone tissue engineering.* Composites Part B: Engineering, 2012. **43**(5): p. 2192-2197.
160. Bhardwaj, N. and S.C. Kundu, *Electrospinning: A fascinating fiber fabrication technique.* Biotechnology advances, 2010. **28**(3): p. 325-347.
161. Shaheed, N., et al., *Synthesis of nanocellulose aerogels and Cu-BTC/nanocellulose aerogel composites for adsorption of organic dyes and heavy metal ions.* Scientific reports, 2021. **11**(1): p. 18553.
162. Semino, R., et al., *Understanding the origins of metal–organic framework/polymer compatibility.* Chemical science, 2018. **9**(2): p. 315-324.